UNITED STATES DEPARTMENT OF COMMERCE
JESSE H. JONES, Secretary
NATIONAL BUREAU OF STANDARDS
Lyman J. Briggs, Director

✦

Journal of Research

of the

National Bureau of Standards

✦

Volume 28, Number 2
February 1942

[Published with approval of the Director of the Budget]

UNITED STATES
GOVERNMENT PRINTING OFFICE
WASHINGTON : 1942

For sale by the Superintendent of Documents, Washington, D. C. - - - - - - Price 30 cents
$3.50 per year on subscription

The prices of the separate Research Papers appearing in this JOURNAL are given on the front cover page. If 100 or more copies of any separate are ordered, a discount of 25 percent is allowed. Those who desire copies of separate Research Papers should send their orders and remittances without delay to the Superintendent of Documents, U. S. Government Printing Office, Washington, D. C. This will aid him to determine the number of copies to be printed for sale. Research Papers are not printed from electrotypes, and usually no more reprints can be had when the first and only printing is exhausted.

MATHEMATICAL TABLES

A list of the mathematical tables now obtainable from the National Bureau of Standards is printed on page 3 of the Journal cover. New tables will be announced from time to time as they become available.

U. S. DEPARTMENT OF COMMERCE NATIONAL BUREAU OF STANDARDS

RESEARCH PAPER RP1449

Part of Journal of Research of the National Bureau of Standards, Volume 28, February 1942

AN ABSOLUTE DETERMINATION OF THE AMPERE, USING HELICAL AND SPIRAL COILS

By Roger W. Curtis, Raymond L. Driscoll, and Charles L. Critchfield

ABSTRACT

The value of an electric current has been measured in absolute units by a current balance, and simultaneously in international units by standard cells and standard resistors. In the current balance a subdivided helix served as the two fixed coils and, as the moving coil, either a short helix or a compact spiral. The two moving coils were the same ones that were described in a previous paper in which the fixed coils were spirals.

The value obtained when using these two moving coils and the subdivided helix differs by only 4 parts in a million from the value obtained when using these moving coils and spirally wound fixed coils. These values are, however, somewhat different from those obtained when using multilayer coils wound with copper wire. The relationship between the absolute and International ampere, from the most dependable measurements at the National Bureau of Standards, may be expressed as

1 NBS International ampere = 0.999 850 absolute ampere.

In the preceding paper published by members of the Bureau staff on this subject the value given was 1 NBS International ampere = 0.999 860 absolute ampere.

CONTENTS

	Page
I. Introduction	133
II. Design and construction of the coils	134
III. Measurements of the dimensions of the coils	136
1. Diameter	136
2. Pitch	139
3. Wire diameter	141
IV. Electrical measurements	142
V. Computation of the force produced by unit current in the coils	144
1. The force between coaxial helices	145
2. The force between a helix and a spiral	148
3. Computation of the absolute value of the current	152
VI. Experimental determination of the maximum force between the coils	152
VII. Discussion of results	155
VIII. References	156

I. INTRODUCTION

The determination of a current in terms of the units of length, mass, and time is usually made by measuring the force between two or more coils carrying the current. The dimensions and positions of the coils can be measured, so that the current in the coils can be computed from their dimensions and the electromagnetic force between them. In most of the determinations made during this century, the coils have been of the multilayer type in which the cross-sectional

dimensions of the windings were small compared with the diameter of the coils. The only important exception is the "current weigher" used at the National Physical Laboratory [1],[1] which was constructed with single-layer helical coils. Previous determinations of the ampere at the National Bureau of Standards, using multilayer coils wound with wire [2, 3], have shown that the effect of the uncertainty in the location of the wires in a multilayer coil is an important factor that cannot be evaluated. The problem has been attacked by building multilayer coils in the form of spiral ribbon windings, as already described [2]. Another approach to the problem has now been made by using single-layer helices exclusively or in combination with spiral ribbon coils, even though the smaller forces obtained reduced somewhat the accuracy of the force measurement. It is unlikely that all the systematic errors will be the same with the two types of fixed coils.

The technique [4] which has been developed at this Bureau for winding single-layer helices in lapped screw threads has produced coils which are well suited for use in a current balance. These coils have very small variations in diameter and in pitch. Two of these helices have been made for use in the current balance.

This report will be devoted to a description of the new coils used, the electric circuit, the formulas used in the computation of the current, and the results obtained. This report is reasonably complete in itself, but it will be necessary to refer to earlier papers for some of the details of the apparatus which have therein been described.

II. DESIGN AND CONSTRUCTION OF THE COILS

The coils for use in a current balance must fulfill the following requirements: (1) The electromagnetic force for the operating current must be sufficiently large to permit its accurate measurement; (2) the mass of the moving coil must be less than that for which the balance was designed; (3) the temperature of the coils when carrying the operating current must be not more than a few degrees above room temperature; (4) the dimensions of the coils must be such that they can be accurately measured; and (5) the distribution of the conductors in the coil must be sufficiently uniform to permit the accurate computation of the electromagnetic force. Spiral and helical coils meet the last condition more satisfactorily than the multilayer coils of wire which were used in an earlier determination [8]. Spiral fixed coils, a spiral moving coil, and a helical moving coil have already been described [2]. This paper gives the results of a determination in which helical fixed coils were used, the moving coils being the spiral and the helix mentioned above. The helical fixed coils for this determination were the two halves of a single helix. The two coils were obtained from one helix by connecting a lead to the midpoint of the winding and having the current flow in opposite directions in the two halves of the helix. The requirements given above will be discussed with reference to the use of the helical fixed coils.

The electromagnetic force between the helical fixed coils and the helical moving coil with an operating current of 1 ampere was about 1.4 g (grams) and with the spiral moving coil about 1.7 g. While these forces were very small, they were sufficiently large to permit the

[1] Figures in brackets indicate the literature references at the end of this paper.

determination of a current within a few parts in a million for a single measurement. An increase in the current did not increase the accuracy because it produced additional heating in the coils.

The mass of the helical moving coil, designated as *P1*, was 700 g and that of the spiral moving coil, designated as *A1*, 475 g. These coils were used on a balance which was designed to take a load of 2 kg. Hence, both of these coils were well within the limits fixed by the balance.

The temperature of the coils was kept within a few degrees of room temperature by designing them to have low resistance, by using a small operating current, and by ventilating the coil case.

It was necessary that the coils be large enough so that their dimensions could be measured with the required accuracy. The moving coil had a diameter of about 25 cm and the fixed coil 45 cm, and these dimensions met the above condition.

A satisfactory helical coil should have extremely uniform diameters and pitch of winding throughout the whole coil. Preliminary measurements were made with a fixed helix which had been used in an absolute determination of the ohm, where it was designated as the short glass solenoid [3]. However, theoretical considerations indicated that the pitch was not sufficiently uniform to give the required accuracy for the investigation on the ampere. Since a helix of the dimensions of this coil could be advantageously used in researches on the absolute ohm as well as on the absolute ampere, C. Moon rewound [2] this form by the method which he had developed for producing helices of very uniform pitch and diameter [4]. Before winding, a helical groove or screw thread having a nominal pitch of 0.8 mm was ground in the cylindrical form. This groove was then lapped with a "saddle" or "half-nut" lap until the profile of the groove was approximately sinusoidal and the diameter of the form uniform. The helix was then wound with carefully selected wire drawn to size through several dies. The final drawing was made onto the grooved cylinder directly from the last drawing die, so that the winding tension of the wire was the tension with which the wire was pulled through the last die, which was about 10 kg. After the winding was completed, elliptically shaped spots were polished on the wire along four lines parallel to the axis of the helix. Two lines were ruled on each spot on turns near the ends and middle of the winding. These ruled lines were used in measuring the pitch of the winding.

Three electric leads were attached to the fixed helix, now designated as *H1*, one at each end and one at the midpoint. They projected radially through amber bushings in a wooden bar running parallel to the axis of the winding and about 2 cm outside of the coil winding. In order to attach the lead wires firmly and accurately, the end of each was notched, tinned, and held firmly against the winding at the desired location by a spring. By careful local heating, each lead wire was soldered onto the desired wire of the winding without disturbing the adjacent turns. This method of fastening the middle lead on the fixed helix made it unnecessary to break the winding at the middle. Hence this coil could be used in the absolute-ohm work as well as in the current balance.

[2] Before rewinding the coil, Moon ground and lapped the screw thread, and, after the winding was completed, polished the "spots" on the wire and ruled the lines on them.

The spiral coil, *A1*, used as the second moving coil consisted of a double winding of aluminum ribbon on a form of aluminum alloy. The ribbon was anodized electrolytically to form an electrical insulating layer of aluminum oxide, which was the only insulation used between the successive turns of the coil. The resistance between the two windings (50 megohms) showed that no appreciable current was leaking between turns. The ratio of the radius of this coil to that of the helical moving coil had been indirectly determined by comparing them with several fixed coils as previously reported [2].

III. MEASUREMENTS OF THE DIMENSIONS OF THE COILS

The dimensions of the coils were measured by methods and with apparatus which had been used previously in similar measurements. It was necessary to measure the diameter and pitch of each helix, and each of these measurements had to be made with high precision. These will be described briefly and the results given in more detail.

1. DIAMETER

A ring micrometer, with a motor-driven screw and a tail stock having a pressure-operated contact, was set up for the measurement of the

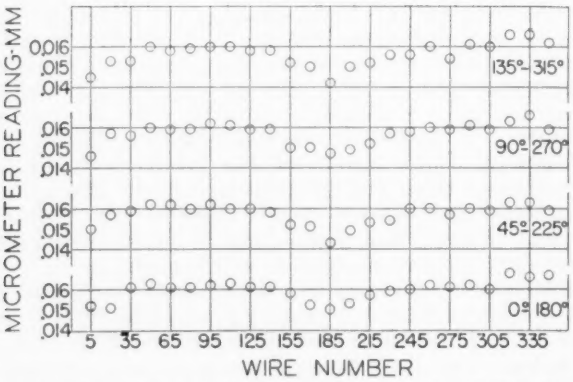

FIGURE 1.—*Variation in the outside diameter of helical coil H1 along four axial planes.*

diameters of the coils [5]. The coil to be measured was mounted on a turntable, with its axis vertical. The micrometer was hung in a horizontal position by three rods from a support which was carried on a vertical track. The coil could be rotated by the turntable to measure any diameter in a given horizontal plane, and the micrometer could be raised or lowered, by running the support up or down the vertical track, to measure any diameter along the length of the coil. The end standard to which the measurements were referred was mounted directly above the coil. The coil, micrometer, and end standard were mounted in a thermostatically controlled cabinet. The micrometer was adjusted and read from outside this cabinet. Readings could be estimated to 0.1 micron and repeated to 0.3 micron.

The diameter of the fixed coil, *H1*, was measured every 12 mm along the axis of the coil in each of four equally spaced axial planes.

The measurements were made at two different temperatures for computing the temperature coefficient of expansion. The results are plotted in figure 1, and the average values at the different axial planes are given in table 1. The value of 3.6 ppm/° C for the temperature coefficient agrees with the value given [6] for the type of Pyrex glass from which the form was made.

TABLE 1.—*Diameter and temperature coefficient of expansion of fixed coil H1*

[The value given for each axial plane is the average of 24 measurements along the length of the coil in that plane. The range in values in any axial plane did not exceed 0.000 26 cm. (See also fig. 1.) Length of fused-quartz end standard at 20° C: 46.316 43 cm. Assumed temperature coefficient of end standard: 0.4 ppm/°C.]

[Date of measurements: August 1940.]

Axial plane	Diameter at 26.0°C	Diameter at 30.9°C	Temperature coefficient
Degrees	*cm*	*cm*	*ppm/°C*
0 to 180	46. 260 26	46. 261 08	3. 6
45 to 225	46. 260 23	46. 261 08	3. 7
90 to 270	46. 260 24	46. 261 03	3. 5
135 to 315	46. 260 22	46. 260 99	3. 4
Average	46. 260 24	46. 261 05	3. 6

Average outside diameter at 30.9°C	46.261 05 cm.
Wire diameter (see table 5)	0.069 96 cm.
Mean diameter of winding at 30.9°C	46.191 09 cm.
Mean diameter of winding at 30.0°C	46.190 94 cm.

The end standard, to which all the diameter measurements were referred, was made of fused quartz (clear silica glass). The ends of this standard were segments of a sphere which had its center at the midpoint of the standard. The length at 20° C was determined by the Interferometry Section of this Bureau. In obtaining the length of the end standard at different temperatures, the temperature coefficient of the fused quartz was assumed to be that given in the International Critical Tables, namely 0.4 ppm/°C.

The diameters given in table 1 were measured without any current in the coil, so that the temperatures of the winding and of the form were the same. With a current in the coil, the temperature of the winding was higher than that of the form. The temperature of the winding under operating conditions was determined from its resistance, but no satisfactory method of measuring the temperature of the form has been developed. In order to obtain the effective temperature of the coil and winding, the diameter of *H1* was measured after it had carried a current of 1 ampere for several days and was under the same conditions as when in the current balance. Then the diameter was 1.8 ppm smaller than that computed from the diameter and temperature coefficient given in table 1 and from the measured temperature of the winding. The appropriate correction was applied to the final result.

Two sets of measurements of the diameters of the moving coil, *P1*, have been made. The measurements made in 1934 were to determine the variation in diameter. The correction for the measuring force was not applied, and the end standard was not accurately calibrated. In 1941 the diameter was measured at 3 different temperatures in 12 different axial planes in each of 11 different axial

positions, from which the mean diameter and its temperature coefficient were determined. A summary of these measurements is given in table 2.

TABLE 2.—*Summary of he measurements of the outside diameter of P1*

[The value given for each axial plane is the average of 11 measurements along the length of the coil in that plane. The average range in values in the different axial planes was 0.000 31 cm. Length of fused-quartz end standard at 20°C: 24.586 18 cm. Assumed temperature coefficient of end standard: 0.4 ppm/°C. Measuring force: 450 g. Date of measurements: February 1941]

Axial plane	Temperature of measurement		
	24.9°C	30.0°C	35.4°C
Degrees	*cm*	*cm*	*cm*
0 to 180	24. 513 03	24. 513 54	24. 514 07
15 to 195	.513 25	.513 75	.514 25
30 to 210	.513 38	.513 85	.514 36
45 to 225	.513 34	.513 88	.514 39
60 to 240	.513 15	.513 58	.514 18
75 to 255	.512 72	.513 22	.513 72
90 to 270	.512 27	.512 78	.513 30
105 to 285	.512 07	.512 56	.513 10
120 to 300	.512 07	.512 56	.513 03
135 to 315	.512 20	.512 68	.513 21
150 to 330	.512 50	.512 92	.513 48
165 to 345	.512 74	.513 27	.513 79
Average	24. 512 73	24. 513 22	24. 513 74

Outside diameter at 30°C corrected to zero measuring force	24. 513 60 cm.
Diameter of wire (see table 5)	0. 051 23 cm.
Mean diameter of winding at 30.0°C	24. 462 37 cm.
Coefficient of thermal expansion in the range 25° to 35°C	3. 9 ppm/°C

Measurements of the diameter with a current in the winding gave the same value (within 1 ppm) as that computed from the measured diameter with no current and the measured temperature of the winding. This showed that the temperature of the winding and form were so nearly the same that no correction for their difference was necessary.

The mean diameter of the spiral moving coil, *A1*, was obtained from the measured diameter of *P1* and the ratio of their radii. This ratio was obtained by comparison of the magnetic fields produced by known currents. Each of these coils was compared with six different fixed coils. The values of the ratio of radii at 22° C when each fixed coil was used as an intermediary were given in table 11 of the previous paper [2]. The diameter of *A1* was 25.154 52 cm at 30° C. The temperature coefficient was 21.0 ppm/°C. With current in the coil, the temperature of the form was substantially the same as that of the winding.

The radial depth of *A1* and an approximate value of its mean diameter were obtained from mechanical measurements. The results depended on a measurement of the outside diameter, which did not give an accurate result because of the uncertainty in the correction for the measuring force. Also, the spacing of the individual ribbons in the radial direction may not have been exactly uniform because of the compression of the inner turns in the process of winding. This compression probably accounted for the fact that the mean diameter by mechanical measurements was 84 ppm larger than that obtained by magnetic measurements. However, the uncertainty in the outside

diameter and the compression of the windings were not sufficient to introduce a significant error in the value obtained for the radial depth, which was 0.6522 cm at 30° C.

2. PITCH

The pitch of the helix, *H1*, was measured with a cathetometer [7, 4] equipped with two microscopes which could be alternately set on the coil and on a meter bar. The coil and the meter bar were mounted with their axes vertical, and the cathetometer was arranged so that it could be rotated about a vertical axis. Each microscope was focused on a ruled line on the wire opposite it. The cross hairs of the filar micrometer eyepiece of each microscope were set on the upper of the two lines in the field of view and the readings recorded. Readings were then taken for the lower lines on the same two spots. The cathetometer was rotated until the meter bar was brought into the field of view of the microscopes. Focusing was done by moving the meter bar with respect to the microscopes so that the original focusing position of the microscopes was not changed. The cross hairs of the filar micrometer eyepieces were then set on the millimeter rulings of the meter bar and the readings recorded. The number of turns between microscopes was chosen so that the distance measured was approximately a whole number of millimeters, and the meter bar was elevated so that the millimeter divisions were in the same part of the field of the eyepiece as the lines on the spots. From these readings and the calibrations of the meter bar and of the filar micrometer, the distance between the two wires was obtained.

Measurements were made on *H1* between five pairs of wires in each of three axial planes. A complete set was made at each of two different temperatures. From the measurement between each pair of wires, the pitch was obtained, and this was multiplied by the number of turns on the coil to give its length. Measurements made from the middle to each end showed that the pitch was only 6 ppm different for the two halves. From the measurements at the two temperatures, the temperature coefficient of thermal expansion in the axial direction was 3.0 ppm/° C. The results of the measurements of the pitch of *H1* are given in table 3.

TABLE 3.—*Axial length and pitch of fixed coil H1*

[The recorded values are the distances between numbered turns. Length standard: calibrated invar meter bar BS3566. Temperature coefficient: 1.13 ppm/°C. Date of measurements: July 1940]

Axial interval	Axial plane[a]					
	0°		180°		270°	
	31.5° C	26.4° C	31.5° C	27.0° C	31.4° C	27.0° C
Turns	*cm*	*cm*	*cm*	*cm*	*cm*	*cm*
350 to 5	27.596 82	27.596 34	27.596 60	27.596 13	27.596 52	27.596 18
349 to 4	.596 44	.596 04	.596 67	.596 30	.596 67	.596 33
348 to 3	.596 60	.596 18	.596 60	.596 30	.596 60	.596 33
347 to 2	.596 77	.596 28	.596 64	.596 38	.596 70	.596 46
346 to 1	.596 67	.596 18		.596 16	.596 67	.596 33
Average	27.596 66	27.596 20	27.596 63	27.596 25	27.596 63	27.596 33
Coefficient of thermal expansion	3.3 ppm/° C		3.1 ppm/° C		2.7 ppm/° C	

Mean axial length of 345 turns	27.596 64 cm at 31.5° C.
Mean pitch	0.079 990 3 cm at 31.5° C.
Mean axial length of 172 turns	13.758 33 cm at 31.5° C.
Mean coefficient of thermal expansion	3.0 ppm/° C.

[a] Measurements made at the 90° position were not satisfactory. This set of spots was ruled first, and, because of difficulties encountered in setting up the ruling device when the spacing between the wires was so small, the lines were not evenly placed with respect to the edges of the wires. Therefore, the few measurements made at this position are not reported.

NOTE.—The half-lengths were measured at the 0° and 180° positions. The pitch of the wires 181 to 1 was 6 ppm greater than that for wires 350 to 175. The length of each half of the helix was taken as the average pitch for the whole helix multiplied by 172, the number of turns in each half.

The pitch of the helical moving coil, *P1*, though relatively unimportant, was measured in somewhat the same way as for *H1*, except that the axis of the coil was mounted in a horizontal position and a single microscope used. This microscope was mounted on a track and its position determined by an accurate micrometer screw. Before and after each set of measurements the screw was calibrated in place by settings made on a line standard. Measurements were made of the length of the whole coil and also of each half. The temperature coefficient was not measured, since the coil was so short that the change in length with any change in temperature encountered in these measurements was negligible. The results of these measurements are given in table 4.

TABLE 4.—*Axial length and pitch of moving coil P1 at 24°C*

[Length standard: stainless steel decimeter bar BS 6. Temperature coefficient: 10.3 ppm/°C. Date of measurements: October 1934]

Axial plane	Axial interval		
	First half, Wires 21 to 1	Second half, Wires 41 to 21	Total length, Wires 41 to 1
Degrees	*cm*	*cm*	*cm*
0	1.2998	1.3001	2.5999
90	1.3000	1.3000	2.6000
180	1.3002	1.2999	2.6001
270	1.3001	1.2999	2.6000
Average	1.3000	1.3000	2.6000

Average length of 40 turns	2.6000 cm.
Pitch	0.065 00 cm.
Axial length of *P1* (41 total turns)	2.6650 cm.

The measurement of pitch for the spiral moving coil, *A1*, has no meaning in the usual sense because there is only one turn in the axial direction, although there are many layers. The corresponding measurement is the axial breadth of the winding, and in this case it is the width of the ribbon itself. This was measured with an ordinary micrometer and a clamp for holding the ribbon flat. Samples of the ribbon, taken before and after winding, were measured. The average width of the ribbon was found to be 0.6364 cm, without insulation and this figure may be taken as the axial breadth of the winding, since, within reasonable limits, the uneven stacking of the winding in an axial direction has been shown to have a negligible effect [2].

3. WIRE DIAMETER

The diameter of the wire was measured with a special micrometer set up for that purpose [4]. The head and tail stock were of the same type as those used in measuring the diameters of the coils, except that the screw was hand-operated and a small light was used to indicate when the contact on the tail-stock was opened. The wire to be measured hung from a support above the micrometer and was kept straight by means of a weight of about 5 kg. The wire was stretched on the form by a force of about 10 kg. A correction to the measured diameter on account of the difference in tension was made using a value of 0.34 for Poisson's ratio. The support could be rotated so that any diameter in a given cross section could be measured, and the micrometer could be raised or lowered to measure at any particular place along the length of the sample. Readings could be made to 0.1 micron and could be repeated to 0.2 micron.

The diameter of the wire of each helix was obtained from samples taken from the beginning and end of the winding. The diameter of each sample was measured in either four or eight different angular positions around the wire. Each sample from *H1* was measured at several places along the wire. In addition, an average value of the diameter of a sample of the wire of *H1* was obtained by measuring its mass, length, and density. A correction was made for the decrease in density of the wire when it was under tension on the coil. Estimates of the accuracy obtained in the measurement of the three quantities used in this method indicated that the precision of the mechanical and density methods was about the same. The results are summarized in table 5.

The wire for *H1* was drawn through a diamond die having a nominal diameter of 0.7 mm. The measurements showed that the wire was slightly elliptical. The wire for the small moving coil, *P1*, was drawn through a sapphire die having a nominal diameter of 0.51 mm. A set of measurements on this wire showed it to be somewhat less elliptical than the wire on *H1*.

The average value of the diameter of the wire was taken as the mean of the values obtained by the mechanical and density methods for *H1* and as the mean of the mechanical measurements for *P1*. However, the important diameter was the one which was perpendicular to the axis of the coil, since it was the one which was subtracted from the outside diameter of the coil winding to get the mean diameter. A small correction to the average value, which was negative in the

case of *H1* and zero in the case of *P1*, was obtained from the data for the variation of the wire diameter with angular position.

The values of the various constants of the coils are assembled in table 6.

TABLE 5.—*Diameter of the wire used on H1 and P1*

[Temperature: between 28° and 29° C. Date of measurements: July 1937 for *P1* and July 1940 for *H1*]

	H1		*P1*	
	End *A*	End *B*	End *A*	End *B*
	mm	*mm*	*mm*	*mm*
Average by mechanical measurements	0.6994	0.7000	0.5124	0.5121
Difference between maximum and minimum diameters	.0012	.0022	.0008	.0006
Average by mechanical measurements	0.6997		0.5123	
Average by density, length, and mass measurements	.7005		-----	
Final average	.7001		-----	
Difference between the diameter perpendicular to the axis of the coil and the average wire diameter	−0.0005	−0.0005	0.0000	0.0000
Final average wire diameter perpendicular to the axis of the coil	0.6996		0.5123	

TABLE 6.—*Constants of the fixed helix H1 and the moving coils P1 and A1*

[All values reduced to 30° C.]

Constant	*H1*	*P1*	*A1*
Average outside diameter, cm	46.260 90	24.513 60	25.8086
Diameter of the wire in the direction perpendicular to the axis of the coil, cm	0.069 96	0.051 23	-----
Mean diameter of coil (cm):			
From mechanical measurements	46.190 94	24.462 37	-----
From magnetic measurements	-----	-----	25.154 52
Axial length (or breadth), cm	27.516 54	2.6650	0.6364
Radial depth of coil, cm	-----	-----	.6520
Number of turns	344	41	45
Mean pitch, cm	0.079 989 9	0.065 00	-----
Resistance of winding in ohms (top or *A* winding is given first)	{11.7958	} 2.8206	{ 2.911
	{11.7916		{ 2.826
Temperature coefficient of expansion, ppm/° C	3.6	3.9	21.
Material of form	Pyrex glass	Pyrex glass	Aluminum alloy
Diameter of the form, cm	46	24.5	24.5
Length of form, cm	30	3.6	1.6
Thickness of form (wall thickness), cm	7.5	1.1	-----
Mass of completed coil, g	68,000	700	473

IV. ELECTRICAL MEASUREMENTS

The measurement of the current through the windings of the coils in NBS International amperes was made by comparing the potential drop across a calibrated resistor with the electromotive force of a standard cell, and computing the current from Ohm's law. A simple circuit was arranged which reduced to a minimum possible troubles from thermal electromotive forces, electric leakage, and calibration errors. A diagram of the circuit is given in figure 2.

The current from the battery, *B*, divided at the midpoint of the fixed helix, *H1*, so that the values of the currents in the two halves had to be determined separately in NBS International amperes. One current was measured directly and the other obtained from the ratio of the two. The current was measured directly by balancing

the potential drop it produced in the calibrated resistor, *R1*, against the electromotive force of the standard cell, *E*. The ratio of currents was measured by a type of bridge circuit in which the calibrated resistor, *R1*, was connected in series with the moving coil and one-half of the fixed coil, and another calibrated resistor, *R2*, was connected in series with an adjustable resistor, *R3*, and the other half of the fixed coil. A storage battery, *B*, was connected in series with an adjustable ballast resistor, *R4*, and a reversing switch, *S1*. The two parallel portions of the circuit extended from the midpoint of the fixed coil to the contact which connects the calibrated resistors, *R1* and *R2*, on the slide wire, *SW*. A galvanometer, *G1*, was arranged

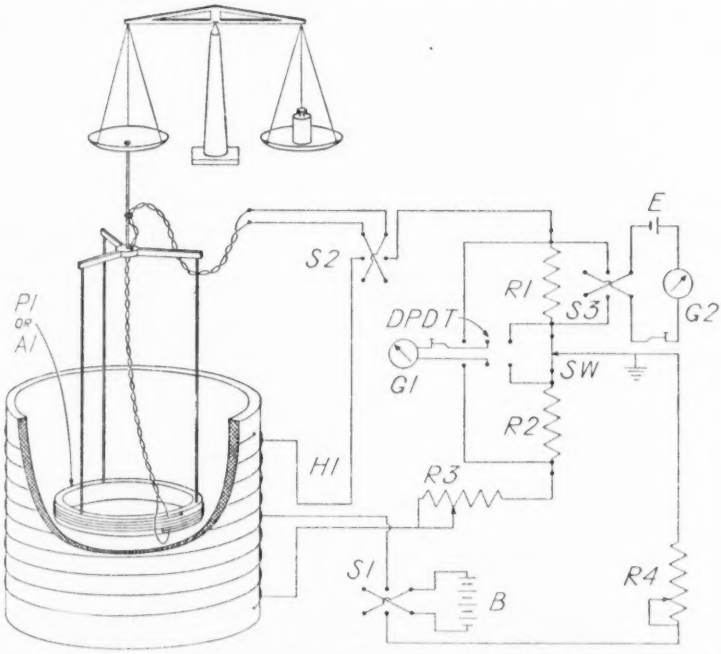

FIGURE 2.—*Diagram of the electric circuit of the current balance when using H1 for the two fixed coils.*

so that it could be connected to either set of the potential terminals of the calibrated resistors through the switch, *DPDT*. By adjusting resistor *R3* and the slide wire, *SW*, the galvanometer deflection could be made zero for both sets of potential terminals. Then the ratio of the currents was equal to the inverse ratio of the resistance of resistors *R1* and *R2*. The current in the upper half of the fixed coil was measured by connecting a standard cell, *E*, and a galvanometer, *G2*, across resistor *R1* and adjusting the ballast resistor, *R4*, until the galvanometer had a zero deflection. This adjustment did not affect the ratio of the currents in the two halves of the coil. When both galvanometers gave no deflection, the current in one-half of the fixed coil and the moving coil was known in NBS International amperes from the resistance of the calibrated resistor *R1* and the electromotive force, *E*, of

the standard cell, and the ratio of the currents was known from the inverse ratio of the calibrated resistors *R1* and *R2*. In practice *R1* and *R2* were very nearly equal, so that the two currents had nearly the same value.

It was more convenient in the computation of the final result to use a mean current rather than the two individual values. This mean current was called the equivalent current and was the square root of the product of the current in the moving coil and the average current in the two halves of the fixed coil.

With a large-capacity storage battery the currents could be kept steady to within 1 or 2 parts in a million by almost continuous adjustment on the part of one observer. A preliminary heating period of 2 or more days was required, since the large mass of the fixed coil made it very slow in attaining an equilibrium temperature.

Sources of error in the measuring circuit were few, and the errors resulting therefrom were made negligibly small by a suitable design and careful measurements. Thermal electromotive forces were made negligible by keeping all parts that were not of copper in constant temperature baths. Observations made on various closed paths, which included a galvanometer but no electromotive force other than thermal, showed that thermal electromotive forces were negligibly small. Leakage to or from the circuit was reduced to a negligible value by a careful choice of insulating materials. Frequent measurements were made of the insulation resisitance between various parts of the circuit and ground to insure that the insulation remained intact. When the circuit was in use, it was grounded at the slide wire, *SW*, so that all potentials were definite with respect to that of ground. The only parts of the circuit requiring careful calibration were the two resistors, *R1* and *R2*, and the standard cell. These were frequently tested by the sections of this Bureau which are responsible for maintaining the units of resistance and of electromotive force. No change in the value of any of these standards other than that caused by temperature was reported during the course of these measurements. The resistors, *R1* and *R2*, were 1-ohm standards of the latest type, which had very low temperature and load coefficients. The resistors were kept in a stirred, thermostatically controlled oil bath, and, when necessary, corrections were made for temperature and load. The standard cells were kept in an underground compartment, where the temperature changed very slowly, so that frequent comparisons with the standards of this Bureau enabled their electromotive force to be determined at any time from the observed temperature. This combination of standard cells and standard resistors gave a current of about 1.018 amperes.

V. COMPUTATION OF THE FORCE PRODUCED BY UNIT CURRENT IN THE COILS

The computation of the force produced by a unit current in both the fixed and the moving coils requires a different formula when the moving coil and the fixed coil are both helices than that required when a helix is used with a spiral coil. The two cases will be considered separately. Because the formulas take quite different forms, the nomenclatures for the two cases are distinct.

1. THE FORCE BETWEEN COAXIAL HELICES

A formula for the force between two coaxial helical wires when each carries unit current has been given by Snow [10]. This formula is perfectly general so far as the relative vertical positions of the two coils are concerned. The permeability at all points is assumed to be unity. The coils of the current balance were arranged as shown in figure 3 in order to obtain the maximum vertical force on the suspended coil, *P1*. In all that follows, Snow's formula has been applied in accordance with the arrangement of the coils as shown.

The following independent variables are used in the formula

r_1 = mean radius of the fixed helix.
r_2 = mean radius of the moving helix.
l_1 = axial length of the fixed helix (pitch × number of turns).
l_2 = axial length of the moving helix (pitch × number of turns).
N_1 = number of turns on fixed coil.
N_2 = number of turns on moving coil.
α = angular separation of the leads on the two helices.

The axial force, f, between the suspended coil, *P1*, and the upper half of the solenoid, *H1*, produced by unit current in each coil, is computed from the same function of three different quantities, X_1, X_2, and X_3, by the equation

$$f=2\omega'(X_1)+\omega'(X_2)-\omega'(X_3).$$

The three quantities, X_1, X_2, X_3, are derived from the lengths of the coils as follows:

$$X_1=\frac{l_2}{2}$$

$$X_2=\frac{l_1-l_2}{2}$$

$$X_3=\frac{l_1+l_2}{2}.$$

The function $\omega'(X)$ is resolved into three components; $\omega'_\theta(X)$, the principal term; $\omega'_\alpha(X, \alpha)$, a correction term depending upon the relative azimuths of the two helices; and $\overline{\omega}'_X(X, \alpha)$, a correction term for the axial component of current in the helices and lead wires. These terms are given by the equations:

$$\omega'_\theta(X)=\frac{2\pi N_1N_2}{l_1l_2}\left\{X\sqrt{X^2+(r_1+r_2)^2}[K-E]+\frac{X(r_1-r_2)^2}{\sqrt{X^2+(r_1+r_2)^2}}[K-\Pi]\right\}$$

$$\omega'_\alpha(X,\alpha)=\frac{\pi X}{6\sqrt{X^2+(r_1+r_2)^2}}\left[\frac{2-k^2}{1-k^2}E-2K\right]$$

$$+\frac{\pi X}{4\sqrt{r_1r_2}}\left\{\cos\frac{\alpha}{2}\sin^{-1}\left(k\cos\frac{\alpha}{2}\right)-\frac{k(2-k^2)}{2(1-k^2)}\sqrt{1-k^2\cos^2\frac{\alpha}{2}}\right.$$

$$\left.+\sin\frac{\alpha}{2}\log_e\left[\frac{k\sin\frac{\alpha}{2}+\sqrt{1-k^2\cos^2\frac{\alpha}{2}}}{\sqrt{1-k^2}}\right]\right\}$$

$$\overline{\omega}'_X(X,\alpha)=\frac{X}{\sqrt{X^2+(r_1+r_2)^2}}\log_e\frac{r_1}{\sqrt{r_1^2+r_2^2-2\,r_1r_2\cos\alpha}},$$

where $k^2=4r_1r_2/[X^2+(r_1+r_2)^2]$

$k_0^2=4r_1r_2/(r_1-r_2)^2$

and K, E, Π are the complete elliptic integrals of the first, second, and third kinds, respectively, to the modulus k and parameter k_0. These integrals can be evaluated conveniently by the AGM method as outlined by King [11] and by Grover [12]. Because the value of f is the difference of quantities that are nearly equal, the computation of the ω' functions must be carried to more significant figures than are required in the result.

As shown in figure 3, the fixed coil, *H1*, was divided into two parts that were practically identical; equal and opposite currents in the

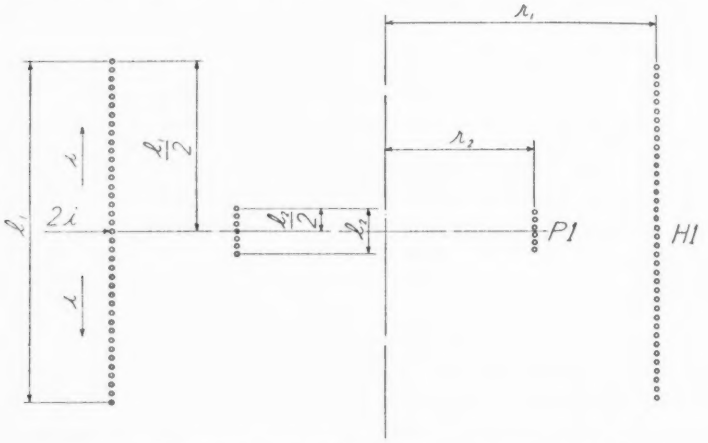

FIGURE 3.—*Section showing relative positions of helices P1 and H1.*

two halves of *H1* doubled the force, f, which, as stated before, was the attraction of unit current in the moving coil, *P1*, for unit current in the upper half of *H1* only. Furthermore, the force measured by the balance was that caused by reversing the current in the fixed coils. This procedure doubled the force that would have been obtained if the observations had been made with the current "off" and "on." The value of f is in dynes if the permeability of the medium surrounding the coils is unity. Hence, the total force, F_{HH}, in dynes for an absolute ampere in each coil is

$$F_{HH}=4f/100.$$

Since the correction terms $\omega'_a(X,\alpha)$ and $\overline{\omega}'_X(X,\alpha)$ are small, adjustments in the value of the force for unit currents corresponding to small

corrections to the nominal values of r_1, r_2, l_1, and l_2 can be made by means of the following variation formula:

$$\frac{\delta f}{f}=\frac{\delta F}{F}=\left\{\frac{\left[\frac{2d\omega'_\theta(X_1)}{dr_1}+\frac{d\omega'_\theta(X_2)}{dr_1}-\frac{d\omega'_\theta(X_3)}{dr_1}\right]r_1}{2\omega'_\theta(X_1)+\omega'_\theta(X_2)-\omega'_\theta(X_3)}\right\}\frac{\delta r_1}{r_1}$$

$$+\left\{\frac{\left[\frac{2d\omega'_\theta(X_1)}{dr_2}+\frac{d\omega'_\theta(X_2)}{dr_2}-\frac{d\omega'_\theta(X_3)}{dr_2}\right]r_2}{2\omega'_\theta(X_1)+\omega'_\theta(X_2)-\omega'_\theta(X_3)}\right\}\frac{\delta r_2}{r_2}$$

$$+\left\{\frac{\left[\frac{2d\omega'_\theta(X_1)}{dl_1}+\frac{d\omega'_\theta(X_2)}{dl_1}-\frac{d\omega'_\theta(X_3)}{dl_1}\right]l_1}{2\omega'_\theta(X_1)+\omega'_\theta(X_2)-\omega'_\theta(X_3)}\right\}\frac{\delta l_1}{l_1}$$

$$+\left\{\frac{\left[\frac{2d\omega'_\theta(X_1)}{dl_2}+\frac{d\omega'_\theta(X_2)}{dl_2}-\frac{d\omega'_\theta(X_3)}{dl_2}\right]l_2}{2\omega'_\theta(X_1)+\omega'_\theta(X_2)-\omega'_\theta(X_3)}\right\}\frac{\delta l_2}{l_2}.$$

The derivatives in these formulas can be computed by the following equations:

$$\frac{d\omega'_\theta(X)}{dr_2}=\frac{2\pi N_1N_2}{l_1l_2}kX\sqrt{\frac{r_2}{r_1}}\left[K+\frac{(r_1-r_2)}{(r_1+r_2)}\Pi\right]$$

$$\frac{d\omega'_\theta(X)}{dr_1}=\frac{2\pi N_1N_2}{l_1l_2}kX\sqrt{\frac{r_1}{r_2}}\left[K+\frac{(r_2-r_1)}{r_1+r_2}\Pi\right]$$

$$\frac{d\omega'_\theta(X)}{dl_1}=M\left[\frac{N_1N_2}{l_1l_2}\right]\frac{dX}{dl_1}-\frac{\omega'_\theta(X)}{l_1}$$

$$\frac{d\omega'_\theta(X)}{dl_2}=M\left[\frac{N_1N_2}{l_1l_2}\right]\frac{dX}{dl_2}-\frac{\omega'_\theta(X)}{l_2},$$

where M is the mutual inductance between coaxial circles of radii r_1 and r_2, the distance between their planes being X. Values of M are tabulated against k^2 in the tables of Nagaoka and Sakurai [14].

A summary of the computations applying these formulas to *H1* and *P1* is given in table 7. In these computations, the preliminary values of the measured dimensions were used. The variation formula was used to obtain the value of the force for unit current when accurate values of the dimensions were available.

TABLE 7.—*Summary of computations on force due to unit currents for the helices P1 and H1*

[The following values of the independent variables were used in the computation:

r_1=23.094 94 cm. l_1=27.516 62 cm. N_1=344 turns. $\alpha=\pi/2$.]
r_2=12.230 84 cm. l_2=2.665 06 cm. N_2=41 turns.

Quantities used in computing functions	Values of terms for—		
	For X_1=1.332 53	X_2=12.425 78	X_3=15.090 84
X^2	1.775 636	154.400 01	227.733 45
$X^2+(r_1+r_2)^2$	1249.686 37	1402.310 74	1475.644 18
k^2	0.904 132 50	0.805 728 74	0.765 687 34
k	.950 858 82	.897 623 94	.875 035 62
$1-k^2$	.095 867 50	.194 271 26	.234 312 66
$\sqrt{1-k^2}$	.309 624 78	.440 762 14	.484 058 53
$X\sqrt{X^2+(r_1+r_2)^2}$	47.106 139 3	465.313 647	579.701 25
K	2.597 967 32	2.270 422 8	2.185 608
$K-E$	1.496 593 8	1.095 811 7	0.984 537 6
$X(r_1-r_2)^2/\sqrt{X^2+(r_1+r_2)^2}$	4.449 016 20	39.164 179 8	46.367 118
$K-\Pi$	−8.986 943 02	−6.951 484 8	−6.469 126 7
$X\sqrt{X^2+(r_1+r_2)^2}(K-E)$	70.498 756	509.896 139	570.737 68
$\frac{X(r_1-r_2)^2}{\sqrt{X^2+(r_1+r_2)^2}}(K-\Pi)$	−39.983 055 1	−272.249 20	−299.954 76
Sum of the two preceding terms	30.515 700 9	237.646 939	270.782 92
$\omega'\theta(X)$	36,875.966	287,178.74	327,221.12
$\omega'_a(X,\alpha)$	−0.005 3	−0.013 4	−0.010 8
$\overline{\omega}'_X(X,\alpha)$	−.004 7	−.041 0	−.048 6

Principal term $[2\omega'_\theta(X_1)+\omega'_\theta(X_2)-\omega'_\theta(X_3)]$=33,709.55 dynes.
Azimuthal correction term $[2\omega'_a(X_1,\alpha)+\omega'_a(X_2,\alpha)-\omega'_a(X_3,\alpha)]$=−0.013.
Axial correction term $[2\overline{\omega}'_X(X_1,\alpha)+\overline{\omega}'_X(X_2,\alpha)-\overline{\omega}'_X(X_3,\alpha)]$=−0.002.
f=33709.54 dynes.
F_{HH}=1348.381 6 dynes.

The computations of the coefficients in the variation formula for these two helices gave the equation

$$\frac{\delta F_{HH}}{F_{HH}}=2.73\frac{\delta r_2}{r_2}-2.81\frac{\delta r_1}{r_1}+0.091\frac{\delta l_1}{l_1}-0.015\frac{\delta l_2}{l_2}.$$

The following adjustments for differences between the measured values of the dimensions and those used in the above computation were made:

$\delta r_1/r_1$=+21.6 ppm ..... δF=−0.0818 dyne.
$\delta r_2/r_2$=+31.1 ..... δF=+0.1145 dyne.
δl_1 and δl_2=0.

Hence for *H1* and *P1* at the dimensions of the coils corresponding to their mean temperatures during the observation of the force,

F_{HH}=1348.414 dynes.

2. THE FORCE BETWEEN A HELIX AND A SPIRAL

In an unpublished paper, Snow has developed a formula for the force produced by unit current in a helix and a spiral. The methods employed were similar to those used on other coil combinations [10, 15]. The coils were coaxial, as shown in figure 4.

The nomenclature used in the formula is:

a_1 = mean radius of fixed helix (same as r_1 in previous section).
a_2 = mean radius of moving spiral.
$2b_1$ = axial length of fixed helix (same as l_1 in previous section).
$2b_2$ = axial length of moving spiral.
$2c_2$ = radial depth of moving spiral.
N_1 = number of turns on fixed helix.
N_2 = number of turns on the moving spiral.

The force, f, for unit current in the moving coil, *A1*, and in either half of the single-layer solenoid, *H1*, is computed as the difference of the same function of two different lengths by the equation

$$f=\omega'(z_2)-\omega'(z_1),$$

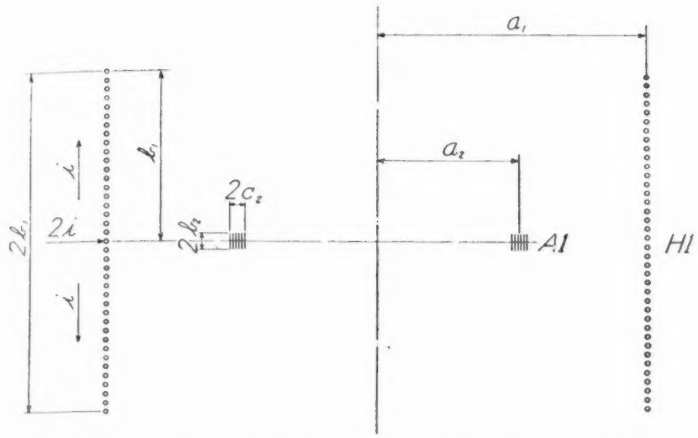

FIGURE 4.—*Section showing relative positions of helix H1 and spiral A1.*

where $z_1=b_1$ and $z_2=0$,

$$\omega'(z)=\frac{N_1N_2}{b_1}\left[\left[1+\frac{c_2^2}{12a_2^2}\right]M(z)\right.$$

$$+\frac{1}{12a_2^2}\left[\frac{F(z)}{z}\right]\left[A^2c_2^2(x^2+\beta)-2a_2^2(b_2^2-c_2^2)\lambda_1(x)\right]$$

$$+\frac{1}{360a_2^2}\left[\frac{F(z)}{z}\right]\left[c_2^2(5b_2^2-3c_2^2)\left\{\beta\left(\frac{2-2\lambda_1(x)-\lambda_2(x)}{x^2}\right)+2\lambda_1(x)-\lambda_2(x)\right\}\right.$$

$$\left.\left.-5b_2^2c_2^2\lambda_1(x)-\frac{a_2^2(3b_2^4-10b_2^2c_2^2+3c_2^4)}{A^2}\cdot\frac{\lambda_3(x)}{x^2}\right]\right].$$

The above formula was simplified by using the following:

$$k^2=4a_1a_2/[z_2+(a_1+a_2)^2]$$
$$A^2=a_1^2+a_2^2$$
$$x=z/A$$
$$\beta=(a_1^2-a_2^2)/(a_1^2+a_2^2)$$

$$\lambda_1(x)=-\frac{3x^4+2x^2-\beta^2+\dfrac{3x^3M(z)}{AF(z)}}{x^4+2x^2+\beta^2}$$

$$\lambda_2(x)=\frac{3\beta^2-2x^2+(5x^4+2x^2-3\beta^2)\lambda_1(x)}{x^4+2x^2+\beta^2}$$

$$\lambda_3(x)=\frac{4x^2-(25x^4+4x^2)\lambda_1(x)+(11x^4+10x^2-\beta^2)\lambda_2(x)}{x^4+2x^2+\beta^2}$$

$$M(z)=4\pi\sqrt{a_1a_2}\left[\frac{2(K-E)}{k}-kK\right]$$

$$\frac{F(z)}{z}=\frac{\pi k}{\sqrt{a_1a_2}}\left[\frac{(2-k^2)}{(1-k^2)}E-2K\right].$$

$M(z)$ is the mutual inductance of two circles whose radii are a_1 and a_2, the distance between their planes being z. $F(z)$ is the force between coaxial circles carrying unit current of radii a_1 and a_2, the distance between their planes being z. Note that

$$\left[\frac{F(z)}{z}\right] \text{ is not zero when } z=0.$$

Values of $F(z)/z$ can be taken from the tables of Nagaoka and Sakurai [14], but the values of $M(z)$ given in those tables may not be sufficiently precise. When necessary, $M(z)$ can be computed by the AGM method as outlined by King [16].

On substituting the two values of z in the above equation for $\omega'(z)$, the following form of the equation for f, suitable for computation purposes, is obtained.

$$\begin{aligned}
f=\frac{N_1N_2}{b_1}\Bigg\{&[M(0)-M(b_1)]\left[1+\frac{c_2^2}{12a_2^2}\right]\\
&+\frac{1}{12a_2^2}[A^2c_2^2\beta-2a_2^2(b_2^2-c_2^2)]\left[\frac{F(z)}{z}\right]_{z=0}\\
&-\frac{1}{12a_2^2}\frac{F(b_1)}{b_1}[A^2c_2^2(x_1^2+\beta)-2a_2^2(b_2^2-c_2^2)\lambda_1(x_1)]\\
&+\frac{1}{360a_2^2}\Bigg[c_2^2\frac{(5b_2^2-3c_2^2)}{\beta}\left\{(2\beta-4)\left[\frac{F(z)}{z}\right]_{z=0}-\frac{3M(0)}{A^2}\right\}\\
&\quad-5b_2^2c_2^2\left[\frac{F(z)}{z}\right]_{z=0}\\
&+\left\{3a_2^2\frac{(3b_2^4-10b_2^2c_2^2+3c_2^4)}{A^2\beta^2}\right\}\left\{4\left[\frac{F(z)}{z}\right]_{z=0}+3\frac{M(0)}{A^2}\right\}\Bigg]\\
&-\frac{1}{360a_2^2}\frac{F(b_1)}{b_1}\Bigg[c_2^2(5b_2^2-3c_2^2)\Bigg\{\beta\left[\frac{2-2\lambda_1(x_1)-\lambda_2(x_1)}{x_1^2}\right]\\
&\quad+2\lambda_1(x_1)-\lambda_2(x_1)\Bigg\}-5b_2^2c_2^2\lambda_1(x_1)-\frac{a_2^2(3b_2^4-10b_2^2c_2^2+3c_2^4)}{A^2x_1^2}\lambda_3(x_1)\Bigg]\Bigg\}
\end{aligned}$$

The formula gives the value of f for the moving spiral and one half of the fixed solenoid, if all the dimensions are measured in the same units and if the medium surrounding the coils has unit permeability. Since there are two fixed coils and since the current is reversed in the fixed coils, the computed force, F_{HS}, is four times f. If F_{HS} is expressed in dynes for an absolute ampere in each coil,

$$F_{HS}=\frac{4f}{100}.$$

The variation in F_{HS} with small variations in a_1, a_2, b_1, b_2, and c_2 is

$$\frac{\delta F_{HS}}{F_{HS}}=\left[1-\frac{b_1F(b_1)}{M(0)-M(b_1)}\right]\left[\frac{\delta a_1}{2a_1}+\frac{\delta a_2}{2a_2}-\frac{\delta b_1}{b_1}\right]$$

$$-\frac{(a_1^2-a_2^2)}{2}\left[\frac{\left[\frac{F(z)}{z}\right]_{z=0}-\frac{F(b_1)}{b_1}}{M(0)-M(b_1)}\right]\left[\frac{\delta a_1}{a_1}-\frac{\delta a_2}{a_2}\right]$$

$$+\frac{c_2^2}{3}\left\{\frac{1}{2a_2^2}+\frac{A^2}{2a_2^2}\left[\frac{\beta\left[\frac{F(z)}{z}\right]_{z=0}-(x_1^2+\beta)\frac{F(b_1)}{b_1}}{M(0)-M(b_1)}\right]\right.$$

$$\left.+\frac{\left[\frac{F(z)}{z}\right]_{z=0}-\lambda_1(x_1)\frac{F(b_1)}{b_1}}{M(0)-M(b_1)}\right\}\frac{\delta c_2}{c_2}$$

$$-\frac{b_2^2}{3}\left[\frac{\left[\frac{F(z)}{z}\right]_{z=0}-\lambda_1(x_1)\frac{F(b_1)}{b_1}}{M(0)-M(b_1)}\right]\frac{\delta b_2}{b_2}.$$

A summary of the computations for this coil combination is given in table 8.

TABLE 8.—*Summary of computations on force produced by unit currents in the helix, H1, and the spiral moving coil, A1,*

[The following constants of the coils were used in the computations:
a_1=23.095 53 cm. b_1=13.758 25 cm.
a_2=12.576 90 cm. b_2=0.3182 cm.
N_1=344 turns. c_2=0.3260 cm.]
N_2=45 turns.

Quantities used in computing ω functions	Values of terms	
	For z=0	For z=13.758 25
z^2	0	0. 273 705
k^2	0. 913 0533	. 794 8224
$M(z)$	153. 801 03	82. 257 44
$F(z)/z$	1. 477 238	0. 402 8606
$\lambda_0(z)$	1	−. 785 656
$\lambda_1(z)$	0	. 332 903
$\lambda_2(z)$	0	4. 924 10
1st term=$\left[1+\frac{c_2^2}{12a_2^2}\right]M(z)$	153. 809 64	82. 262 05
2d term	0. 032 272	0. 012 466
3d term	−. 000 016	. 000 002
Sum [1+2+3]	153. 841 90	82. 274 52
$\omega'(z)$	86 547. 07	46 285. 30

f=40261.77 dynes.
F_{HS}=1610.4708 dynes.

The computations of the coefficients in the variation formula for helix *H1* and spiral *A1* gave the equation

$$\frac{\delta F_{HS}}{F_{HS}}=2.78\frac{\delta a_2}{a_2}-2.85\frac{\delta a_1}{a_1}+0.066\frac{\delta b_1}{b_1}-0.00085\frac{\delta b_2}{b_2}+0.00151\frac{\delta c_2}{c_2}.$$

The following adjustments for differences between the measured values of the dimensions and those used in the above computation were made:

$\frac{\delta a_2}{a_2}$=27.8 ppm ..... δF_{HS}=0.1244 dyne.

In the computation the measured values were used for all the other dimensions. Hence for *H1* and *A1*,
F_{HS}=1610.595 dynes
for the dimensions of the coils corresponding to their mean temperatures during the observations of the force.

3. COMPUTATION OF THE ABSOLUTE VALUE OF THE CURRENT

The absolute value of the equivalent current, I_{eq} is computed by the formula $I^2_{eq}=mg/F$. In this formula m is the mass required to restore the equilibrium of the balance when the current is reversed in the fixed coil, g is the value of gravity, and F is the computed force in dynes for an absolute ampere in each coil. The value of the acceleration of gravity at the elevation of the balance has been taken as 980.095 cm/sec^2, as has been used in the earlier reports.

VI. EXPERIMENTAL DETERMINATION OF THE MAXIMUM FORCE BETWEEN THE COILS

The determination of the maximum force between the coils was made in practically the same manner as described in the previous reports. The fixed and moving coils were mounted with their axes vertical and with the center of the moving coil in the same horizontal plane as the center of the fixed coil. This same plane also contained the lead to the midpoint of the fixed coil. The planes of the ends of the coil forms were made horizontal by means of sensitive levels and leveling screws. In order to ascertain the correct position of the moving coil with respect to the fixed coil, a series of force measurements was made with a constant current in the coils. The series consisted of measurements with the moving coil at different positions along each of three perpendicular axes, one of which was vertical. The measured force, when plotted as a function of the position of the moving coil along each of the axes, had a maximum value at the correct position on the vertical axis and a minimum value at the correct position on each of the horizontal axes. The moving coil was concentric with the fixed helix when it was at the position of maximum force for vertical adjustments and at the position of minimum force for horizontal adjustments. When the coils were set to the correct positions for all adjustments, the force was measured carefully and at the same time the equivalent current was measured in terms of the NBS International ampere, as described in section IV. From the measured force and the dimensions of the coils, the value of the current was computed in absolute amperes, as outlined in section V. The ratio of these two values for the same current gave the inverse ratio of the two units of current.

As an additional check on the vertical position of the moving coil, measurements of the force were taken when the current in both halves of the fixed helix were in the same direction—that is, when there was no current in the center lead of the fixed helix. Under this condition there was no force on the moving coil when it was midway between the two ends of the fixed helix, but there was a force, either positive or negative, when the moving coil was displaced up or down from the midpoint of the fixed helix. The graph showing the measured force plotted against the vertical displacement of the moving coil was a straight line. From this line, the position of the moving coil at which the force on it was zero was determined. Experimentally, this position was found to be the same as the position for maximum force when the currents in the two halves of the helix were in opposite directions. This was expected, since both methods indicate the position at which coils are concentric. However, the method using the currents in the same direction located the concentric position more accurately than could be done when using the currents in opposite directions.

The effect of the leads was measured by short-circuiting the twisted lead-in wires as near to the coil windings as possible and measuring the force with normal current in the other coil and in the leads of the coil in question. This force was added to or subtracted from the total force measured to get the true force. A small residual effect might still remain, caused by the fact that a long helix has to have a long axial return for the leads. This was made negligibly small by keeping these return leads in a vertical plane, and by keeping the area of the loop formed by the leads small. The lead residual effect was a function of the projected area of this loop area on a horizontal plane, so that it was not difficult to keep the effect of the loop below 1 ppm.

The force was measured as in the previous work by observing the change in the rest point of the balance when the current in the fixed coils was reversed and the weight added (or removed). One person observed and recorded the swings of the balance and another regulated the currents. A series of turning points (usually five) was used to determine the rest point of the balance. Then the current in the fixed coils was reversed, the weight changed, and the rest point was again determined. A series of at least five of these rest points was obtained in determining the mass required to compensate the electromagnetic force under any given set of conditions. The difference in the rest points for the "on" and "off" positions of the weight multiplied by the sensitivity of the balance gave the amount to be added to (or subtracted from) the mass of the weight to give the mass required to balance the electromagnetic force on the moving coil.

The accuracy of the measurement of the force was limited by the irregular oscillations of the balance. The principal cause of these irregularities was the heating produced by the electric currents in the fixed and moving coils. Water cooling was not feasible even for the fixed coils, so that all the heat had to be dissipated into the air. With normal currents the coils generated heat at the rate of about 25 watts for the fixed coil and 2 or 3 watts for the moving coils. If allowed to come to equilibrium, the air in the closed coil case was heated about 3° C above the room temperature when the coils were 9° or 10° C above room temperature. Under such conditions the swings of the balance were somewhat erratic. However, when the coil case was ventilated by small openings at the top and bottom, or by drawing air from the top of the coil case with a fan, the temperature of the air in the coil case was the same as that of the room and and the coil temperatures were 6° or 7° C above room temperature. The swings of the balance became more regular after the ventilating system was installed. All of the final results were taken with either the natural or artificial ventilation of the coil case.

The interior of the fixed coil formed a chimney through which flowed the air that both cooled and disturbed the moving coil. In an attempt to streamline the air flow through the chimney and around the moving coil, a honeycomb made of small tubes was placed in the chimney directly under the moving coil. Some improvement in the operation of the balance was noted after the installation of the honeycomb so that it was used when the final observations were made.

After the coils were adjusted to be coaxial and concentric, about 10 determinations of the force were made with the same currents and with the coils at nearly constant temperatures. The conditions were

sufficiently constant so that average values of temperature and force could be taken for the whole set and the computation made for this average condition. The mechanical measurements of the dimensions of the coils were made after the force measurements. In order to reduce the uncertainty caused by temperature corrections, one set of the mechanical measurements was carried out while each coil was held at a temperature approximately the same as the average temperature it attained in the current balance.

Tables 9 and 10 contain a summary of all the sets of observations which were taken after the coils were adjusted to their correct positions, and after the erratic oscillations of the balance had been minimized. From these the final average result for each set of coils is obtained. This computation is outlined in table 11.

TABLE 9.—*Results of measurements of force with helices H1 and P1*

[Note: δ=average difference in scale reading of rest points of the balance corresponding to "on" and "off" positions of weight. Sensitivity of balance: 1.21 mg per cm. Mass of weight (a platinum cylinder): 1.427 655 grams]

Date 1940	Temperature					Difference in rest points=δ
	Room	Coil case	*P1*	*H1*		
				Upper half	Lower half	
	°C	°C	°C	°C	°C	cm
May 2	22.5	22.2	29.24	29.06	28.01	0.19
9	24.2	23.8	31.08	31.51	30.13	.20
9	23.7	23.8	30.99	31.06	29.76	.22
10	23.8	23.8	30.88	30.70	29.51	.18
10	23.8	23.8	30.67	30.68	29.49	.18
11	23.7	23.5	30.31	30.29	29.21	.14
14	23.4	23.3	30.25	30.05	29.00	.21
15	23.5	23.3	30.24	30.13	29.05	.19
16	24.C	24.8	31.90	32.57	31.25	.19
16	24.4	24.6	31.76	32.13	30.81	.20
17	23.6	23.8	30.68	30.74	29.58	.20
Average			30.77	30.81	29.62	0.19 ±0.005
				30.22° C		

Average δ × sensitivity of balance = 0.231 ±0.006 mg.

TABLE 10.—*Results of measurements of force with coils H1 and A1*

[Note: δ is the average difference in scale reading of the rest points of the balance corresponding to "on" and "off" positions of weight. Sensitivity of balance: 1.17 mg per cm. Mass of weight (a platinum cylinder): 1.705316 grams]

Date 1940	Temperature					Difference in rest points=δ	
	Room	Coil case	*A1*	*H1*		Observed	Corrected for departure of *A1* from 29.94° C
				Upper half	Lower half		
	°C	°C	°C	°C	°C	cm	cm
June 15	25.1	25.2	30.08	31.90	31.00	0.09	0.07_9
17	25.3	25.4	30.26	32.04	31.14	.11	$.08_4$
17	25.4	25.5	30.37	32.19	31.31	.06	$.02_4$
18	25.4	25.5	30.42	32.22	31.34	.11	$.07_9$
18	25.3	25.5	30.42	32.24	31.35	.09	$.05_9$
25	24.2	24.5	29.41	31.16	30.32	−.01	$.03_4$
25	24.2	24.6	29.50	31.27	30.42	.03	$.06_9$
26	24.4	24.7	29.68	31.43	30.56	.02	$.04_4$
27	24.5	24.7	29.66	31.47	30.60	.03	$.05_5$
27	24.5	24.7	29.70	31.48	30.62	.07	$.09_1$
Average			29.94	31.74	30.87	0.06$_9$	0.06_6 ±0.005
				31.30			

Average δ × sensitivity of balance = 0.072 ±0.006 mg.

TABLE 11.—*Calculation of final results*

[Value of acceleration of gravity 980.095 cm/sec.²]

	P1, H1	*A1, H1*
Mass of weight.....g	1.427 655	1.705 316
Buoyancy correction	−.000 077	−.000 092
Lead correction:		
Moving coil	−.000 068	+.000 008
Fixed coil	−.000 018	−.000 021
½×sensitivity of balance (from tables 9 and 10)	+.000 231	+.000 072
Net compensating mass.....g	1.427 723	1.705 283
Measured electromagnetic force (compensating mass×gravity).....dynes	1399.304	1671.339
Calculated force for unit current for average temperatures involved (from tables 7 and 8).....dynes	1348.414	1610.595
Equivalent current in absolute amperes $=\sqrt{\frac{\text{measured force}}{\text{calculated force}}}$	1.018 696	1.018 683
Emf of standard cell....NBS International volts (average during time of runs)	1.018 366	1.018 360
Resistance of standard resistor *R1*.....NBS International ohms	0.999 531	0.999 531
Resistance of standard resistor *R2*.....NBS International ohms	.999 527	.999 527
Equivalent current.....NBS International amperes	1.018 847	1.018 841
Ratio of equivalent currents I_{ABS}/I_{NBS}	0.999 851	0.999 845

VII. DISCUSSION OF RESULTS

The ratio of the value of a current in absolute amperes to its value in NBS International amperes, as obtained from measurements with the helix *H1* as the fixed coils of the current balance, is the average of the two ratios given at the end of table 11. This average ratio is

1 NBS International ampere=0.999 848 absolute ampere.

In the previous investigations the sources of error have been discussed in detail [2,8]. In general the same discussion applies to this determination. However, several of the larger sources of error have been reduced in size. Table 12 gives the errors that are estimated to be as large as 1 part in a million. The uncertainty appears to be about 10 parts in a million for the results involving *A1* and somewhat less for the results with *P1*. This does not include the uncertainty in the value of gravity, which may be as large as 10 ppm.

TABLE 12.—*Sources of error causing an uncertainty in ratio I_{NBS}/I_{ABS} as large as 1 ppm*

	Fixed coil *H1*			Fixed coil *H1*	
	Moving coil *P1*	Moving coil *A1*		Moving coil *P1*	Moving coil *A1*
	ppm	*ppm*		*ppm*	*ppm*
Adjustment of coils	1	1	Finite cross section of moving coil		3
Temperature of coils	1	1	Distribution of current over cross section of wire	1	1
Measurement of the force	2	2	Calibration of standard of mass	2	2
Lead corrections	2	2	Acceleration of gravity	10	10
Radius of the fixed coil	1	1			
Radius of the moving coil	1	3			

The result of this determination differs by 14 parts in a million from the weighted mean as published in 1939 [2]. That weighted mean included some results taken with the older type multilayer wire-

wound coils. Since the position of the wires in those coils was uncertain, the uncertainty in the distribution of current over the cross section of the coils introduced an uncertainty in the absolute value of the current. Since the results obtained when using the two types of improved coils agree among themselves but differ considerably from the average of the diverse results obtained with the multilayer wire-wound coils, the values based on the work with helical and spirally wound coils are the only ones that are included in the final résumé. All the results in which only the spiral and helical coils were used are summarized in table 13.

TABLE 13.—*Summary of the results with spiral and helical coils*

Fixed coils		Moving coil		Ratio of the value of a current in absolute amperes to its value in NBS International amperes	Deviation from mean
Designation	Type	Designation	Type		
					ppm
B1, B2	Spiral of aluminum ribbon on aluminum form	*A1*	Aluminum ribbon	0.999 853[a]	−3
		P1	Copper wire	.999 851[a]	−1
H1	Helix of copper wire on glass form	*A1*	Aluminum ribbon	.999 845	+5
		P1	Copper wire	.999 851	+1
Average				0.999 850	±3

[a] These values were taken from the preceding paper [2].

The determinations given in table 13 with the two different types of fixed coils are nearly independent. In the determination with the fixed coils, *B1* and *B2*, the ratio of radii of each moving coil to each fixed coil was individually determined by an electrical method. From these data, the ratio of the radii of the moving coils, *A1* and *P1*, was obtained. This ratio was used to obtain the radius of *A1* from the measured radius of *P1*. Hence only the one result obtained when using *H1* and *P1* was entirely independent of the electrical method of measuring the ratio of the radii.

The authors are of the opinion that the best value of the ratio of the units of current as the result of the work at the National Bureau of Standards is

1 NBS International ampere = 0.999 850 absolute ampere.

The authors acknowledge assistance from many members of the staff of the National Bureau of Standards and in particular from H. L. Curtis, C. Snow, and C. Moon.

VIII. REFERENCES

[1] P. Vigoureux, *An absolute determination of the ampere*, Roy. Soc. Phil. Trans. (London) **236A,** 133 (1936).

[2] H. L. Curtis, R. W. Curtis, and C. L. Critchfield, *An absolute determination of the ampere, using improved coils*, J. Research NBS **22,** 485 (1939) RP1200.

[3] H. L. Curtis, C. Moon, and C. M. Sparks, *An absolute determination of the ohm*, J. Research NBS **16,** 1 (1936) RP857.

[4] H. L. Curtis, C. Moon, and C. M. Sparks, *A determination of the absolute ohm, using an improved self inductor*, J. Research NBS **21,** 375 (1938) RP1137.

[5] C. Moon, *Apparatus for comparison of length of gages*, BS J. Research **10,** 249 (1933) RP528.
[6] C. G. Peters and C. H. Cragoe, *Measurements on the thermal dilatation of glass at high temperatures*, Sci. Papers BS **16,** 449 (1920) S393.
[7] C. Moon, *A precision cathetometer*, J. Research NBS **14,** 363 (1935) RP774.
[8] H. L. Curtis and R. W. Curtis, *An absolute determination of the ampere*, BS J. Research **12,** 665 (1934) RP685.
[9] H. L. Curtis, Electrical Measurements (McGraw-Hill Book Co., New York, N. Y., 1937).
[10] C. Snow, *Mutual inductance and force between two coaxial helical wires*, J. Research NBS **22,** 239 (1939) RP1178.
[11] L. V. King, On the Direct Numerical Calculation of Elliptic Functions and Integrals (Cambridge University Press 1924).
[12] F. W. Grover, *On the use of arithmetico-geometric mean series for the calculation of elliptic integrals, with special reference to the calculation of induction*, Phil. Mag. [7] **15,** 1115 (1933).
[13] H. Nagaoka and S. Sakurai, The Tables of the Elliptic Integrals K and E, Sci. Papers Inst. Phys. Chem. Research (Table No. 1), Tokyo (1922).
[14] H. Nagaoka and S. Sakurai, Tables for Facilitating the Calculation of Self-Inductance of Circular Coil and of Mutual Inductance of Coaxial Circular Currents. Sci. Papers Inst. Phys. Chem. Research (Table No. 2), Tokyo (1927).
[15] C. Snow, *The attraction between coils in the Rayleigh current balance*, BS J. Research **11,** 681 (1933) RP615.
[16] L. V. King, *On some new formulae for the numerical calculation of the mutual induction of coaxial circles*, Proc. Roy. Soc. (London) **[A], 100,** 60 (1921).

WASHINGTON, February 21, 1941.

U. S. Department of Commerce National Bureau of Standards

RESEARCH PAPER RP1450

Part of Journal of Research of the National Bureau of Standards, Volume 28, February 1942

RECTANGULAR PLATE LOADED ALONG TWO ADJACENT EDGES BY COUPLES IN ITS OWN PLANE

By William R. Osgood

ABSTRACT

A. and L. Föppl give an approximate solution for the stresses in the rectangular knee of an L-shaped plate loaded by couples acting on the legs in the plane of the plate. A solution is presented here that is exact in the sense that the equations of equilibrium and the condition of compatibility (for two-dimensional systems) are satisfied at every point. Small self-equilibrated stresses remain along the free edges of the knee.

The stresses in the knees of rigid frames are of considerable interest to engineers, and theoretical analyses, as well as experimental results, may be worth while. Such an analysis for the rectangular knee of a rigid frame has appeared recently.[1] Part of the analysis involves the stresses produced in the knee by couples acting on the legs in the plane of the rigid frame. The solution used for this condition of loading was not derived in the paper presenting it; and since it appears to be new and not quite obvious, the derivation is presented here for the essentially similar but simpler, special case of a rigid frame without flanges, that is, an L-shaped plate.

Figure 1 illustrates the problem. The linear distribution of stress of the ordinary flexure formula is assumed to apply in the legs at a distance from the knee. At the sharp reentrant corner the stress must become infinite, according to the theory of elasticity, so that the distribution along the inner edges of the knee, shown dotted in the figure, is, according to this theory, probably somewhere between a logarithmic distribution, such as is characteristic of a curved beam, and the linear distribution of a straight beam. Since in practice the theoretically infinite stresses at the corner would be reduced by plastic flow, the final distribution of stress would be represented by a curve with finite ordinates everywhere. In the present paper it is assumed that this distribution can be approximated by a nearly linear distribution, and a polynomial solution is obtained for the stresses in the knee which satisfies the equations of equilibrium and the condition of compatibility (for two-dimensional systems). There is some experimental evidence[2] that the assumption of a linear distribution is practically justifiable, at least in a rigid frame with flanges running through along the dotted lines in figure 1. The stresses in the web of the knee are almost surely not appreciably affected by the exact manner of distribution at the junctions between knee and legs. For

[1] W. R. Osgood, *Stresses in a rectangular knee of a rigid frame*, J. Research NBS **27**, 443 (1941) RP1431.
[2] A. H. Stang, Martin Greenspan, and W. R. Osgood, *Strength of a riveted steel rigid frame having straight flanges*, J. Research NBS **21**, 269 (1938) RP1130.

practical purposes of design and analysis of the knee, therefore, the assumption of a nearly linear distribution of stress along the inner edges of the knee, the junctions between knee and legs, seems sufficiently accurate.

A. and L. Föppl [3] give a solution for the knee in which they assume a strictly linear distribution along the inner edges. Their solution

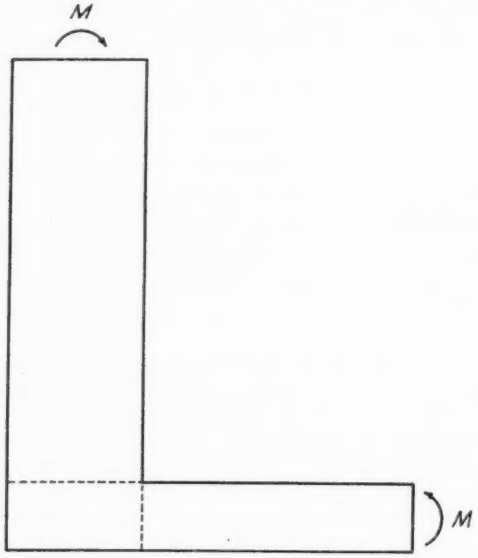

FIGURE 1.—L-*shaped plate loaded by couples.*

satisfies the boundary conditions and the equations of equilibrium at every point, but it does not satisfy the condition of compatibility. The solution proposed here may be built up by judiciously superposing known solutions for cantilever beams. The equations of equilibrium

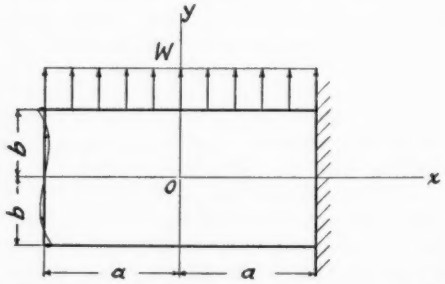

FIGURE 2.—*Cantilevered plate acted on by uniformly distributed load.*

and the condition of compatibility are satisfied at every point, but small self-equilibrated stresses remain on the outer edges of the knee. Since these boundary stresses are relatively small and their effect can be readily judged, it seems preferable to sacrifice the boundary conditions rather than the condition of compatibility, the consequences of

[3] Drang und Zwang **1**, 340 (1924).

the latter sacrifice not being so readily apparent. (Rather large self-equilibrated stresses do in fact occur. See footnote 2.)

We proceed now to the proposed solution. The solution for the uniformly loaded cantilever beam or cantilevered plate of thickness t shown in figure 2 is [4]

$$\left.\begin{aligned}\sigma_x&=-\frac{3Wa}{8b^2t}\left(1+\frac{x}{a}\right)^2\frac{y}{b}-\frac{W}{4at}\frac{y}{b}\left(\frac{3}{5}-\frac{y^2}{b^2}\right),\\ \sigma_y&=\frac{W}{4at}\left(1-\frac{y}{2b}\right)\left(1+\frac{y}{b}\right)^2,\\ \tau_{xy}&=-\frac{3W}{8bt}\left(1+\frac{x}{a}\right)\left(1-\frac{y^2}{b^2}\right).\end{aligned}\right\}\tag{1}$$

The solution for the cantilevered plate of thickness t carrying a uniformly varying total load W as shown in figure 3 is [5]

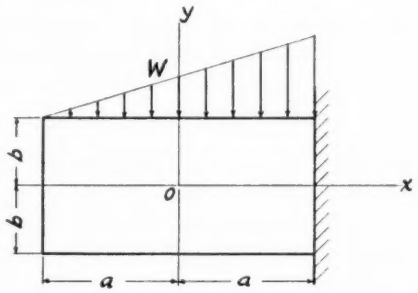

FIGURE 3.—*Cantilevered plate acted on by uniformly varying load.*

$$\left.\begin{aligned}\sigma_x&=\frac{Wa}{8b^2t}\left(1+\frac{x}{a}\right)^3\frac{y}{b}+\frac{W}{4at}\left(1+\frac{x}{a}\right)\frac{y}{b}\left(\frac{3}{5}-\frac{y^2}{b^2}\right),\\ \sigma_y&=-\frac{W}{4at}\left(1+\frac{x}{a}\right)\left(1-\frac{y}{2b}\right)\left(1+\frac{y}{b}\right)^2,\\ \tau_{xy}&=\frac{3W}{16bt}\left(1+\frac{x}{a}\right)^2\left(1-\frac{y^2}{b^2}\right)+\frac{Wb}{16a^2t}\left(\frac{1}{5}-\frac{y^2}{b^2}\right)\left(\frac{1}{5}-\frac{y^2}{b^2}\right).\end{aligned}\right\}\tag{2}$$

If we superpose these two solutions, we obtain the solution for a plate loaded by couples $M=Wa/3$ on the two edges $x=a$ and $y=b$, figure 4:

$$\left.\begin{aligned}\sigma_x&=-\frac{3M}{4b^2t}\left(1+\frac{x}{a}\right)^2\left(1-\frac{x}{2a}\right)\frac{y}{b}+\frac{3M}{4a^2t}\frac{x}{a}\frac{y}{b}\left(\frac{3}{5}-\frac{y^2}{b^2}\right),\\ \sigma_y&=-\frac{3M}{4a^2t}\frac{x}{a}\left(1+\frac{y}{b}\right)^2\left(1-\frac{y}{2b}\right),\\ \tau_{xy}&=-\frac{9M}{16abt}\left(1-\frac{x^2}{a^2}\right)\left(1-\frac{y^2}{b^2}\right)+\frac{3Mb}{16a^3t}\left(1-\frac{y^2}{b^2}\right)\left(\frac{1}{5}-\frac{y^2}{b^2}\right).\end{aligned}\right\}\tag{3}$$

Along the edge $y=b$ the forces are uniformly varying but not along the edge $x=a$. This "unsymmetrical" condition is not of much

[4] R. V. Southwell, Theory of Elasticity, p. 377 (1936).
[5] S. Timoshenko, Theory of Elasticity, p. 42 (1934).

interest. Moreover, for large values of b/a the self-equilibrated normal stresses (second term on right-hand side of expression for σ_x) at $x=-a$ become relatively large. These objections may be overcome

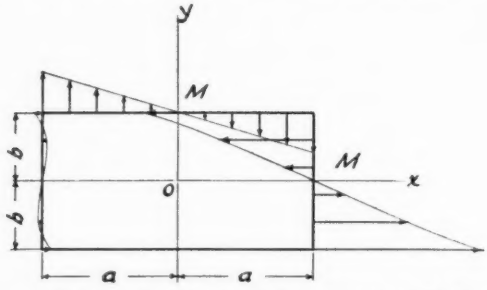

FIGURE 4.—*Rectangular plate loaded unsymmetrically by couples.*

as follows. We write first the solution for a uniformly varying load along the edge $x=a$ by interchanging x and y and a and b in solution 3:

$$\left.\begin{aligned}
\sigma_x &= -\frac{3M}{4b^2t}\left(1+\frac{x}{a}\right)^2\left(1-\frac{x}{2a}\right)\frac{y}{b},\\
\sigma_y &= -\frac{3M}{4a^2t}\,\frac{x}{a}\left(1+\frac{y}{b}\right)^2\left(1-\frac{y}{2b}\right)+\frac{3M}{4b^2t}\,\frac{x}{a}\,\frac{y}{b}\left(\frac{3}{5}-\frac{x^2}{a^2}\right),\\
\tau_{xy} &= -\frac{9M}{16abt}\left(1-\frac{x^2}{a^2}\right)\left(1-\frac{y^2}{b^2}\right)+\frac{3Ma}{16b^3t}\left(1-\frac{x^2}{a^2}\right)\left(\frac{1}{5}-\frac{x^2}{a^2}\right),
\end{aligned}\right\} \tag{4}$$

Now if we replace M by αM in solution 3 and M by $(1-\alpha)M$ in solution 4 and then superpose these two solutions, we obtain another solution for a plate loaded by couples M on adjacent edges; and by varying α the distribution of the loads may be made to vary between that required by solution 3 and that required by solution 4:

$$\left.\begin{aligned}
\sigma_x &= -\frac{3M}{4b^2t}\left(1+\frac{x}{a}\right)^2\left(1-\frac{x}{2a}\right)\frac{y}{b}+\frac{3\alpha M}{4a^2t}\,\frac{x}{a}\,\frac{y}{b}\left(\frac{3}{5}-\frac{y^2}{b^2}\right),\\
\sigma_y &= -\frac{3M}{4a^2t}\,\frac{x}{a}\left(1+\frac{y}{b}\right)^2\left(1-\frac{y}{2b}\right)+\frac{3(1-\alpha)M}{4b^2t}\,\frac{x}{a}\,\frac{y}{b}\left(\frac{3}{5}-\frac{x^2}{a^2}\right),\\
\tau_{xy} &= -\frac{9M}{16abt}\left(1-\frac{x^2}{a^2}\right)\left(1-\frac{y^2}{b^2}\right)+\frac{3M}{16t}\left[\frac{\alpha b}{a^3}\left(1-\frac{y^2}{b^2}\right)\left(\frac{1}{5}-\frac{y^2}{b^2}\right)\right.\\
&\quad\left.+\frac{(1-\alpha)a}{b^3}\left(1-\frac{x^2}{a^2}\right)\left(\frac{1}{5}-\frac{x^2}{a^2}\right)\right].
\end{aligned}\right\} \tag{5}$$

If we wish to keep the ratio of the self-equilibrated normal stress to the remaining normal stress the same for equal values of x/a and y/b, inspection of the first two of eq 5 shows that we must have

$$\frac{b^2\alpha}{a^2}=\frac{(1-\alpha)a^2}{b^2}$$

or

$$\alpha=\frac{a^4}{a^4+b^4}.$$

With this value of α eq 5 become

$$\left.\begin{aligned}
\sigma_x &= -\frac{3M}{4b^2t}\left(1+\frac{x}{a}\right)^2\left(1-\frac{x}{2a}\right)\frac{y}{b}+\frac{3Ma^2}{4(a^4+b^4)t}\frac{x}{a}\frac{y}{b}\left(\frac{3}{5}-\frac{y^2}{b^2}\right),\\
\sigma_y &= -\frac{3M}{4a^2t}\frac{x}{a}\left(1+\frac{y}{b}\right)^2\left(1-\frac{y}{2b}\right)+\frac{3Mb^2}{4(a^4+b^4)t}\frac{x}{a}\frac{y}{b}\left(\frac{3}{5}-\frac{x^2}{a^2}\right),\\
\tau_{xy} &= -\frac{9M}{16abt}\left(1-\frac{x^2}{a^2}\right)\left(1-\frac{y^2}{b^2}\right)\\
&\quad +\frac{3Mab}{16(a^4+b^4)t}\left[\left(1-\frac{x^2}{a^2}\right)\left(\frac{1}{5}-\frac{x^2}{a^2}\right)+\left(1-\frac{y^2}{b^2}\right)\left(\frac{1}{5}-\frac{y^2}{b^2}\right)\right].
\end{aligned}\right\} \quad (6)$$

This solution is symmetrical, and the self-equilibrated stresses, represented by the second of each of the two terms on the right-

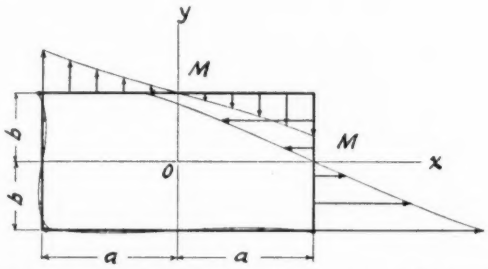

FIGURE 5.—*Rectangular plate loaded symmetrically by couples.*

hand sides, can never become excessive. At $x=a$, $y=b$, for example, the second term of σ_x or of σ_y is equal to $a^2b^2/[5(a^4+b^4)]$ times the first term. The maximum value this fraction can have is 1/10, when $a=b$. Figure 5 shows the distribution of stress along the boundary for $a/b=2$. The self-equilibrated shearing stresses are too small to appear in the drawing.

WASHINGTON, September 17, 1941.

435456—42——3

U. S. DEPARTMENT OF COMMERCE NATIONAL BUREAU OF STANDARDS

RESEARCH PAPER RP1451

Part of Journal of Research of the National Bureau of Standards, Volume 28, February 1942

SPARK SPECTROGRAPHIC ANALYSIS OF COMMERCIAL TIN[1]

By Bourdon F. Scribner

ABSTRACT

A procedure is described in detail for the simultaneous spectrographic determination of antimony, arsenic, bismuth, cadmium, copper, indium, iron, lead, silver, and zinc in tin metal of commercial grades. The preparation of standards and samples by chill-casting of tin in open molds and in evacuated tubes is described. The use of a press is found convenient in forming electrodes from tin metal. The characteristics of the tin spark under varied operating conditions are discussed in connection with the selection of optimum conditions of excitation. Application of the step sector provides a means of extending the range of line intensity measurements with the microphotometer as well as for plate calibration. Rapid reduction of the photometric measurements to intensities is made by a modified graphical calculator. The shapes of the analytical curves derived from measurements on tin standards are compared, and deviations from the ideal case are discussed. Repeated determinations on homogeneous samples show a standard deviation of from 1.0 to 2.5 percent. Single determinations in routine analysis are estimated to fall within 5 percent of the actual concentration, with few exceptions. The analyses are carried out on groups of six samples in a working time of 5 minutes per determination.

CONTENTS

	Page
I. Introduction	165
II. Preparation of samples and standards	168
1. Sample rods formed by melting or pressing	168
2. Chemically analyzed standards	169
3. Standards synthesized by vacuum melting	170
III. Spark excitation of tin	172
1. Types of spark sources employed	172
2. Effects of operating conditions	173
3. Characteristics of the spark adopted	175
IV. Analytical procedure	177
1. The spectrograph and its illumination	177
2. Choice of spectral lines for analysis	178
3. Photometric measurements	179
4. Analytical curves	182
V. Discussion	185
1. Precision and accuracy	185
2. Advantages and limitations of the method	188
VI. References	189

I. INTRODUCTION

The National Bureau of Standards has been assigned the responsibility for testing a number of products of tin metal for conformity with Federal and departmental specifications of composition. Of major importance is the determination of impurities in fusible plugs

[1] Presented at the Ninth Summer Conference on Spectroscopy and Its Applications at Massachusetts Institute of Technology, Cambridge, Mass., July 21–23, 1941.

employed as safety devices for boiler protection; other materials examined include tin pipe and tin linings of pipes and fittings, as well as samples of pig tin purchased by the Government. The problems presented by the analysis of tin have proved tedious and time-consuming for application of the usual wet-chemical methods, primarily because of the low concentrations of impurities involved, usually below 1 percent. For reasonable accuracy, the analyst requires rather large samples and must exercise painstaking care in the analytical operations.

The possibility that the spectrographic method of analysis might relieve the chemist of labor was recognized as early as 1922 by Meggers, Kiess, and Stimson [1],[2] of this Bureau, who described a method for estimating the impurities in fusible plugs. The method provided for visual comparison of the photographed spectral lines from the sample under test with the lines from samples of graded known composition. In the years intervening since the publication of this pioneer paper, a number of contributions have appeared in the literature on various aspects of the spectrographic analysis of tin. Gerlach [2] showed that the effects of variations in spectral exposure and in photography could be largely eliminated by referring the intensity of the impurity line to a neighboring line of the major constituent as standard. This principle, now known as internal control, was embodied in the method of homologous pairs applied to the analysis of tin by Negresco [3], Schweitzer [4], Gerlach [5], and Smith [6, 7]. Quantitative estimations were based upon observation of pairs of impurity and control lines. Each selected pair at equality of intensity could be relied upon to represent a definite concentration. The method is undoubtedly useful where photometric measurements are not made, but it is subject to the inconveniences and uncertainties of interpolation, especially when the available number of pairs of matching lines is small.

A distinct advantage resulted from application of the rotating logarithmic spiral sector to the comparison of line intensities in the analysis of tin. This method, in which the length of the wedge-shaped line image serves as a measure of the line intensity, was applied by Töpelmann and Shuhknecht [8] to the determination of lead in concentrations as high as 3 percent in tin. Hitchen [9] describes the determination by this method of antimony, arsenic, bismuth, copper, iron, lead, and zinc in tin, with deviations seldom exceeding 5 percent. This paper is especially recommended for its thorough discussions of line selection and of sampling problems. A recent paper by Stewart [10] describes a similar method for determining antimony, bismuth, copper, iron, and lead in commercial tin.

The development of the microphotometer and its use in spectrographic analyses provides a truly objective method of measuring relative spectral line intensities. The earliest mention of microphotometric measurements in tin analysis is found in a paper by Scheibe, Linström, and Schnettler [11], who describe the determination of lead in concentrations up to 9 percent. Follet [12] employed the microphotometer combined with a stepped wedge to provide calibration of the photographic plate and illustrated this procedure by the determination of lead in tin. In the range from 0.02 to 0.6 percent of lead, the probable error was reported to be ± 1.5 percent for a single determination.

[1] Figures in brackets indicate the literature references at the end of this paper.

All of the investigations mentioned have favored the excitation of the tin spectrum by the condensed spark discharge. The arc, however, has been employed by Smith [6], by Hitchen [9], by Breckpot [13], and undoubtedly by many others who have found it satisfactory for qualitative analysis and for quantitative estimation particularly in the range of low concentrations of impurities. Where both arc and spark excitation have been available, the spark has generally been found more reproducible and convenient.

At this Bureau an increasing burden of routine testing in the chemical laboratory led to renewed interest in the spectrographic method. A procedure was developed whereby the required determinations of impurities in tin could be made with a considerable saving in time and labor and with the requisite accuracy. The specifications under which the tin is tested are given in table 1; these are fixed mostly by the requirement for metal of high purity in many of the uses of tin. For example, impurities in fusible plugs may cause an increase in the melting point beyond the limit of safety protection of boilers [14]. Zinc is especially effective in raising the melting point of the plug in service, apparently by formation of a network of zinc oxide in the tin matrix. Tin piping for distilled-water lines must be free of impurities which might be absorbed by the water; a minimum concentration of lead is specified here because of the numerous chemical determinations of this element, in which contamination by lead must be avoided. The specifications call for the determination of a number of elements either explicitly, as in the case of Federal Specification QQ–T–371, or inferred in other cases where the minimum limit for tin involves the determination of the total of impurities. The major impurities encountered are copper, lead, arsenic, and antimony. In fusible plugs, copper and lead have been observed as high as 2 percent each. Other elements are generally below 0.1 percent. The analytical problem therefore involves both the requirement for the precise determination of the major impurities and the requirement for a degree of sensitivity sufficient to permit certain determinations as low as 0.01 percent or less. In addition to achieving the desired accuracy and sensitivity, it was proposed to simplify the manipulations, as far as possible, to realize the potential advantages of speed and convenience in the spectrographic method.

TABLE 1.—*Specifications for metallic tin*

Source of specification	Material	Sn, min	Pb, max	Sb, max	Zn, max	Cd, max	As, max	Cu, max	S, max	Fe, max	Bi, max
		%	%	%	%	%	%	%	%	%	%
Federal Government QQ-T-371.	Pig tin, grade *A*.	99.75	0.10	0.10	None[1]	None[1]	0.10	0.10	0.01	0.01	0.01
Federal Government QQ-T-371.	Pig tin, grade *B*.	98.00	1.50	1.50	do.[1]	do.[1]	.10	.10	.01	.10	.10
U. S. Department of Commerce, Bureau of Marine Inspection and Navigation.	Fusible safety plugs.	99.3	.10	.....	0.10	.....	.....	.50	.....	.....	.....
U. S. Department of Commerce, National Bureau of Standards.	Block tin pipe.	99.9	.03	.....	.....	.....	.....	.....	.....	.....	.....
U. S. Department of Agriculture, Bureau of Agricultural Chemistry and Engineering.	Linings of pipes and fittings.	99.9	.09	.....	.....	.....	.....	.....	.....	.....	.....

[1] "As determined on a 20-g sample." It is assumed that this is equivalent to less than 0.01 percent.

The author, surveying methods of comparing spectral line intensities [15], described preliminary results on the use of the step sector and plate calibration for the determination of copper in fusible tin plugs. This method has now been extended to cover the analytical requirements of the specifications outlined above except for the determination of sulfur. The measurement of a single spectral exposure suffices in most cases for the determination of 10 elements in tin—namely, antimony, arsenic, bismuth, cadmium, copper, indium, iron, lead, silver, and zinc. Reduction of photometric measurements to line-intensity ratios is made by a graphical calculator modified to permit rapid use with stepped spectra. The general procedure is adapted to the routine analysis of commercial metals, with a minimum chance of error on the part of the observer. It is the purpose of this paper to describe the procedure employed in the analysis of tin, with particular regard to sampling, preparation of standards, spark excitation, and photometry.

II. PREPARATION OF SAMPLES AND STANDARDS

1. SAMPLE RODS FORMED BY MELTING OR PRESSING

The form of the tin submitted for analysis cannot, in general, be controlled. A typical group of samples is shown in figure 1. The majority of the samples submitted for test are fusible plugs (group *C* of fig. 1) in which the tin core, heated in contact with the brass casing during manufacture, is known to absorb varying amounts of the constituents of the brass. The procedure previously employed to provide a homogeneous sample for chemical analysis was to melt the tin from the casing, to catch it in a warm crucible, and, finally, to cast it in a cold mold. A similar procedure was followed in obtaining the spectrographic sample, but the design of the mold was modified to produce a two-fingered casting from which short rods suitable for spark electrodes could be cut. The first castings provided rods ⅛ in. in diameter; later the diameter was increased to ¼ in. to realize the advantages gained in sparking a larger electrode area. To obtain electrodes, two pieces of the rod at least ½ in. long are cut from the casting and the ends to be sparked are turned flat on a lathe. The cast specimens exhibit a high degree of homogeneity, as will be shown later by the results obtained.

Samples in forms other than fusible plugs formerly were fabricated into rods by melting and casting a few grams of turnings in glass tubes, sealed under vacuum. This lengthy procedure has recently been replaced by compressing the turnings, millings, or scrapings into small rods for electrodes. A commercially available hydraulic pressing machine is used to prepare two 2-g rods, ¼ in. in diameter and 5/16 in. long. The spectra of electrodes prepared from castings and from compressed drillings of the same sample were compared to observe any significant differences, as illustrated in figure 2. Apparently the only differences are those caused by contamination of the sample, not during the pressing operation, but in the machining and handling of the turnings. The maximum observed increase in iron was 0.004 percent when fine turnings were cut. The extraneous impurities may be removed by washing the turnings in dilute hydrochloric acid. Where preparation of the sample can be controlled, a more satisfactory procedure is to use a tool made of a material which will not interfere in the analysis, for example, tungsten carbide. The magnesium in-

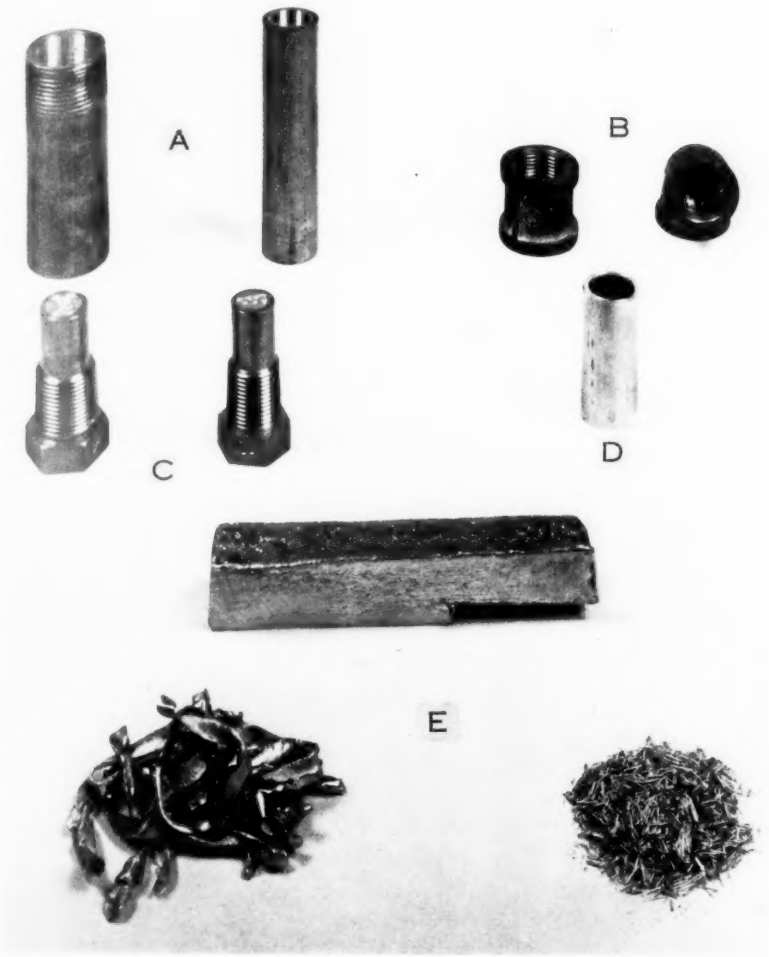

FIGURE 1. — *Typical samples submitted for analysis of tin.*

A, Tin-lined copper and brass pipe; *B*, tin-lined fittings; *C*, tin fusible plugs in brass casings; *D*, block tin pipe; *E*, samples of pig tin in various forms.

UNIV. OF MICH.

troduced in handling the turnings can easily be avoided. The usual rules of representative sampling should be obeyed in obtaining the portion for analysis.

The pressed rod provides an electrode sparking surface composed of several turnings, which is an advantage in obtaining an average sample. The prepared set of electrodes will provide a number of spectral exposures when machined to a clean surface after each run.

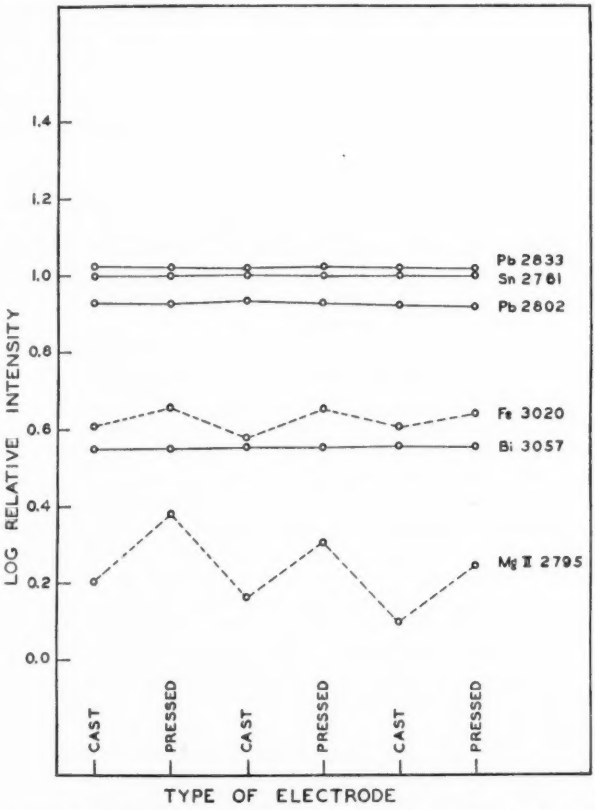

FIGURE 2.—*Comparison of line intensities in spark spectra from cast electrodes and electrodes prepared by pressing machined turnings of the same sample.*

It may be noted that repeated tests on samples submitted for analysis have seldom shown deviations exceeding ± 5 percent from their mean, although wider deviations have been observed in some of the prepared standards, especially for iron in tin, as will be described in the following section.

2. CHEMICALLY ANALYZED STANDARDS

Reference standards of tin metal containing known concentrations of impurities were obtained by (1) selection of samples previously analyzed by chemical methods, (2) melting the constituents in an

open crucible and casting in rod form, followed by chemical analysis, and (3) melting weighed amounts of the constituents in glass tubes sealed in vacuum. Samples analyzed by routine chemical methods in this Bureau were found in good agreement on spectrographic examination, except for a few determinations of small concentrations of the order of 0.05 percent or less. To cover the required ranges of concentrations, melts of tin containing copper, iron, lead, and zinc were prepared in the Metallurgy Division by adding known amounts of master alloys to tin of high purity. These melts were heated in graphite crucibles, stirred, cast in a graphite mold, and finally swaged to rod. Both the master alloys and the standards were analyzed in the Chemistry Division. The analyses were found necessary because of losses of zinc and variations in the iron content occurring during melting.

With the exception of the melts containing over 0.05 percent of iron, the standards showed agreement within ±5-percent average deviation on spectrographic examination and were employed in the analysis for copper, lead, and zinc Only two melts gave consistent results for iron. The iron in the standard of highest concentration, 0.3 percent, was segregated to such an extent that the spark employed in excitation was affected, tending to burn to localized areas high in iron on the electrode surface. Another alloy containing 0.015 percent of iron by chemical analysis was found to vary from 0.008 to 0.040 percent by spectrographic analysis. The low solubility of iron in tin undoubtedly accounts for the observed discrepancies.[3] Satisfactory standards containing as high as 0.36 percent of iron were later obtained in our laboratory by dissolving the iron in tin at an elevated temperature and chill-casting in an iron mold. The melt of tin was stirred in an open graphite crucible with a stirrer made of 1/16-in. iron wire bent at the end to form a compact spiral. A few crystals of zinc chloride and ammonium chloride were added as fluxing agents to permit the tin to wet the iron. After a few minutes, determined by trial, the stirrer was removed (thus effectively removing all undissolved iron) and the metal was chill-cast. The iron concentration was determined by chemical analysis. In the range from 0.01 to 0.1 percent, the spectrographic results for the iron standards prepared in this way deviated less than ±6 percent from their means. In practice, iron is rarely encountered in concentrations of more than a few hundredths percent in pig tin; where irregular results are observed, repeated determinations should be made to provide an average survey of the sample.

3. STANDARDS SYNTHESIZED BY VACUUM MELTING

To supplement the available standards for all of the elements except iron, a number of melts were prepared in evacuated tubes, as suggested by Smith [6]. The earlier melts, containing copper and lead in concentrations of 1 to 2 percent, exhibited definite segregation. The extreme deviations in spectrographic results amounted to ±10 percent along a casting in some cases, despite cooling of the well-mixed melt by an air blast. Improved results followed the adoption of half the quantity of metal for each melt (20 g) and cooling the

[3] Phase relations in tin alloys are discussed in detail by Mantell [16].

melting tube by immersion in water. In general, the standards prepared by the latter method showed larger deviations caused by segregation than were observed for the same elements in the chill-cast samples. However, this did not preclude their use, since the average of the spectral measurements made at various points (usually four) on the bars gave values in agreement with the chemically analyzed standards. The analytical data for antimony, arsenic, bismuth, indium, and silver are based entirely on the vacuum-melted standards.

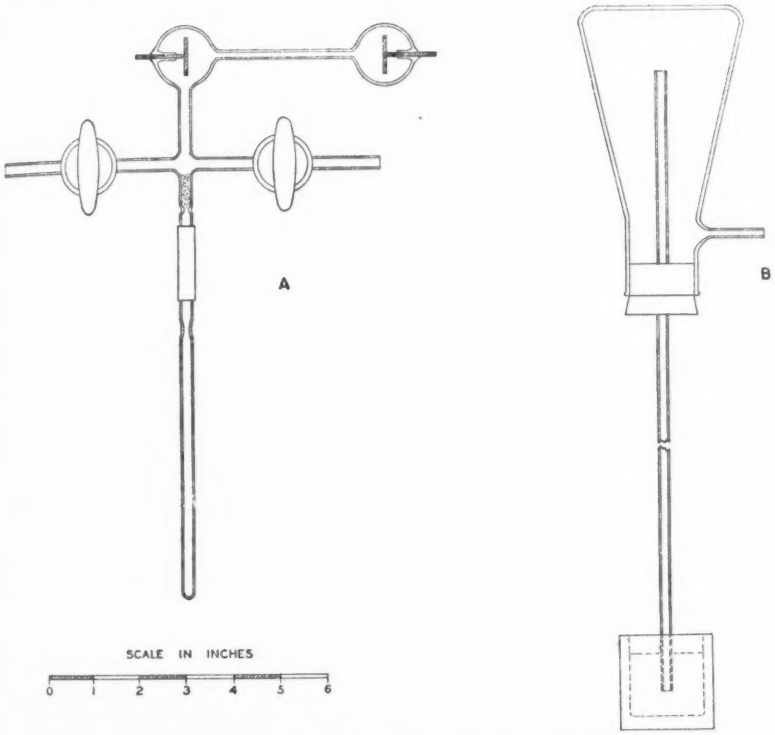

FIGURE 3.—*Apparatus used in preparing vacuum-melted tin standards.*

A, melting tube connected to vacuum line; *B*, arrangement for obtaining tin in rod form to be used in preparation of standards.

For copper, lead, and zinc the vacuum-melted standards are supplemented by chemically analyzed standards.

The vacuum-melting technique requires considerable care to avoid time-consuming failures. The procedure found most suitable will be described in detail for the benefit of those contemplating similar operations. A convenient arrangement for vacuum melting is shown in figure 3. Tin rod of diameter slightly less than that of the final melting tube, ¼ in. (fig. 3, *A*), is prepared by drawing the molten metal up in a glass tube by suction, as demonstrated in figure 3 (*B*). The glass is broken from the cast rod only when the metal is required. The weighed amount (20 g) of this rod and the other constituents are placed in the glass melting tube closed at one end. After a con-

striction is made above the charge, the tube is attached by a rubber connector to the vacuum line, as shown in figure 3 (*A*). The contents of the melting tube are protected from contamination by a wad of glass wool. The discharge tube, excited by a small sign-lighting transformer, acts as a simple vacuum gage. After evacuation, the melting tube is sealed off neatly at the constriction, placed in the open end of a long U-shaped wire holder, and heated carefully in a large flame. The melted charge is mixed by pouring from one end of the tube to the other for about 15 minutes, after which the melt is cooled by removing the tube from its holder and dipping it cautiously first in hot and then in cold water. The castings are tested for homogeneity by comparing electrodes cut from the two ends and the middle. A series of standards may be prepared by diluting the master melts with pure tin. To avoid pitted castings and segregation of impurities, the tube and metals should be clean. Oxide films, soiled surfaces on the metals, or bits of rubber or sulfur from the rubber connections should be avoided, since these cause serious drossing with attendant difficulty in mixing. The loss of weight observed after the dross film had been wiped from the cast rod rarely exceeded 2 mg on a 20-g melt. A loss of 5 mg or more was regarded as an indication of excessive drossing. Heating the tin to a high temperature in contact with glass produced considerable dross, probably from attack of the hot metal on the glass surface. Spectrographic examination of the dross showed a much higher concentration of impurities than the body of the metal and exhibited significant amounts of silicon and boron, which undoubtedly were introduced from the glass.

The following sources of added constituents were found satisfactory:

Antimony and bismuth: pieces freshly broken from cast slabs.

Arsenic: crystals freed from oxide by warming in a glass tube under reduced pressure (aspirator).

Copper: oxygen-free copper sheet.

Lead and indium: pellets cut from bars and sealed in the melting tube immediately after weighing.

Silver: electrolytic crystals.

Zinc and cadmium: pellets with clean surfaces.

It was not found possible to introduce weighed quantities of iron (of the order of 0.1 percent) into the tin at the temperature employed in vacuum melting. Melts containing a number of constituents showed greater tendency toward segregation. Mixtures containing 1 to 2 percent of arsenic and antimony were kept molten only with difficulty.

III. SPARK EXCITATION OF TIN

1. TYPES OF SPARK SOURCES EMPLOYED

The high-voltage condensed spark was found sufficiently sensitive, as well as reproducible, for the requirements of this analysis of tin. Both the simple spark circuit and the spark circuit with synchronous interrupter have been employed with satisfactory results. The simple oscillating circuit was fed by a 1-kva 15,000-volt transformer operated with a current of 2.50 to 2.55 amp in the primary. A condenser bank of capacitance 0.0030 μf and an inductance [4] of 19 μh were in the

[4] The inductance in the spark circuits was calculated from measurement of the capacitance of the condensers and the frequency of oscillation of the circuit, both measurements being made by direct-reading meters. The resistance in the circuit was assumed to be negligible, and the value of inductance, L, was calculated from tabulated values of LC for various frequencies, based on the formula $\lambda=1884\sqrt{LC}$.

circuit with the spark in the secondary. With this low power, the spark gave a steady discharge with very uniform attack on the electrodes; however, an exposure time of 2 minutes was required to provide sufficient strength in the spectrum. Later, a commercial 2-kva spark unit equipped with a synchronous interrupter was installed in the laboratory, since a source of higher power was desired for work on other problems. This unit, equipped with controls to facilitate the change from one set of operating conditions to another, was found convenient for studies of the tin spark.

2. EFFECTS OF OPERATING CONDITIONS

The general characteristics of spark discharges have been extensively investigated by Kaiser and others [17, 18]. It is of importance to examine the particular characteristics of the tin spark to establish optimum conditions for analysis. The observations to be described were made on a spark between tin electrodes separated by a gap of 4 mm and fed by the interrupted spark circuit. The electrodes were cylindrical, having a diameter, at first, of 5 mm, and later of ¼ in. (6.4 mm); the ends were turned flat and edges slightly beveled. Electrodes of this shape are easily faced on a lathe and conform to the shape recommended by Kaiser for spark electrodes.

The choice of power for this spark is limited by the low melting point of the metal; excessive power produces marked distortion of the surface of the electrodes, finally resulting in fusion of the ends. The power chosen was 2/3 kva with a capacitance of 0.0090 μf. The addition of inductance to the circuit, as is well known, suppresses the spark-like characteristics of the discharge, that is, decreases the intensity of spectral background, air lines, and lines from ionized atoms. To establish an optimum value of inductance, the effect of its increase on the intensities of the spectral lines was determined as shown in figure 4. The apparatus provided four steps of 24, 60, 152, and 335 μh. The expected reduction of intensity of ionized atoms is shown by the sharp drop in the intensity of Sn II 2896A; this is accompanied by a decrease in background intensity. For the lines of neutral atoms, however, an increase in intensity is observed between 24 and 152 μh almost diametrically opposed to the decreased intensity of the Sn II line. The further increase of inductance from 152 to 335 μh resulted in little change in the intensity of lines of neutral atoms, but the spark lines and background were further reduced. The attack of the spark on the electrodes varies considerably with the amount of inductance. At the lowest inductance the electrode surface is only partially burned in a ringlike area near the edge. As the inductance is increased, a more uniform attack of the electrodes results until at values of 152 or 335 μh the surface is almost uniformly pitted.

The fact that added inductance up to 152 μh produced an increase in the intensity of lines of neutral atoms, at the expense of lines of ionized atoms and background, indicated that higher sensitivity of detection of minor impurities would be attained with higher inductance. This was confirmed by tests with samples of low concentration of impurities. Consideration of the requirements for sensitivity and freedom from background indicated a choice of one of the higher

values of inductance for the analysis.[5] Studies of reproducibility showed little difference between the last two steps of inductance. The highest value, 335 μh, was adopted in view of the slight gain in the intensity of most of the lines over background.

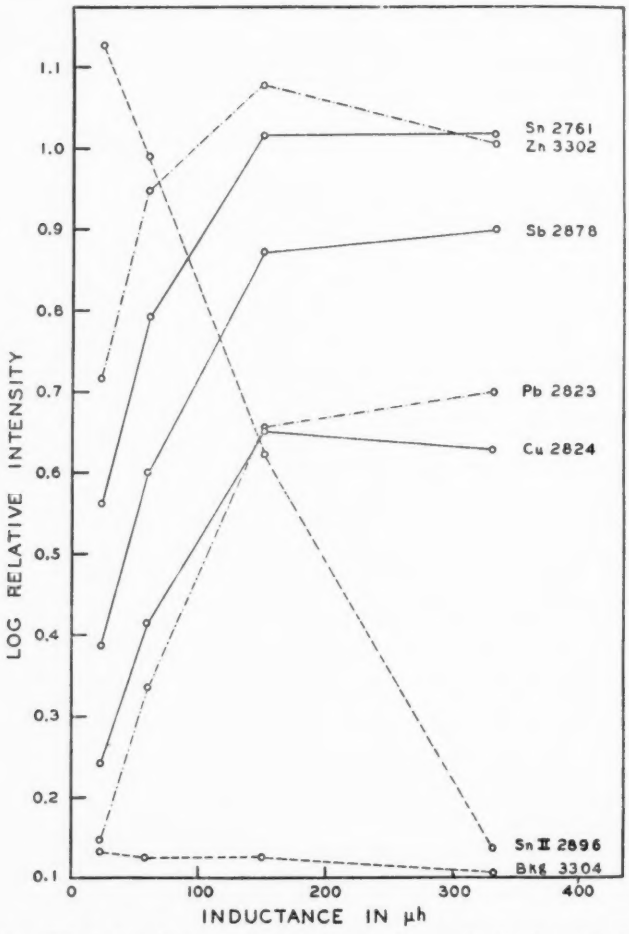

FIGURE 4.—*Effect of variation of inductance in the spark circuit on the intensities of spectral lines and background.*

As a factor in the reproducibility of the measurements, it is of importance also to observe the effects of variation in inductance on the intensity ratios of the line pairs chosen for the analysis. In figure 5 this effect is observed to be small for the analytical line pairs

[5] Previous observers have differed widely in their choice of inductance for the tin spark, and in one case recommendation was made that inductance be omitted entirely to obtain higher sensitivity. It is obvious that the effect of inductance will depend on the other variables in the circuit, and therefore the optimum amount of inductance should be determined for the particular conditions employed. In any case, however, the inclusion of a moderate amount of inductance for the analysis of tin is indicated from results obtained in this laboratory on both the simple and interrupted spark circuits.

shown, especially at the higher values of inductance. Similar behavior was observed for the other spectral lines chosen for the analysis.

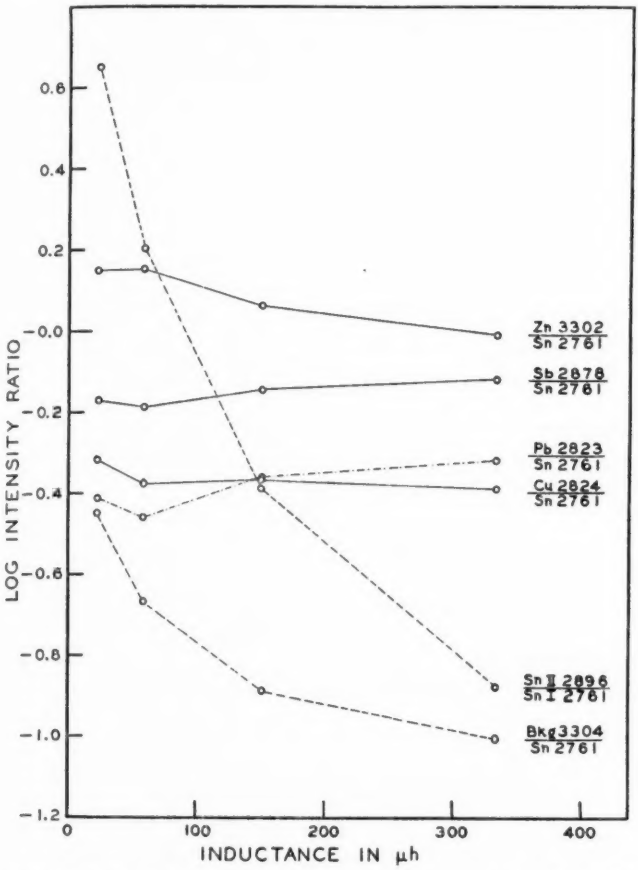

FIGURE 5.—*Effect of variation of inductance in the spark circuit on the ratio of spectral line intensities.*

3. CHARACTERISTICS OF THE SPARK ADOPTED

The tin spark, under conditions of high inductance, produces a spectrum closely resembling that of the arc and, in fact, the excitation may be described as a controlled arc. It is of interest to observe the change in spectral radiation during the discharge period, as shown in the typical case illustrated in figure 6. The discharge is characterized by three stages: (1) a short induction period of generally increasing line intensity in which the vapors of the spark gap approach an equilibrium condition; (2) a period 4 or 5 times as long, depending on the area of the electrode, in which the intensities of most of the lines are at a maximum and show little change in relative values; and (3) an abrupt decrease in the intensities of the lines as the discharge

is weakened and confined to one spot on the electrode, apparently by the surface film of oxide which is formed on the electrode surface. The behavior of zinc lines is markedly different from the general case; these show a maximum intensity for the first few seconds and then a steady decrease with time, probably as a result of more rapid volatilization. This behavior leads to a pronounced loss of sensitivity

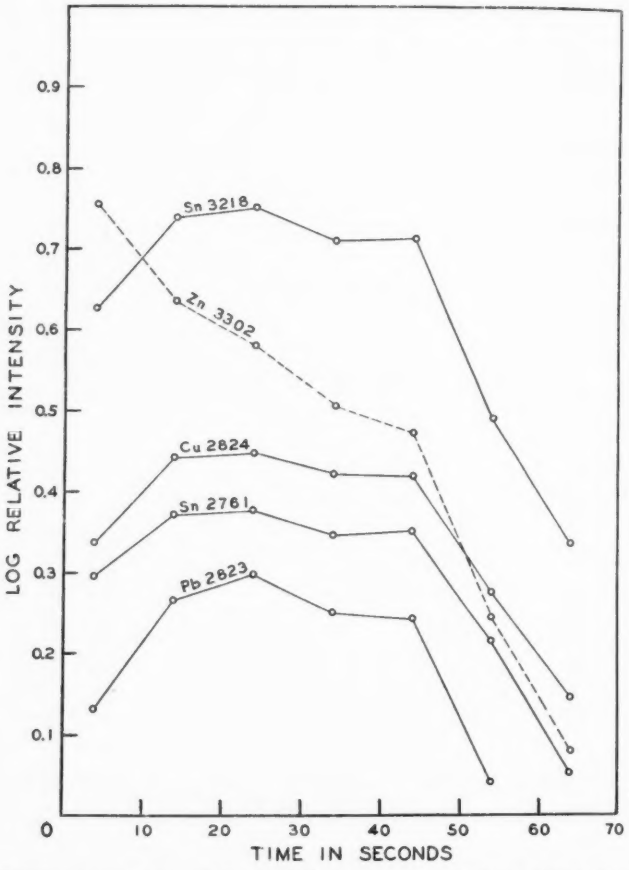

FIGURE 6.—*Change of spectral line intensity with time of sparking.*

The points represent a series of 8-second exposures, with intervals of 2 seconds between successive exposures. Electrodes were 5-mm rod containing 2.0 percent of Cu, 1.0 percent of Pb, and 0.10 percent of Zn.

of zinc when the electrodes are sparked for an interval before the exposure is made. The effect of oxidation of tin electrodes in reducing the intensity of the spark has been observed by Töpelmann and Shuhknecht [8], who measured the variation in current in the oscillating circuit with time of sparking. Their curves indicate a rise and fall of current during the first minute of sparking, which is similar to the rise and fall of the line intensities in the "normal" cases of copper, lead, and tin in figure 6.

Ideally, the second phase of the discharge would appear most reproducible for the determination of copper in lead. In practice, however, the exposure time is adjusted to cover both the first and second phases of the sparking cycle to provide sufficient line strength for the detection of minor impurities. With ¼-in. electrodes, oxidation of the electrodes becomes effective in reducing the line intensity, only after 1 minute; the exposure is limited to this interval.

Changes in other variables in the spark circuit—such as output energy, controlled by the synchronous interrupter, and the gap distance between the electrodes—affect the over-all intensity of the spectrum and are kept constant to minimize photometric errors. The intensity ratios of copper, lead, and bismuth lines to tin internal control were found to be little affected by changes in the adjustment of the interrupter; zinc showed a noticeable variation. The constants of the circuit now employed are summarized as follows:

Circuit: Commercial spark unit, 35,000-volt transformer feeding an oscillating circuit across a condenser. This circuit consists of the condenser connected to a solenoidal induction coil, a rotary interrupter run by a synchronous motor, and the spark gap.
Input voltage: 106 volts.
Power: 2/3 kva.
Capacity of condensers: 0.0090 μf.
Inductance of circuit: 335 μh.
Interrupter adjustment: Intermediate between the positions for high energy and low energy in circuit (40–42 volts on the indicating instrument furnished with the unit).
Electrode form: Two electrodes of circular rod ¼ in. (6.4 mm) in diameter, turned flat on discharge ends, and edges slightly beveled. Length not less than ¼ in.
Electrode holder: Heavy metal spring clips.
Electrode gap distance: 4 mm.
Exposure time: 1 minute, no prespark.

IV. ANALYTICAL PROCEDURE

1. THE SPECTROGRAPH AND ITS ILLUMINATION

A spectrograph of moderately high dispersion, although not essential to certain determinations in metallic tin, nevertheless provides the advantages of reduced background intensity and wider separation of lines. This is especially important when the spectrograph slit is widened for accurate photometric measurements. A large Littrow quartz-prism spectrograph of focal length $f_D = 183$ cm was employed throughout the work.

The simplicity of the tin spectrum, which is an advantage in avoiding interferences of lines, is a disadvantage when selecting tin lines of suitable low intensity for internal control. In order to utilize the available tin lines over the various ranges of concentrations of the impurities, a reduction of the intensity of the lines is accomplished by means of a step sector rotated at the slit of the spectrograph. In addition, the step sector provides a line pattern of intensities for calibrating the photographic plate [19]. Proper use of the sector requires uniform illumination of the sector and slit combination. For this, an image of the source is focused on the spectrograph collimator lens by a lens at the slit of the spectrograph. The sector is mounted close to the slit. The system, which provides uniform illumination over about 1 cm of the slit length, is illustrated in figure 7.

An image of the full spark column (spark gap 4 mm) is focused on the collimator lens of the spectrograph by means of a thin crystal quartz lens, L_1 (1-mm edge thickness, 2.5-cm diameter, and focal length f_D=34 cm), mounted in the cover of the slit, S. Since the focal length of lens L_1 determines the distance of the spark source, X, from the slit, a focal length was chosen which provides the requisite uniformity of slit illumination without too great a loss in light intensity. The step sector, R, made in the Bureau shop, has 5 steps each 2 mm high cut in the periphery of the disk, the ratio of successive steps being 1.585, so that the logarithm of the ratio is the simple value 0.200. The sector disk is mounted as close to the slit cover, D, as possible (0.5 mm) and rotates at a speed of 1,700 rpm. The position of the spark source, X, for the spectral region 2700 to 3400 A, is fixed by photographing full-length images of the slit for successive displacements of the source and choosing that position of the source which provides most nearly uniform intensity along the slit image. An auxiliary lens, L_2, behind the spark stand, projects an enlarged

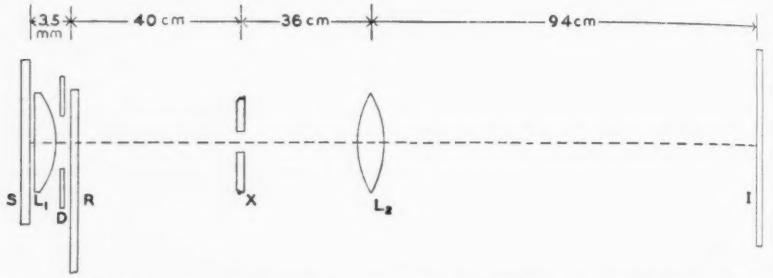

FIGURE 7.—*Diagrammatic sketch of the illuminating system employed with the spectrograph.*

image of the electrodes to a marked position on the screen, I, permitting rapid and accurate adjustment of both the position of the spark on the optical axis and the gap distance between the electrodes. The spectrograph slit is opened to 40 microns.

The spectra of six samples, each exposed for 1 minute through 5 steps of the sector, are photographed on a 4- by 10-in. Eastman Spectrum Analysis Plate No. 1. The plate is developed in D-11, M–Q developer, with fixed time (2 min) and temperature (20°C). Uniform agitation was found especially important in obtaining reproducible results with this plate; the Eastman Process plate previously used (with twice the developing time) was much less sensitive to irregular agitation. Improved results were observed with a mechanically operated rocking device for the development.

2. CHOICE OF SPECTRAL LINES FOR ANALYSIS

Typical spectrograms of tin are reproduced in figure 8. The 2 samples represented by these exposures together contained the 10 elements determined by this procedure. The lines selected for the determination of impurities are marked on the illustration and a list is given in table 2. The choice of lines for the determinations of the lower concentrations of the impurities is limited to those disappearing

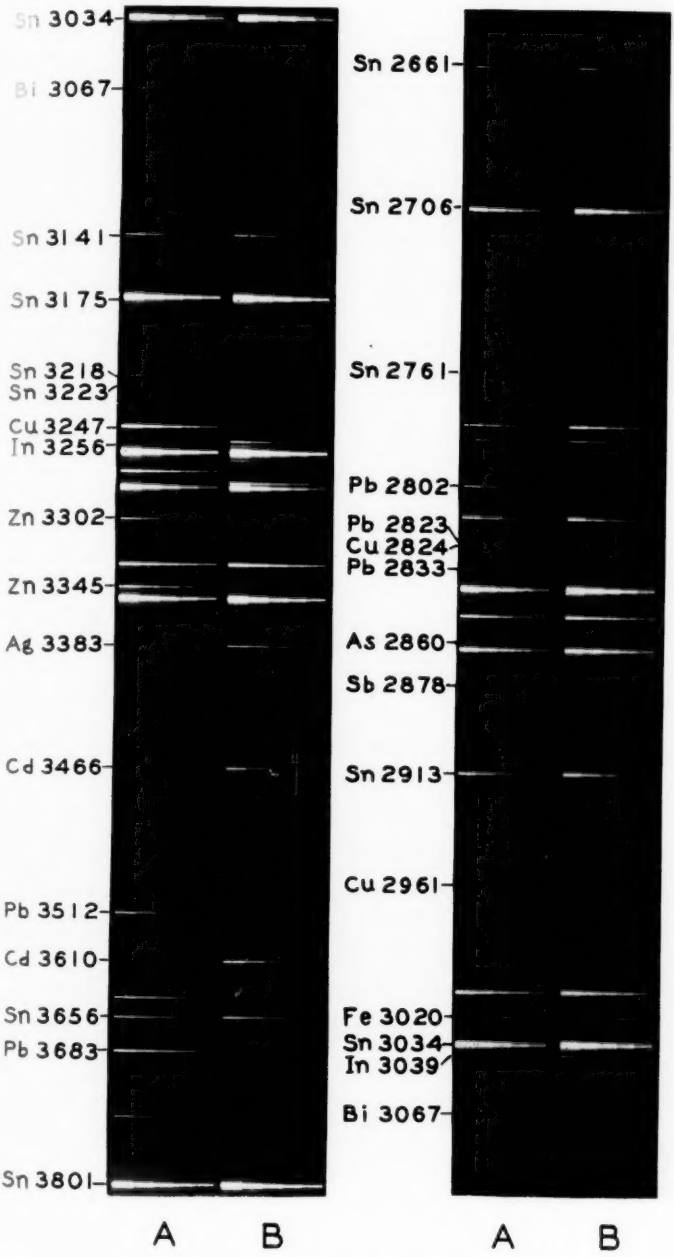

FIGURE 8.—*Typical spectrograms of tin samples.*

A, Sample containing 2.0 percent of Cu, Pb, and 0.2 percent of Bi, Zn; *B*, sample containing 2.0 percent of As, Sb, and 0.2 percent of Ag, Cd, In. A trace of iron is present in both samples.

UNIV. OF MICH.

last as the element is progressively diluted in tin. They are usually the strongest lines produced by neutral atoms of the impurities in the spectral region chosen as most convenient for analysis, 2600 to 3600 A. For higher concentrations of copper and lead (above 0.1 percent), the most sensitive lines of these elements were too intense for accurate photometric measurement and the weaker lines, Cu 2824 A and Pb 2823 A, were selected. In combination with Sn 2671 A, as internal control, the intensity ratios obtained with the two lines exhibited a high degree of precision. Marked similarity was observed in the behavior of the radiations during the sparking cycle previously described. In addition to the Sn 2761 A, a survey of the tin spectrum in this region reveals only two more lines of tin at the low level of intensity suitable for internal control lines. These tin lines, 3218 and 3223 A, may be employed as controls for the group of impurity lines at 3300 A. The line 2761 A was found most generally applicable, lying near the important group of impurity lines at 2800 A for several of the elements determined. This line is free from interference with other lines with the exception of iron 2761.78 A, which adds perceptible intensity to the tin line at iron concentrations above 0.04 percent. Iron has not been observed higher than 0.03 percent, and was usually below 0.01 percent, in many hundreds of determinations. The probability of interference of iron with the tin line is slight.

TABLE 2.—*Wavelengths employed in the analysis of tin*

Element	Wavelength	Concentration range	Remarks
	A	%	
Antimony	2877.92	0.06 to 2.0	
Arsenic	2860.45	.06 to 2.0	Wing of Sn 2863 A affects intensity measurements of this line.
Bismuth	3067.72	.001 to 0.2	
Cadmium	3466.20	.01 to 0.2	
	3610.51	<.01	Used for qualitative detection.
Copper	2824.37	.1 to 2.0	Avoid confusing this line with Pb 2823 A.
	3247.54	.001 to 0.05 (0.03 to 0.3).	Requires a weaker exposure (e. g., 30 sec) to cover the higher concentration range.
Indium	3039.36	.01 to 0.2	
	3256.09	.002 to 0.2	
Iron	3020.6d	.01 to 0.4	Most sensitive for iron in this region.
Lead	2802.00	.01 to 0.5	
	2823.19	.1 to 2.0	Avoid confusing this line with Cu 2824 A.
	2833.07	.003 to 0.5	Wing of Sn 2839 A affects intensity measurements of this line below 0.01 percent of Pb.
Silver	3382.89	.002 to 0.03	
Zinc	3302.8d	.01 to 0.2	Avoid confusing this line with Cu 3307.95 A.
	3345.57	<.01	Used for qualitative detection.
Tin	2761.78	Internal control line	Most generally useful control line, but iron line interferes above 0.04 percent of Fe.
	3218.68	do	
	3223.57	do	

3. PHOTOMETRIC MEASUREMENTS

The line blackenings on the photographic plate are measured by a commercial microphotometer modified [15] to provide ease and accuracy in measurement. The blackening deflections, as defined by Thomson and Duffendack [20], are observed by means of a barrier-layer cell and galvanometer on a scale from zero corresponding to the clear plate reading to 310 mm for the dark cell (opaque shutter). The important requirement that the full-scale deflection (zero reading) should remain unchanged during the series of measurements on a plate is met by drawing power for the 200-watt projection lamp from a large battery. After an initial stabilization period of about 15

minutes, the full-scale deflection becomes practically constant, except for a slight drift (1 mm in ½ hour) caused by cell fatigue.

The photometric procedure, in common with other methods involving plate calibration, consists in making two related series of measurements. First, to provide a plate-calibration curve, blackenings are measured for the consecutive steps of two or more line images selected to cover the blackening scale. The blackening values are plotted against the corresponding logarithms of the relative exposures calculated from the sector aperture ratios, and a smooth curve is drawn. For purposes of analysis, the exposure scale may be considered equivalent to an intensity scale, thus permitting conversion of blackening measurements to intensities.

The second series of measurements on the plate is that of the lines selected for analysis. Since a choice of blackenings in two or more

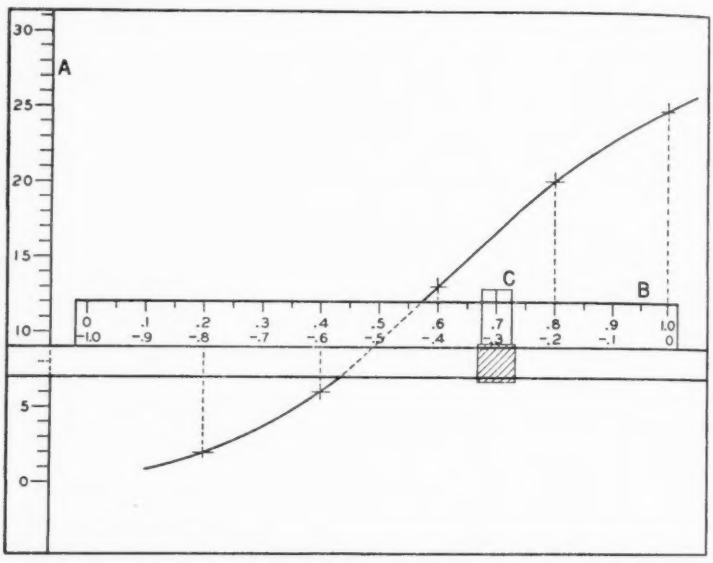

FIGURE 9.—*Graphical calculator used in rapid determination of log-intensity ratios from measured blackenings.*

steps of the stepped image may be possible, those measurements are favored which fall in the central part of the blackening scale. Usually two blackenings are measured for two consecutive steps of the line image. The recorded blackenings of the lines are reduced to log I values by means of the calibration curve. For the pairs of lines employed in the determinations, subtraction of the log I values gives log I_1/I_2. Where the blackening of each of the two lines is not measured in the same sector step, a correction is applied.

These operations are laborious and subject to error if carried out by arithmetical calculation. The possibility of increasing the speed by means of a graphical calculator similar to that devised by Owens [21] was investigated. By changing the scales of a commercially available calculator, it was found possible to plot the calibration curve rapidly and then to read directly log I_1/I_2 for two lines, irrespective

of the steps in the sectored image in which the individual blackenings are measured. A diagrammatic sketch of the calculator is given in figure 9. The ordinate scale, A, corresponds to the microphotometer scale, and the abscissa scale, B, to the logarithm of relative intensity. Scale B is movable horizontally along a rigid arm, which can be moved vertically. The plate-calibration curve is plotted from the blackening readings for Sn 2761 A in the five steps provided by the stepped sector. A typical section of a data sheet is shown in table 3. Since the logarithm of the aperture ratios of the successive sector steps is 0.200, step blackening values are plotted at the 0.200 intervals on the scale, as shown by the dotted lines on the diagram in figure 9. In practice the plotted points are checked by values from another line before the calibration curve is drawn. The determinations of log I_1/I_2 values from the blackening measurements of impurity and control lines are now made. The simplest case is one in which both blackenings are in the same step—for example, for Pb 2833 A and Sn 2761 A in step 3, as given in table 3. The arm, B, is raised to 13.1 on scale A, and scale B is moved sidewise until the zero value (left end of scale) lies at the intersection of the scale with the curve. An index marker, C, is moved over to this point to fix the position of the scale. The scale arm is then raised to 17.1 on scale A, and the reading at which the curve intersects scale B is recorded as log I Pb 2833/I Sn 2761. When the blackenings are measured in different steps, scale B is moved sidewise an interval of 0.200 or 0.400, depending on the relative apertures of the steps, before the log I_1/I_2 value is read. When the blackening of the impurity line, in the same step as the control, is lower than that of the control, the negative scale must be used. This is true also when the blackening of the impurity line is measured in a step of larger aperture than the control line. The recorded log I_1/I_2 values are applied to preestablished analytical curves to obtain the concentration of the impurity, which is entered in the column headed by the percent sign on the working sheet.

TABLE 3.—*Typical section of data sheet*

[Values in italics are log I_1/I_2 determined by graphical calculation from the measured line blackenings]

Wavelength	Step 1	Step 2	Step 3	Step 4	Step 5	Concentration
A Sn 2761	*cm* 2.0	*cm* 6.0	*cm* 13.1	*cm* 20.1	*cm* 24.8	%
Pb 2833		10.0 *0.114*	17.1 *0.109*			0.178
Sb 2878					5.5 *−0.609*	.172
Ag 3383	15.0 *0.451*					.023

The operations with the calculator are more easily carried out than explained, and a considerable saving in time has resulted. The internal control line Sn 2761 A usually serves for plate calibration from 2700 to 3500 A, although above 3300 A the contrast of the plate

increases. To avoid the construction of a second calibration curve for this region for the few measurements involved, the curve for Sn 2761 A is used under conditions which minimize the error. This is done by measuring the blackenings of the impurity lines near a fixed value on the lower end of the blackening scale where possible. When highest accuracy is desired for the lines affected (zinc, silver, and cadmium), internal control lines should be chosen near the impurity lines and the plate calibrated in this region.

To summarize the procedure, a single, sectored, spectral exposure is employed (1) to calibrate the plate by line images, (2) to provide usually two intensity measurements for each line, and (3) to provide accurate measurement of intensity ratios over a wider range than is possible with a single-step exposure.

4. ANALYTICAL CURVES

The measured values of log I impurity/I control are plotted for a series of known concentrations of the impurity to obtain the analytical

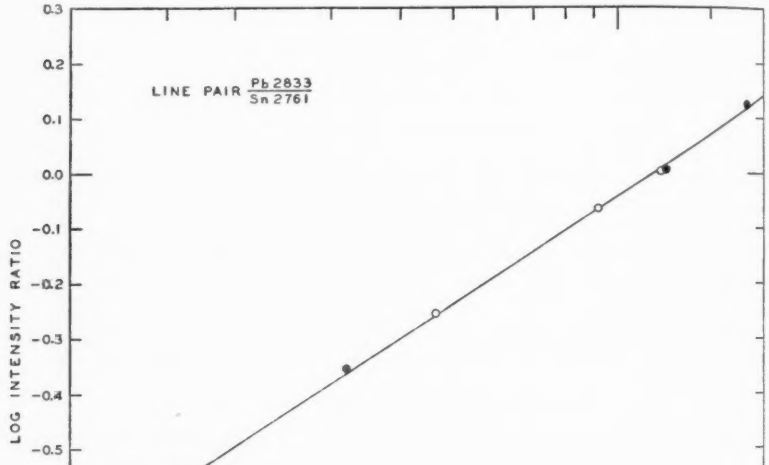

FIGURE 10.—*Typical analytical curve.*

Determination of lead between 0.01 and 0.2 percent in tin.

curve for each impurity. Convenience in plotting is provided, as is customary, by constructing the analytical curve on semilogarithmic coordinate paper, with log I_1/I_2 values plotted on the linear scale and with percentage concentrations on the logarithmic scale. A typical analytical curve is shown in figure 10, constructed for the determination of lead between 0.01 and 0.2 percent. The points representing standards based on synthetic vacuum melts and others based on chemical analysis fall close to the smooth curve. The chemical value for the lead standard at 0.015 percent apparently was too high, but

the deviation from the curve is only 0.001 percent; the agreement in general indicates a high accuracy in the chemical determinations. Similar curves were obtained for the other impurities. The agreement of the plotted points with the analytical curves in the more important ranges of concentrations is exhibited in table 4. For the ranges covered, the average deviation of the points from the curve is of the order of ± 2.5 percent and the extreme deviations were within ± 5 percent with few exceptions. A few standards showing abnormal disagreement on repeated measurement were discarded.

TABLE 4.—*Agreement of plotted points, based on standards, with the analytical curve*

Element	Wavelength (Sn 2761 · control)	Concentration range	Average deviation of standards from curve
	A	%	%
Antimony	2877.92	0.1 to 2.0	±1.6
Arsenic	2860.45	.1 to 2.0	±2.5
Bismuth	3067.72	.003 to 0.1	±2.5
Cadmium	3466.20	.01 to 0.2	±2.0
Copper	2824.37	.2 to 2.0	±2.5
Indium	3256.09	.004 to 0.2	±4.2
Iron	3020.6d	.01 to 0.05	±2.4
Lead	2823.19	.01 to 2.0	±2.3
Lead	2833.07	.006 to 0.4	±3.3
Silver	3382.89	.002 to 0.2	±3.2
Zinc	3302.8d	.01 to 0.2	±2.4

The determination of the impurity is made by applying the value of the log I_1/I_2 ratio to the curve to find the concentration. The determination of the amount of tin in the sample, required by the specification for minimum tin content, is, of course, made by difference after the total concentration of the impurities is ascertained. In all cases the spectra are examined qualitatively for possible impurities before photometric measurements are made. In testing samples under the specifications listed in table 1, p. 167, it is usually unnecessary to make photometric measurements for more than four elements. A single determination is deemed sufficient for each element in the analysis of fusible plugs when the sample meets the specification. A duplicate determination is made with an additional set of electrodes of the sample when the fusible plug fails to meet the specification. For other samples, prepared by less refined sampling conditions, two or more determinations are made per element to ensure an average value of the concentration.

The procedure set up for this analysis affords an opportunity to compare the behavior of a number of analytical curves for different chemical elements in the same matrix. The method of plotting the analytical curves described above is equivalent to plotting log I_1/I_2 against log concentration. If a given added increment in concentration produces an equivalent change in the intensity of the spectral line radiated by the vaporized metal, a linear relation should be obtained and has been observed in many cases in spectrographic analysis. Under ideal conditions the relation between log intensity and log concentration should be represented by a straight line, inclined at 45° to the log-concentration axis or, in other words, having a slope equal to unity. The curves established for the tin analysis in many cases are linear, having slopes which in a few cases approach but do not equal unity. In some cases marked deviation from linearity is

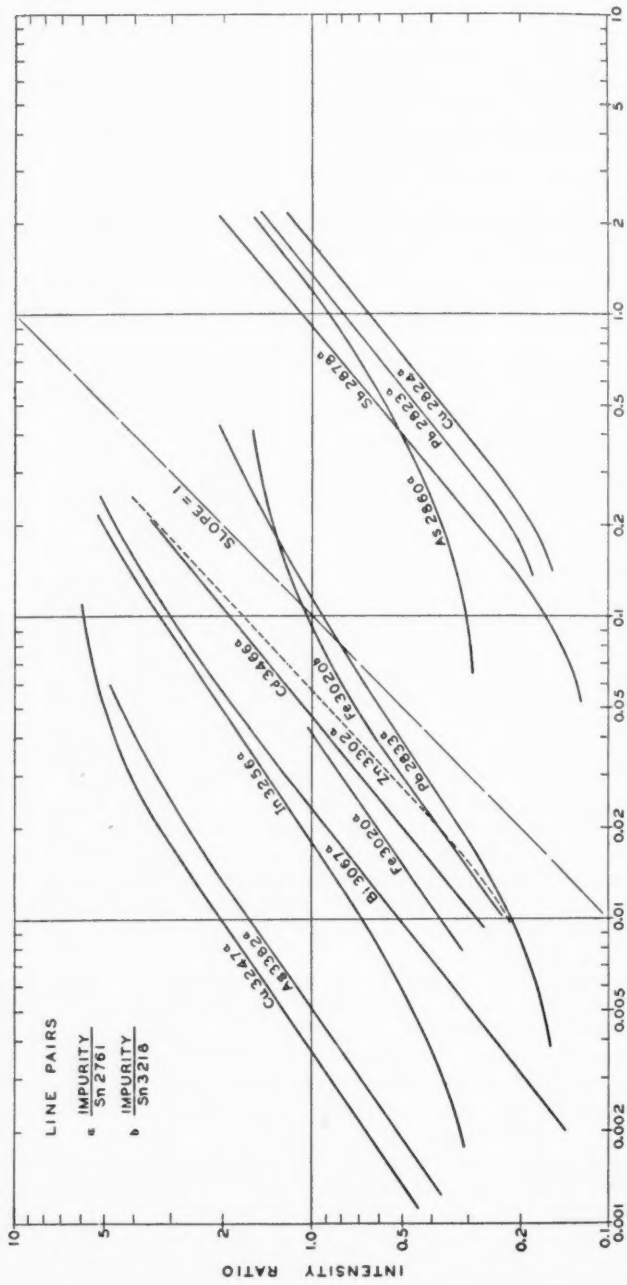

FIGURE 11.—*The system of analytical curves for the analysis of tin, arranged for intercomparison.*

observed. To illustrate the types of curves obtained, the 30 large-scale plots of the curves employed in the analysis of tin have been compressed to the scale of figure 11. A straight line of unit slope has been added for comparison. The closest approach to ideal behavior is shown for the zinc line 3302A, followed by Cd 3466A, Sb 2878A, Pb 2823A and Cu 2824A. Other lines exhibit either a smaller slope or a marked departure from linearity, or both. The different behavior of the various spectral lines is explained by two underlying causes: First, the presence of background in the spectrum which, when uncorrected, affects the photometric measurements of line intensities; and second, the tendency for certain radiations to lose energy by self-absorption in the vapors of the spark.

The effect of background in the spectrum in adding intensity to the spectral line becomes larger as the line intensity decreases with lowered concentration. This is observed in the plotted curves as a gradual decrease in slope at the lower end as the intensity of the line-plus-background approaches the background intensity asymptotically as a limit. Examination of the curves shows this effect in varying degrees, the most serious being observed for As 2860A, which, as previously mentioned, is measured on the background associated with Sn 2862A. Obviously the precision of the determinations will be adversely affected for these cases. A correction, by actual measurement of the background intensity, was not made because of the uncertainty involved. It was found preferable, when an accurate determination of arsenic is desired, to expose one or two standards on the same plate for reference under conditions which ensure comparable values of background.

The effect of self-absorption has been observed in spectographic analysis whenever an easily absorbed radiation, that is, one derived from a low-energy transition in the atom, is employed in determinations of concentrations of more than a few hundredths percent. This effect is observed here as a decreasing slope at the upper end of certain of the analytical curves. The shape of the curve for Cu 3247A above 0.02 percent indicates strong self-absorption, as might be expected from the nature of this line. Similarly, Ag 3383A exhibits the effect above 0.02 percent and, to a lesser degree, the deviation is observed for Bi 3067A above 0.04 percent, Fe 3020A above 0.05 percent, and Pb 2833A above 0.1 percent. In most cases these regions of decreased accuracy can be avoided; but, because of the scarcity of suitable spectral lines for copper, the line Cu 3247A is employed up to a concentration of 0.1 percent. The observation that curves fall roughly into two groups having different values for the slopes of their linear portions is probably related to the phenomenon of self-absorption. Those lines most affected by self-absorption fall into the class giving, in general, the smaller slope values, as will be seen by inspection of figure 11.

V. DISCUSSION

1. PRECISION AND ACCURACY

The precision of the method may be measured by the agreement of repeated determinations made on the same sample. To arrive at knowledge of the reproducibility of the spectrographic procedure independent of the effects of inhomogeneity in the sample, a care-

fully mixed and chill-cast sample is employed. The results of repeated determinations, on two photographic plates, for copper, lead, iron, and bismuth in the sample are shown in table 5. The results exhibit excellent reproducibility; the standard deviation ranges from 1.09 percent for copper to 2.52 percent for iron, the most troublesome case.

TABLE 5.—*Reproducibility of determinations on a single chill-cast sample of tin*

Plate number	Copper			Lead			Iron			Bismuth		
	Observed concentration	Deviation from mean	Percentage deviation	Observed concentration	Deviation from mean	Percentage deviation	Observed concentration	Deviation from mean	Percentage deviation	Observed concentration	Deviation from mean	Percentage deviation
	Pct.			*Pct.*			*Pct.*			*Pct.*		
1	0.670	0.003	0.4	0.132	0.001	0.8	0.0107	0.0004	3.9	0.00510	0.00001	0.2
	.677	.010	1.5	.133	.000	.0	.0106	.0003	2.9	.00517	.00008	1.6
	.662	.005	0.8	.132	.001	.8	.0103	.0000	0.0	.00507	.00002	0.4
	.681	.014	2.1	.137	.004	3.0	.0104	.0001	1.0	.00530	.00022	4.3
	.675	.008	1.2	.132	.001	0.8	.0103	.0000	0.0	.00510	.00001	0.2
	.658	.009	1.4	.132	.001	.8	.0103	.0000	.0	.00501	.00008	1.6
2	.665	.002	0.3	.134	.001	.8	.0097	.0006	5.8	.00497	.00012	2.4
	.661	.006	.9	.132	.001	.8	.0103	.0000	0.0	.00500	.00009	1.8
	.660	.007	1.0	.129	.004	3.0	.0100	.0003	2.9	.00494	.00015	2.9
	.662	.005	0.8	.137	.004	3.0	.0103	.0000	0.0	.00522	.00013	2.6
	.667	.000	.0	.132	.001	0.8	.0101	.0002	1.9	.00505	.00004	0.8
	.668	.001	.1	.129	.004	3.0	.0102	.0001	1.0	.00510	.00001	.2
Mean	.667			.133			0.0103			0.00509		
Average deviation		.0058	0.87		0.002	1.5		0.00017	1.6		0.00008	1.6
Standard deviation= $\sqrt{\Sigma D^2/n-1}$		.0073	1.09		0.0025	1.88		0.00026	2.52		0.00011	2.16

In routine analyses there are several factors involved which preclude attainment of this same degree of precision. In addition to the errors in photometric measurements previously discussed, an important factor is small-scale inhomogeneity in composition. To exhibit the degree of reproducibility of determinations on samples submitted for routine analysis, table 6 was prepared. This compares the results of duplicate determinations of copper and lead on a series of fusible plugs which failed to meet the specification. In most cases, the deviation between the pairs of values is well within 5 percent, and the mean should be good to ± 2.5 percent. However, wider deviations have been observed in a few cases, for example the 19-percent deviation for copper in sample 9849. Segregation of copper in this sample, one of the first group to be analyzed spectrographically, was confirmed by further determinations. Precautions are now taken to provide more complete mixing of the sample before casting, to minimize errors from this source. Another factor which enters into considerations of precision is the day-to-day stability of the procedure. In preparing the analytical curves, a shift in the plotted values was observed as high as 3 percent over a period of several days. This is apparently caused by a variation in the excitation conditions which has not yet been explained. Where this shift might be important, as for determinations requiring the highest accuracy, a standard may be photographed on the plate with the

unknown, to provide correction. In practice, when a sample fails to meet the specification, a second determination is made with a reliable standard for reference. A comparison of repeated runs of standards employed in this way over a period of weeks is shown in table 7, in which the agreement is usually within 6 percent except for iron, where segregation was apparent in the standards.

TABLE 6.—*Agreement of duplicate determinations on various samples of fusible plugs which failed to meet specifications*

Sample number	Copper			Lead		
	Observation 1	Observation 2	Deviation	Observation 1	Observation 2	Deviation
	Percent	*Percent*	*Percent*	*Percent*	*Percent*	*Percent*
9761	0.53	0.52	1.9	0.063	0.063	0.0
9798	.70	.67	4.4	1.30	1.17	10.7
9849	.174	.21	19.0	0.306	0.316	3.2
9897	.57	.57	0.0	.110	.108	1.8
10012	.50	.50	.0	.20	.20	0.0
10046	.52	.53	1.9	.050	.050	.0
10047	.63	.64	1.6	.055	.054	1.8
10049	.20	.21	5.0	.147	.148	0.7
10053	2.31	2.35	1.7	.187	.193	3.2
10054	1.47	1.44	2.1	.153	.150	2.0
10109	1.25	1.28	2.4	.127	.128	0.8
10110	1.08	1.11	2.7	.053	.053	.0
10187	0.54	0.53	1.9	.024	.023	4.1
10259	.28	.28	0.0	.79	.79	0.0
10260	.22	.21	5.0	.84	.81	3.7
10261	.96	.94	2.1	.039	.039	0.0
10346	.69	.74	6.9	.35	.38	8.3
10347	.235	.25	6.2	1.46	1.48	1.3
10348	.80	.76	5.0	0.035	0.032	9.1
10389	.73	.71	2.8	.070	.067	4.4
10428	.30	.30	0.0	.21	.22	4.5
10429	.42	.42	.0	.23	.24	4.2
10430	.28	.27	3.6	.182	.188	3.2
10431	.32	.32	0.0	.161	.162	0.6
10434	.29	.30	3.3	.25	.26	3.8

TABLE 7.—*Deviations of results from accepted values on periodic check runs of standard samples*

Element	Range of concentrations	Total runs	Deviation from accepted value				
			0 to 2 percent	2 to 4 percent	4 to 6 percent	6 to 10 percent	10 to 14 percent
	Percent						
Copper	0.29 to 0.94	23	15	5	3	0	0
Lead	.01 to .17	24	12	7	4	1	0
Iron	.015 to .07	28	9	6	4	6	3

The accuracy of the results depends not only on the precision of the spectrographic determinations but on the care in sampling the tin and on the reliability of the reference standards. The precision has been discussed. Serious sampling errors are probably avoided in the methods employed in preparing the samples. The reliability of the reference standards is perhaps best indicated by the agreement of the measurements with the analytical curves (table 4), where the average deviations were shown to be about ± 2.5 percent. It is believed that the deviation of the routine single determinations from the actual

concentrations is, in general, less than 5 percent and may be reduced to 2 percent under favorable conditions.

2. ADVANTAGES AND LIMITATIONS OF THE METHOD

The spectrographic method of analysis described in this paper offers several advantages over the chemical analysis. Of primary importance is the gain in speed; other advantages lie in the certainty of detection of metallic impurities, the attainment of higher accuracy for low concentrations, the ease of carrying out the analysis, and the possibility of analyzing very small samples. The following discussion of these points is of interest in evaluating the method.

The time required by one observer for the spectrographic analysis of six samples of fusible plugs, where four determinations are usually required on each sample, is a total of 2 hours. This includes preparation of electrodes, photography, photometry, and determination of concentrations from analytical curves. The average time per determination is 5 minutes. The wet chemical determination of the same elements in the six samples requires 2 days after the sample has been milled in the shop. The time required for the spectrographic analysis of other types of tin samples, such as pig tin, is not much longer than that for fusible plugs. The equivalent, complete, wet chemical analysis for 8 or 10 elements would require at least 4 days.

The spectrographic routine method permits a check on the presence of 10 elements, thus eliminating the danger that important metallic impurities will be overlooked. The chemical analysis, on the other hand, may be limited by the time available to the determination of a few impurities most likely to occur. For example, the routine chemical analysis of fusible plugs covers the determination of copper, lead, iron, and zinc; however, four fusible plugs recently subjected to spectrographic analysis each contained 0.2 percent of antimony, which was readily detected and determined. This impurity, which raised the value for the total impurity above the permissible limit of the specification, would probably not have been detected chemically by the short routine procedure used.

The accuracy of the spectrographic method compares favorably with that of the routine chemical method in the region of 1 percent of impurity and exceeds it below 0.1 percent, where the errors of separations and weighings become appreciable. The spectrographic method consists in a series of operations with physical instruments and involves a minimum of reliance on the observer's judgment. Therefore, after the method has been established and the instruments are functioning properly, comparable results might be expected, and, in fact, have been observed for measurements made by different observers having varying degrees of experience.

This method involves the alteration of only the small surface area of the electrodes during sparking; consequently, it may be adapted to studies of inhomogeneity of specimens as well as to the analysis of small samples. In the latter case, millings or drillings can be pressed into a thin layer on the end of each of two tin rods to form electrodes for analysis.

Limitations of the method may lie in the requirements for complex equipment, an insufficient sensitivity for certain nonmetallic elements, and the possibility of errors caused by segregation of impuri-

ties. The equipment, of course, can be employed for the analysis of a wide variety of metals and alloys under conditions similar to those outlined for the analysis of tin. It must be recognized that success of the step-sector method rests on the uniform illumination of the sector and the alinement of the spectrograph slit jaws. An occasional check of the line intensity over the effective slit length, with the sector open, will demonstrate the reliability of the adjustments. If a sensitivity of test higher than that provided by the procedure described is desired, two possibilities are open. First, the time of exposure of the spark may be increased, preferably by photographing a composite of two or more 1-minute exposures of the same electrodes, machined between exposures. Second, for the elements arsenic, antimony, cadmium, and zinc, recourse may be had to more sensitive spectral lines, some of which lie in the lower ultraviolet region of the spectrum. Segregation in tin samples, which can be studied by this method, as mentioned above, is a possible source of error when information on the average composition of a sample is desired. By taking the precautions of proper sampling outlined earlier in the paper, the danger of serious error from this source should be eliminated.

The spectrographic method, as described, has been adopted at the National Bureau of Standards for the routine analysis of commercial tin samples submitted for test under the various governmental specifications.

The author is indebted to H. L. Mullin for assistance in making many of the spectrographic observations. Standard samples were provided through the generous cooperation of J. G. Thompson, of the Metallurgy Division, and W. D. Mogerman, of the Chemistry Division. The suggestions made during tbe course of the work by W. F. Meggers, of the Spectroscopy Section, and by C. E. White, of the University of Maryland, are sincerely appreciated.

VI. REFERENCES

[1] W. F. Meggers, C. C. Kiess, and F. J. Stimson, BS Sci. Pap. **18,** 235 (1922) S444.
[2] W. Gerlach, Z. anorg. allgem. Chem. **142,** 383 (1925).
[3] T. Negresco, Recherches expérimentales d'analyse spectrale quantitative sur les alliages métalliques (Presses Univ., Paris, 1927).
[4] E. Schweitzer, Z. anorg. allgem. Chem. **164,** 127 (1927).
[5] W. Gerlach and E. Schweitzer, Foundations and Methods of Chemical Analysis by the Emission Spectrum (A. Hilger, Ltd., London, 1931).
[6] D. M. Smith, Metallurgical Analysis by the Spectrograph, British Non-Ferrous Metals Research Assoc., Research Monograph No. 2, London (1933).
[7] D. M. Smith, The Spectrographic Analysis of Tin. Tech. Pub. Int. Tin Research Development Council, Series A, No. 46 (1936).
[8] H. Töpelmann and W. Shuhknecht, Z. anal. Chem. **86,** 160 (1931).
[9] C. S. Hitchen, Am. Inst. Mining Met. Engrs., Tech. Pub. No. 494 (1932–33).
[10] J. W. Stewart, Proc. Am. Soc. Testing Materials **39,** 788 (1939).
[11] G. Scheibe, C. F. Linström and O. Schnettler, Z. angew. Chem. **44,** 145 (1931).
[12] D. H. Follett, J. Sci. Instr. **13,** 221 (1936).
[13] R. Breckpot and J. Eeckhout, Natuurw. Tijdschr. **20,** 92 (1938).
[14] John R. Freeman, Jr., J. A. Scherrer, and J. Rosenberg, BS J. Research **4,** 1 (1930) RP129.

[15] B. F. Scribner, Proc. 5th Summer Conference on Spectroscopy and Its Applications, p. 51 (John Wiley & Sons, New York, N. Y., 1938).
[16] C. L. Mantell, Tin (The Chemical Catalog Co., New York, N. Y., 1929).
[17] H. Kaiser and A. Wallraff, Ann. Physik **34,** 297 (1939).
[18] H. Kaiser, Spectrochimica Acta **1,** 477 (1941).
[19] L. W. Strock, Spectrum Analysis with the Carbon Arc Cathode Layer (A. Hilger, Ltd., London, 1936).
[20] K. B. Thomson and O. S. Duffendack, J. Opt. Soc. Am. **23,** 101 (1933).
[21] J. S. Owens, Metals & Alloys **9,** 15 (1938).

WASHINGTON, October 27, 1941.

U. S. Department of Commerce National Bureau of Standards

RESEARCH PAPER RP1452

Part of Journal of Research of the National Bureau of Standards, Volume 28, February 1942

CALCULATION OF PROTEIN-ANION AFFINITY CONSTANTS FROM ACID TITRATION DATA

By Jacinto Steinhardt [1]

ABSTRACT

It has been shown earlier that the titration curves of wool and other proteins obtained with different strong acids differ widely in position with respect to the pH coordinate. By assuming that these differences were due to combination of the protein with anions as well as with hydrogen ions, it was possible to calculate from the pH of the midpoint of each curve numerical values of the affinity of each anion for wool. In the present paper modifications of the equations for calculating anion affinity are described. It is shown that the new equations describe the titration curves as a whole instead of merely the positions of their midpoints. The new forms are also shown to describe the effects of the presence of salts on the titration curves at least as adequately as did the earlier ones.

CONTENTS

	Page
I. Introduction	191
II. The calculation of affinity with the modified equations	192
III. Experimental justification of the modified equations	195
1. Data obtained in the absence of salt	195
2. Data obtained in the presence of salt	196
IV. References	199

I. INTRODUCTION

It has been shown previously that wool combines reversibly with different acids to very different extents [2, 6].[2] The titration curves obtained with each acid (amounts combined plotted against pH), while essentially congruent with one another, differ widely in position with respect to the pH coordinate. The existence of these differences, which have also been found with the soluble protein, egg albumin, distinguishes the reaction of proteins with acids from other acid-base equilibria, and indicates that more is involved than a proton exchange. Earlier experiments concerned with the effect of potassium chloride on the titration curves obtained with hydrochloric acid suggested an interpretation in terms of combination of the protein with anions as well as with hydrogen ions [3]. A simple extension of the earlier

[1] Research Associate at the National Bureau of Standards, representing the Textile Foundation.
[2] Figures in brackets indicate the literature references at the end of this paper.

analysis was therefore employed to calculate numerical values of the several anion-protein dissociation constants (values of K_A' corresponding to titration with each acid, which were shown to differ from one another many thousandfold. The equations employed and the constants so calculated were used in analyzing the effects on the curves of the presence of salts of some of the acids, and in calculating the heats of dissociation from the protein of a number of the anions involved.

The present paper describes a slight modification in the method of calculation, which is made in order to extend the range of usefulness of the previously formulated equations. With this modification, the equations represent quite closely the course of the entire curves and not merely, as before, the relative positions of their respective midpoints.

II. THE CALCULATION OF AFFINITY WITH THE MODIFIED EQUATIONS

The equations previously used to represent the dependence of the amounts combined on the hydrogen ion and anion activities (a_H and a_A) were derived by considering the following postulated equilibria, each governed by its corresponding constant:

$$\begin{array}{ll} K_H' & WHA \rightleftharpoons WA^- + H^+ \\ K_A' & WA^- \rightleftharpoons W^* + A^- \\ K_H & WH^+ \rightleftharpoons W^* + H^+ \\ K_A & WHA \rightleftharpoons WH^+ + A^-, \end{array}$$

in which W^*, WH^+, etc., represent ionic states of wool. The constants are not independent but are necessarily interrelated by the equation $K_H' K_A' = K_H K_A$.

Two different expressions for the amounts of acid combined in the absence of salt were obtained by combining these equilibria:

$$\frac{[WHA]+[WH^+]}{[WHA]+[WH^+]+[WA^-]+[W^*]} = \frac{1}{1+\frac{K_H'}{a_H}\left[\frac{a_H+K_A'}{a_H+K_A}\right]} \quad (1)$$

$$\frac{[WHA]+[WA^-]}{[WHA]+[WH^+]+[WA^-]+[W^*]} = \frac{1}{1+\frac{K_A}{a_H}\left[\frac{a_H+K_H}{a_H+K_H'}\right]}. \quad (2)$$

On the basis of the methods used earlier for measuring the amounts of acid combined with wool, eq 1 represents the fraction of the wool fully combined with acid when the parameters are such that $[WH^+] > [WA^-]$. Equation 2 represents this fraction in the opposite case, $[WA^-] > [WH^+]$. Because of this difference in the conditions of their applicability, eq 1 and 2 are referred to hereafter as the low-affinity and the high-affinity equations, respectively. K_A' may be obtained

directly from a_H, the value of a_H at which half the maximum amount of acid is bound, by means of the relations:

$$K_A' = \frac{a_H(a_H - K_H')}{K_H'} \times \frac{K_H}{K_H - a_H} \tag{1'}$$

$$K_A' = \frac{a_H(a_H + K_H')}{K_H'} \times \frac{K_H}{K_H + a_H}, \tag{2'}$$

which apply respectively to the same conditions as eq 1 and 2.

It is evident that the simple equations used to calculate K_A' were derived from the law of mass action by treating the dissociation of each ion from the protein as if each dissociation occurred in a different molecule (i. e., as if the protein molecules were strictly monovalent). Formulations based upon this obviously unreal assumption must fail to describe accurately the dependence of the amounts of acid (or of hydrogen ion) combined (i. e., undissociated) as a function of pH, regardless of their usefulness in predicting the dependence of the position or shape of the titration curve with a given acid relative to other titration curves, or its dependence on other variables, such as the anion concentration. When sets of dissociating groups are present in a single molecule instead of being uniformly distributed among different molecules, interaction between the members of each set is bound to result—that is, the state of ionization of the molecule as a whole determines its charge, and must have an influence on the tendency of any one group to ionize. The formulation of an equation in terms of a *single* dissociation constant disregards that influence. However, it was pointed out previously [2, 3, 5] that the oversimplified equations could be made to represent the entire course of the individual titration curves very closely if the concentration terms were permitted to enter into the equations as square roots. The constants K_H', K_A', etc., must then be changed for numerical consistency in the computation to the corresponding square roots $(K_H')^{1/2}$, $(K_A')^{1/2}$, etc., although the actual average values of the dissociation constants may be still given by the first powers [5,[11]]. Equations of this type (in which, however, the only variable was the hydrogen-ion concentration) have been used by Kern [1] in describing titration data obtained with a number of compounds of high molecular weight. In the present work the anion concentration terms must also be changed to square roots, since it has already been demonstrated [3] that hydrogen-ion and anion terms affect the acid-combination function to approximately equal extents.

If, in order to gain the advantages described, all activity terms and constants are introduced as square roots, $\left([WH^+] = \frac{[W^-][H^+]^{1/2}}{K_H^{1/2}}, \text{etc.}\right)$ the foregoing equations become the following:

$$\text{Fraction combined} = \frac{1}{1 + \left(\frac{K_H'}{a_H}\right)^{1/2}\left[\frac{a_H^{1/2} + (K_A')^{1/2}}{a_H^{1/2} + (K_A)^{1/2}}\right]} \tag{3}$$

$$\text{Fraction combined} = \frac{1}{1 + \left(\frac{K_A}{a_H}\right)^{1/2}\left[\frac{a_H^{1/2} + (K_H)^{1/2}}{a_H^{1/2} + (K_H')^{1/2}}\right]} \tag{4}$$

and K_A' should be calculated by the relations:

$$(K_A')^{1/3} = \frac{a_H^{1/3}[a_H^{1/3} - (K_H')^{1/3}]}{(K_H')^{1/3}} \times \frac{k_H^{1/3}}{K_H^{1/3} - a_H^{1/3}} \tag{3'}$$

$$(K_A')^{1/3} = \frac{a_H^{1/3}[a_H^{1/3} + (K_H')^{1/3}]}{(K_H')^{1/3}} \times \frac{K_H^{1/3}}{K_H^{1/3} + a_H^{1/3}} \tag{4'}$$

It is apparent that the values of K_A' and K_H', calculated from the modified equation, will differ somewhat from those previously calculated from the equations which lack the empirical exponent. The extent of this difference is small, as is made evident elsewhere [7].

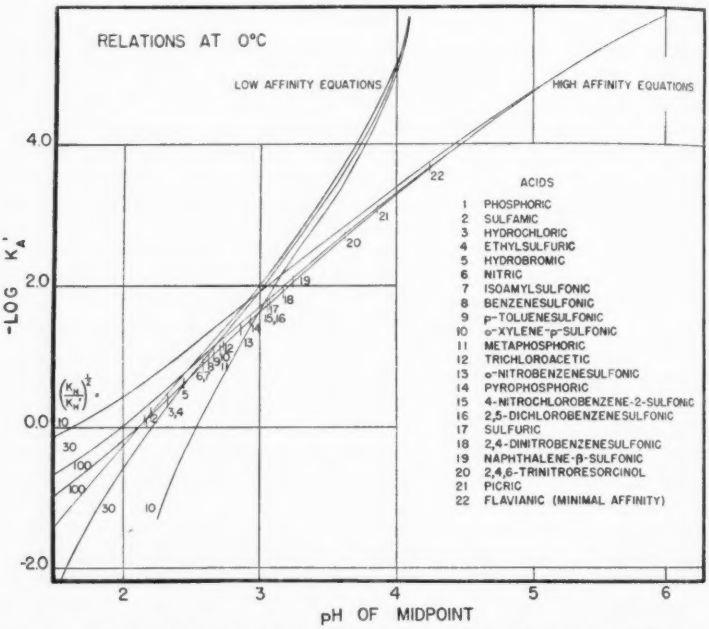

FIGURE 1.—*Relation between the position of the acid titration curve with respect to* pH *and the affinity of the anion of the acid for protein.*

Two sets of curves are shown, representing eq 3′ (low affinity) and 4′ (high affinity), respectively. The individual curves within each set were obtained by assuming three different ratios of $(K_H)^{1/3}$ to $(K_H')^{1/3}$. The point for *o*-phenolsulfonic acid, which has been omitted, would coincide with the point for *p*-toluenesulfonic acid.

In the earlier treatment K_H, which cannot be evaluated directly, was eliminated by an approximation which further simplified eq 1′ and 2′. The simplified equations were represented graphically, and the values of K_A' tabulated were obtained from the graph [2, 6]. In the present paper, advantage is taken of the exact forms (eq 3′ and 4′) to appraise the effect of uncertainty as to the value of K_H on the values of K_A' calculated. This has been done (fig. 1) by plotting both equations 3′ and 4′ for three different ratios of $(K_H/K_H')^{1/3}$. The values selected for this ratio, 10, 30, and 100 are greater than unity because of electrostatic considerations which have been discussed elsewhere [2, 6]. It is apparent that for each equation the relation

between affinity and midpoint pH becomes relatively independent of the ratio chosen if the affinity is high, but is increasingly dependent upon it as the anion affinity decreases. The highest ratio of the three represented has been adopted in further calculations because it leads to the results most compatible with the shapes of the individual titration curves, and with the effect of chlorides on the position of the hydrochloric acid titration curves previously described [3].

Fortunately, with the highest of these ratios it is practically immaterial whether eq 3′ or 4′ be used for the calculation of affinity in the case of the only anions (i. e., those with the lowest affinities) for which the choice between the two equations is not immediately apparent. In figure 1 the position of the midpoint of each of the titration curves at 0° C has been indicated by a short vertical line intercepting the curve which represents eq 4′ and a ratio of 100. Since all the points indicated fall in a region for which the curve representing eq 4′ is lower than the curve representing eq 3′, it is obvious that with this ratio eq 4′ rather than eq 3′ must be used to calculate the affinity for wool of all of the anions represented.[3] In another paper [7] values of K_A' for 33 different acids obtained by the use of eq 4′ are tabulated and compared with those previously given.

III. EXPERIMENTAL JUSTIFICATION OF THE MODIFIED EQUATIONS

1. DATA OBTAINED IN THE ABSENCE OF SALT

The accuracy with which the modified equation describes in detail individual titration curves is shown in figure 2. The curves in this figure represent the theoretical relations which are obtained when values of K_A', shown in figure 1 for a number of acids selected to cover a wide range of affinity, and the value of K_H' at 0°C previously established [3, 5] are inserted in eq 4. The logarithmic ordinate has been chosen because it yields approximation to a linear relation to pH [3], and furnishes a more critical visual criterion of fit than a linear ordinate allows. Because of the exaggerated sensitivity of this form of function to experimental error when either very large or very small amounts of acid are combined, the data represented are limited to amounts combined between about 5 percent and 95 percent of the maximum. An additional reason for this restriction is the existence of an "excess" take-up of acid beyond 0.82 millimole per gram; it cannot be expected that a function based on this "maximum" will be entirely successful in representing data which approach this value. 0.03 millimole has been subtracted from all the amounts combined, in order to eliminate the estimated contribution of the histidine content of the fibers; the data are thus restricted to the results of back-titrating a single set of groups, the carboxyls.

The good agreement of the curves with the experimental data shows that practically the same values of K_A' as these calculated from the midpoint pH values of each of the titration curves would be obtained if points representing any other extent of combination had been consistently chosen, and used in conjunction with the appropriately modified eq 4′. This would not have been the case if the

[3] The pH at which eq 3′ and 4′ intersect for any given ratio of $(K_H/K_H')^{1/2}$, is the pH above which $[WA^-]$ is larger than $[WH^+]$. By definition, eq 4′ applies when $[WA^-]$ is larger than $[WH^+]$.

integral power equation previously employed had been used. This ability of eq 4 to describe the titration curves in detail is essential to a treatment of more complicated systems, such as mixtures of acids

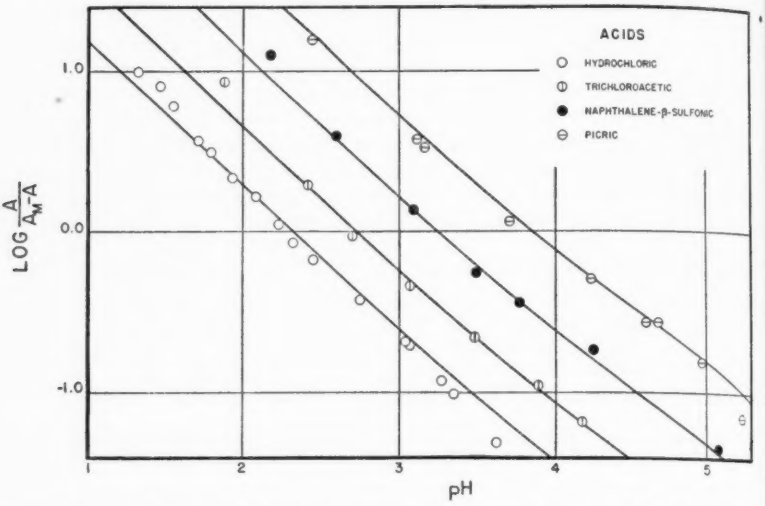

FIGURE 2.—*The amounts of 4 different acids combined by wool as a function of* pH.

The curves are theoretical (eq 4) and have been calculated for each acid by using the values of K_A given by eq 4'.

or acids and salts, since attention cannot then be confined to the points of half-maximal combination [4].

2. DATA OBTAINED IN THE PRESENCE OF SALT

Curves obtained in the presence of salt (constant concentrations of the anions of each respective acid) have a more gradual slope (about −0.5 instead of −1.0 in a logarithmic plot such as that used in fig. 2). The relation between the amounts of acid bound and pH for these curves is described almost equally well by the modified equations. This is illustrated in figure 3; the curve drawn through the experimental points for hydrochloric acid is theoretical, using the value of K_A' calculated from the experiment *without salt*. The equation used to calculate this curve was

$$\text{Fraction combined} = \frac{[WHA]+[WH^+]+\frac{a_H}{a_A}([WA^-]-[WH^+])}{[WHA]+[WH^+]+[WA^-]+[W^\pm]}$$

$$= \frac{1}{1+\left(\frac{K_H'}{a_H}\right)^{1/2}\left[\frac{a_A^{1/2}+(K_A')^{1/2}}{a_A^{1/2}+K_A^{1/2}}\right]} + \frac{\frac{a_H}{a_A}\left[\left(\frac{a_A}{K_A'}\right)^{1/2}-\left(\frac{a_H}{K_H}\right)^{1/2}\right]}{\left(\frac{a_H}{K_H}\right)^{1/2}\left[\left(\frac{a_A}{K_A}\right)^{1/2}+1\right]+\left(\frac{a_A}{K_A'}\right)^{1/2}+1} \quad (5)$$

This equation differs from eq 3 only by the presence of a correction term which affects appreciably only the upper part of the curve. This *low-affinity* form (eq 3), rather than the high-affinity form, is required because when salt is present the amounts of *acid* bound should be almost wholly given by the sum of the terms [WHA] and [WH^+]. Even though [WA^-] is larger than [WH^+], the resulting negative charge on the fibers should be neutralized almost entirely by cations other than hydrogen ions—that is, salt as well as acid is combined. The small correction term is inserted to account for the part of this neutralization brought about by adsorption of hydrogen ions. If the high-affinity form were used, the quantity calculated would be the sum of acid *plus salt* combined.

The variation with pH of the amounts combined in the case of the other two acids (fig. 3) is also well described by eq 5, but the positions with respect to pH of the predicted curves differ appreciably from those required by the data. This discrepancy is illustrated by the curve

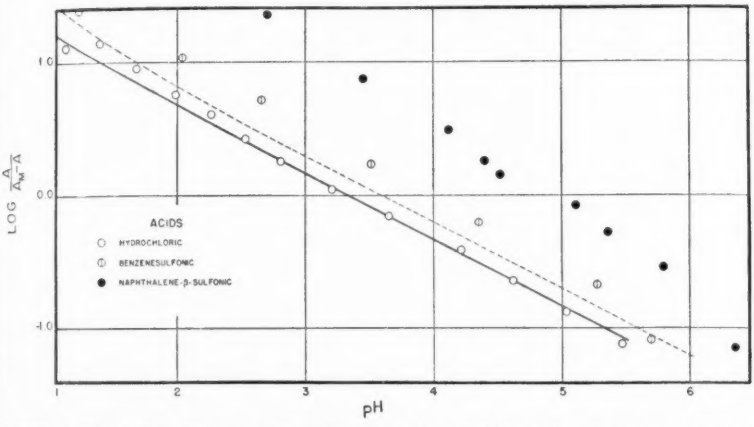

FIGURE 3.—*The amounts of three different acids combined by wool as a function of* pH, *in the presence of a constant concentration (0.1 M) of their anions.*

The solid line is theoretical (eq 5) and has been calculated by using the value of K_A' for chloride ion given by eq 4'. The broken line was calculated with the value of K_A' for benzenesulfonate.

given for benzenesulfonic acid (the broken line), calculated by using the value of K_A' given by the experiments with this acid without salt. Such a discrepancy is inherent in the use of eq 5 with anions of high affinity, because this equation cannot represent curves with midpoints at pH values above 4.2, the value of pK_H'; thus the equation tends to compress the wide range of midpoints observed experimentally into the pH range below this value. The high-affinity form, eq 4, despite its obvious inapplicability to experiments with salt, is more successful in predicting the large displacements between the upper parts of the curves obtained with different acids, even in the presence of salt [6]. This may signify that there is a greater inherent probability of neutralizing a negative charge on a fiber with a hydrogen ion than with a sodium or potassium ion. Should this be true, the calculation of accurate values of K_A' under the more complicated conditions represented in the experiments with salt requires accurate measurements of

the combination of *acid plus salt*, to which the simple assumptions underlying eq 4 can be applied. It has been determined experimentally that appreciable amounts of salt are combined. The amounts, however, appear to be smaller than the difference in uptake predicted by eq 4 and 5.

Since it has been shown previously that the equations without the fractional exponent are of the right form to describe the nature of the dependence of the position of the hydrochloric acid titration curves on the concentration of added salt, it is necessary to show that eq 5 can be used to describe those relations quantitatively, or at least equally well. The extent to which this may be done is shown in figure 4, in which the pH of the midpoint of the titration curves

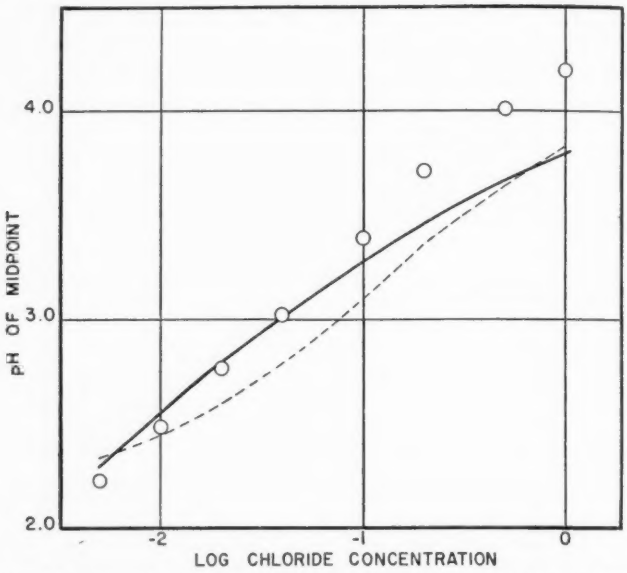

FIGURE 4.—*The dependence of the* pH *of half-maximal combination with hydrochloric acid on the level at which the chloride concentration is held constant.*

The solid line represents eq 5. The broken line was calculated from the equations previously used [3].

obtained with hydrochloric acid is plotted as a function of the total chloride-ion concentration. The solid curve represents the relation between these variables predicted by eq 5 with a ratio of $(K_H/K_H')^{\frac{1}{2}}$ of 100, and the value of K_A' used in figure 2. The agreement with the experimental data is satisfactorily close for solutions of less than 0.1 *M* concentration. The discrepancy at higher concentrations is probably not important in view of the consistent neglect in this analysis of all questions of the relation between thermodynamic activity and concentration in both the wool and the aqueous phases.[4] High values of the ratio $(K_H/K_H')^{\frac{1}{2}}$ give a better approximation to the data than do low values.

[4] The discrepancy at high concentrations could be greatly reduced by adopting a smaller value for K_H'. Consistent use of a smaller value of K_H' would change the numerical values of K_A' but would have little effect on theoretical functions other than the one considered here.

The relationship predicted by an exact analysis in terms of the earlier equations [3] is shown by the broken line; the actual experimental values are fitted less well by these earlier equations than by eq 5. Since the simple assumptions underlying the present analysis are more likely to be applicable to the most dilute solutions, the fact that eq 5 yields the correct slope as well as the best approximation to the absolute experimental values in the most dilute range is definitely in its favor. In every particular in which they have been tested, therefore, relationships based on eq 3 and 4 of this paper have proved equally useful or superior to those based on the older forms. In experiments with mixtures, the new modifications are of still wider general utility [4].

IV. REFERENCES

[1] W. Kern, Z. physik. Chem. [A] **189,** 249 (1938); Biochem. Z. **301,** 338 (1939).
[2] J. Steinhardt, Ann. N. Y. Acad. Sci. **41,** 287 (1941).
[3] J. Steinhardt and M. Harris, J. Research NBS **24,** 335 (1940) RP1286; Textile Research **10,** 181 (1940); Am. Dyestuff Reptr. **29,** 103 (1940).
[4] J. Steinhardt and M. Harris, Proc. Am. Soc. Biological Chemists XXXV, J. Biol. Chem. **140,** cxxiv (1941). A more complete account is in preparation.
[5] J. Steinhardt, C. H. Fugitt, and M. Harris, J. Research NBS **25,** 519 (1940) RP1343; Textile Research **11,** 72 (1940); Am. Dyestuff Reptr. **29,** 607 (1940).
[6] J. Steinhardt, C. H. Fugitt, and M. Harris, J. Research NBS, **26,** 293 (1941) RP1377; Textile Research **11,** 259 (1941); Am. Dyestuff Reptr. **30,** 223 (1941).
[7] J. Steinhardt, C. H. Fugitt, and M. Harris, J. Re earch NBS **28,** 201 (1942) RP1453.

WASHINGTON, November 7, 1941.

U. S. DEPARTMENT OF COMMERCE NATIONAL BUREAU OF STANDARDS

RESEARCH PAPER RP1453

Part of Journal of Research of the National Bureau of Standards, Volume 28, February 1942

FURTHER INVESTIGATIONS OF THE AFFINITIES OF ANIONS OF STRONG ACIDS FOR WOOL PROTEIN

By Jacinto Steinhardt,[1] Charles H. Fugitt,[1] and Milton Harris [1]

ABSTRACT

Titration curves of wool with 18 strong acids at 0°, 25°, or 50° C have been added to the data for 19 others presented earlier. Several have been investigated at more than one temperature. The reversibility of the equilibria measured has been demonstrated quantitatively. New anion-wool dissociation constants, based on modifications of equations previously used to calculate anion-wool affinities, are tabulated for 33 anions, and heats of dissociation of a few anion-wool complexes are also given. The previously reported tendency of affinity to rise with molecular-weight is confirmed; fairly consistent relationships between the affinity and the molecular weights of strong organic acids appear.

CONTENTS

	Page
I. Introduction	201
II. Experimental procedure	202
1. Wool	202
2. Source of acids and specific procedures	203
3. Measurement of reversibility of the combination with acids	205
4. Allowance for the effects of hydrolytic decomposition	205
III. Results and discussion	207
1. Titration curves	207
2. The scale of anion affinities	212
3. Effect of temperature on affinity	214
IV. Relation of chemical structure to affinity	214
V. References	214

I. INTRODUCTION

It has been shown in a previous paper that the titration curves of wool and of other proteins obtained with a number of strong acids are not identical but occupy very widely different positions with respect to the pH coordinate [16].[2] These wide differences have been interpreted as due to combination of protein with anions as well as with hydrogen ions, the combination with each anion being governed by its own distinct dissociation constant. It has been shown also that by making a number of simple assumptions these dissociation constants (or their reciprocals, the affinities) may be calculated from the titration data.

The existence of differences in the affinities of anions for protein has a direct bearing on dyeing theory. A serious difficulty in "chemical" theories of dyeing, which have attempted to draw a close analogy between the combination of fibers with hydrochloric acid and their combination with acid dyes, has been the lack of an explanation of

[1] Research Associates at the National Bureau of Standards, representing the Textile Foundation.
[2] Figures in brackets indicate the literature references at the end of this paper.

why the combination of dyes is relatively fast to water and dilute alkalies while that of hydrochloric acid is not. If the equilibrium of fibers with both of these acids is considered solely in terms of an acid-base (i. e., hydrogen ion) equilibrium, one would conclude that both acids should be bound equally well. The existence of a second dissociation equilibrium involving each anion provides a basis for understanding these differences, and encourages exploitation of the many attractive features of the "chemical" theory of acid dyeing.

Experiments reported elsewhere [14] have shown that the quantitative formulation of the anion affinity concept may be applied to mixtures of acids or of acids and salts, systems which more nearly approach in complexity the dyebaths commonly employed in industry than do the simple systems involved in measurement of titration curves. Measurements of the amounts of each of the anions combined with the fiber have indicated the nature of some of the factors controlling fastness and degree of exhaust. In addition, they have suggested a consistent explanation of the part played by various widely used assistants (such as Glauber's salt) in promoting level or solid dyeing, which will be discussed elsewhere. Since it is indicated by these experiments that the relative effectiveness of such assistants is directly related to their affinities, it has appeared particularly important to determine the affinities of a still larger number of compounds of more diverse types than those previously investigated in order to establish with greater certainty the relation between affinity, size, and structure of ions. Such information, especially if it is combined with more detailed knowledge of the variation of affinity at higher temperatures, would provide a basis for selecting economically practical leveling agents having the desired range of affinities for wool.

The present paper, besides describing measurements of the affinity for wool of the anions of an additional number of strong acids, makes use of certain refinements in the methods of calculating affinity [11] which make possible a more detailed comparision of theoretical predictions with experimental data. On the basis of these refinements, the data previously presented are recomputed and a recapitulation is made of the results obtained with 33 strong acids. As a result, the discussion of the relation between chemical structure and affinity in this paper is based on a broader survey than was previously available.

II. EXPERIMENTAL PROCEDURE

Methods of purification of the wool, measurement of pH values, and determination of the amounts of acid combined have been described in earlier publications [12, 15, 16]. Additional details concerning the specific materials and procedures used in the present investigation are described in the following subsections.

1. WOOL

All of the new measurements described in this paper were made with a single lot of purified wool having a slightly higher acid-binding capacity than the wool used in earlier work. In order to allow for this small difference (about 0.03 millimole), the pH at which 0.415 millimole per gram is combined has been taken as the "midpoint pH," by means of which the position of each curve with respect to the pH coordinate has been expressed, in place of the pH at which 0.40

millimole is combined, which was previously used. When this is done, the half-combination points of curves obtained on both lots of wool with the same acid occur at the same pH value; therefore the anion dissociation constants calculated are the same.

As in previous work, allowance was made for acid neutralized by the small amount of combined cation in the purified fibers. The hydrogen-ion equivalence of their cation content, as shown by electrodialysis [9], was 0.015 millimole per gram, less than one-half as great as in the wool used in the earlier work. As previously explained, the validity of this procedure is in question only when small amounts of acids of high affinity are combined; since this occurs at very high dilution of the acid, it is possible that a fraction of the combined cations remains on the fiber in competition with the few hydrogen ions present. At most a very small number of the measurements in this paper were made under conditions admitting such a possibility; therefore the full correction has been applied to all the data.

When solutions more concentrated than 0.02 *M* were used, the usual corrections were made for the selective absorption of water from the solution by the fibers, and where necessary, for the effects of any hydrolysis undergone by the wool. (See 4 in this section.)

2. SOURCE OF ACIDS AND SPECIFIC PROCEDURES

Except where particularized further below, commercial cp products were employed, and all procedures used were the same as those previously described [12, 15, 16].

(1) Sulfamic and sulfosalicylic acids were Eastman products recrystallized from water to remove sulfuric acid present as an impurity.

(2) Naphthalene-β-sulfonic acid (Eastman) was separated from traces of naphthalene by filtration of the moderately dilute stock solutions.

(3) Isoamylsulfonic acid was prepared from the sodium salt (Eastman) by precipitation with lead nitrate and treatment of the lead salt, suspended in water, with hydrogen sulfide.

(4) Pyrophosphoric acid was prepared from tetrasodium pyrophosphate (Monsanto) by precipitation with lead nitrate and treatment of the lead salt, suspended in water, with hydrogen sulfide. Determination of the titration curve of the free acid showed that two equivalents of hydrogen ion (one-half of the available acidity) are almost completely dissociated in the pH range above 2.0 and that the third and fourth hydrogens are practically undissociated in solutions below pH 4.8. Since most of the measurements made with this acid fall between these two values, the curve obtained represents combination of wool with the divalent dihydrogen pyrophosphate ion. Assays of solutions of this acid were made by titrating to an electrometric endpoint at pH 4.8 and calculating the results as two equivalents per mole. Tests showed that the material was not appreciably hydrolyzed at 0° C during the time required for the attainment of equilibrium with the wool.

(5) Dodecylsulfonic acid was prepared from dodecylsulfonyl chloride made by the method of Sprague and Johnson [10] from lauryl bromide (Eastman). The sulfonyl chloride was hydrolyzed by refluxing with 1.5 *M* sodium hydroxide, and the lead salt was precipi-

tated with lead acetate after acidifying the mixture with acetic acid. The free acid was obtained from the lead salt by the method of Noller and Gordon [6]. Special care was required to assure the removal of all perceptible traces of hydrochloric acid in this procedure. The affinity of dodecylsulfonate ion for wool is so great that the presence of even small amounts of hydrochloric acid will affect materially the pH at which a given amount of dodecylsulfonic acid is combined; that is, the pH will be determined by the hydrochloric acid present rather than by the extremely small proportion of dodecylsulfonic acid left uncombined.

Concentrated solutions of this acid appear to be incompletely dissociated [18], but a good titration end point may be obtained with bromocresol purple or bromothymol blue.

(6) Dodecylsulfuric acid and octylsulfuric acid were prepared from sodium salts kindly supplied by the research laboratories of E. I. du Pont de Nemours & Co., Inc. The first was precipitated with lead nitrate and the lead salt was decomposed with hydrogen sulfide; the second was precipitated as the barium salt which was subsequently decomposed with dilute sulfuric acid. It was necessary to coagulate the sulfide precipitate by adding ethanol, subsequently removed by vacuum distillation.

(7) Diphenylsulfonic acid (Monsanto) was separated from sulfuric acid, present as an impurity, by precipitating its silver salt and decomposing it with hydrogen sulfide. The silver sulfide was filtered off after coagulating it by the addition of alcohol, which was subsequently distilled off in vacuum at low temperature.

(8) *p*-Diphenylbenzenesulfonic acid was prepared from its sodium salt (Eastman) by treatment similar to that described for diphenylsulfonic acid.

(9) Isopropylnaphthalenesulfonic acid was prepared from its sodium salt (the commercial product Aerosol OS) by precipitation with lead nitrate, and treatment of the lead salt, suspended in 50 percent ethanol, with hydrogen sulfide followed by concentration in vacuum at low temperature. The starting material consisted of mixed isomers.

(10) Anthraquinone-β-sulfonic acid was prepared from its sodium salt (Eastman) by precipitating the lead salt and treating it, suspended in 50 percent ethanol, with a small excess of hydrochloric acid. Silver oxide was added in small portions until no further precipitation of silver chloride occurred. The excess silver at this point was determined by the Volhard method, and an equivalent quantity of hydrochloric acid was added to precipitate it. Most of the alcohol was then removed by vacuum distillation at room temperature. The free acid is not entirely stable in concentrated aqueous solutions, being transformed slowly to a substance which undergoes a color change (to red) in the pH range 6 to 7. However, very little change occurred in the interval required by the measurements.

(11) *p*-hydroxyazobenzene-*p'*-sulfonic acid was prepared from its sodium salt (Eastman) by precipitation with lead nitrate from a saturated solution. Further stages of the preparation were the same as for anthraquinone-β-sulfonic acid. This dye, unlike Orange II, which it somewhat resembles in structure, apparently forms no complexes with silver ion. Thus, use can be made of silver oxide in preparing the acid form.

(12) Sodium metaphosphate was prepared by strongly heating sodium dihydrogen phosphate, as in the method of Briggs [2]. The sodium glass obtained by rapidly cooling the fused material dissolved slowly in cold water (0° C) without hydrolyzing. Titration with hydrochloric acid at 23° C showed that the amount of hydrogen ion combined was only one-third as great as the sodium or phosphorus present. Thus, two-thirds of the hydrogen in hexametaphosphoric acid is strongly acidic, as Hisar has also found [5]. The apparent pK at 23° C of the weakly acidic group is 2.28. The sodium glass is therefore regarded as trisodium trimetaphosphate, or a higher polymer of this compound, consistent with the findings of Partridge, Hicks, and Smith [7]. Although this interpretation differs from that of Briggs [2], it is not inconsistent with his data.

The experimental solutions were made up by adding various amounts of hydrochloric acid to solutions of a constant amount of the sodium glass. They thus differ from the other experimental solutions in containing, in addition to hydrogen ion and anion (monohydrogen trimetaphosphate or a polymer), equivalent amounts of sodium chloride plus residual amounts of the dissolved glass.

(13) The acid form of Orange II was prepared as previously described [16]. When stored in Pyrex bottles in the cold, no insoluble impurity was formed.

3. MEASUREMENT OF REVERSIBILITY OF THE COMBINATION WITH ACIDS

A number of the measurements were obtained by first allowing the wool to come into equilibrium with a solution which initially contained a relatively high concentration of acid, determining the amount combined by the usual methods, and then diluting a known volume of the solution (which still contained all the wool) with a known volume of water. After a suitable interval, a second aliquot of the solution was titrated, and the acid *given off* by the fiber was calculated. The acid remaining on the fiber was then entered in the table against a new pH determination. Measurements made in this way thus represent approach to a final state from the opposite direction to that represented by the other measurements.

4. ALLOWANCE FOR THE EFFECTS OF HYDROLYTIC DECOMPOSITION

When amide bonds in the wool are hydrolyzed, the *apparent* acid-binding capacity as measured by our method increases by an amount corresponding to the ammonia liberated. Accordingly, a correction for the effect of this ammonia was made wherever required. If peptide bonds also are hydrolyzed and soluble decomposition products only are formed, no additional correction is required except for the decrease in weight of the undissolved protein, which is usually negligible. However, if some *insoluble* decomposition products are formed, a real increase in acid-binding power may be observed. In earlier work with hydrochloric acid, only small amounts of ammonia (negligible at 0° C) were formed, even with high concentrations of acid; of other dissolved products only traces could be detected. With acids of higher affinity, however, ammonia is liberated more rapidly; it may be detected in experiments made at 25° C or 50° C with initial con-

centrations of certain acids as low as 0.005 *M*. The necessary corrections (table 1) show a tendency to increase as the affinity of the anion of the acid increases, and have reached extreme values for the most concentrated solutions (0.05 *M* or less) of over 0.3 millimole per gram of wool in equilibration experiments requiring 3 to 4 days at 50° C. Even at room temperature these acids have a noticeably destructive effect. Analyses for ammonia were made by the usual alkaline distillation, as well as by adsorption of the ammonia on

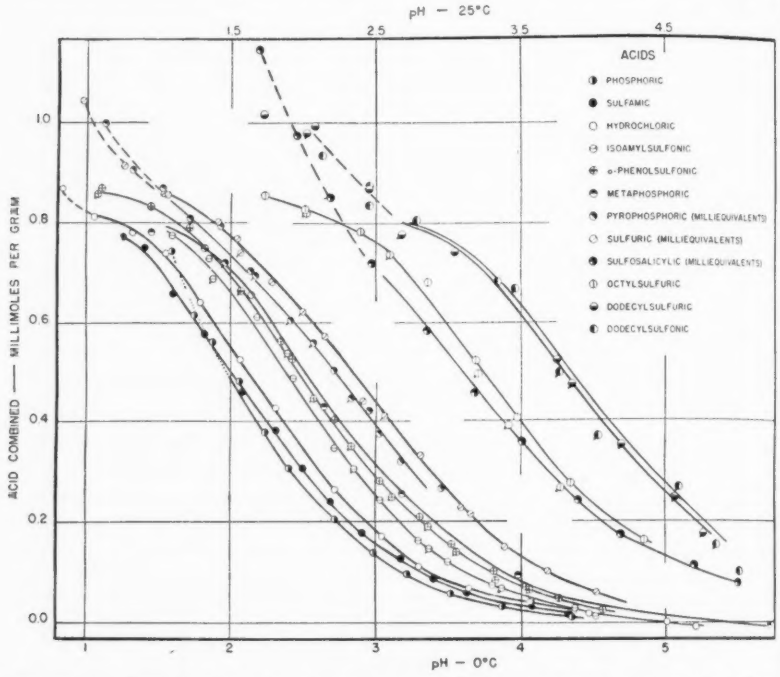

FIGURE 1.—*Combination of wool protein with 12 different strong acids at 0° or 25° C.*

The pH scale at the bottom of the figure applies to the data obtained at 0° C. The scale at the top of the figure refers to the data obtained at 25° C. The significance of the tagged circles is described in the text.

permutit, followed by alkaline distillation. The good agreement between the methods indicates that the ammonia found is a primary decomposition product rather than the product of secondary breakdown of dissolved protein during the alkaline distillation. Kjeldahl digestion of other aliquots has shown that appreciable amounts of nonammonia nitrogen are also present; thus, considerable hydrolysis of peptide bonds has probably occurred in these extreme cases. The corrections applied for the effects of hydrolysis at or near the tops of the curves obtained with the acids of highest affinity at 25° and 50° C may therefore be inadequate to transform the data to values characteristic of the unchanged wool. It is in these cases, especially, that the flattening in the neighborhood of 0.83 to 0.84 millimole per gram combined, which characterizes the curves for the acids of lower affinity, disappears.

III. RESULTS AND DISCUSSION

1. TITRATION CURVES

The data obtained with 18 different acids at 1 or more of 3 different temperatures are summarized in table 1 and are represented graphically in figures 1 (0° and 25° C) and 2 (50° C). With most of the acids used the data represented have been obtained by approaching equilibrium from both sides, that is, by starting with fibers which are combined with more than their equilibrium amount of acid as well as with fibers that are initially uncombined. The "reversed" measurements are indicated in table 1 by italics, and by tagged circles in the figures. It is clear that the sets of data obtained in both ways are

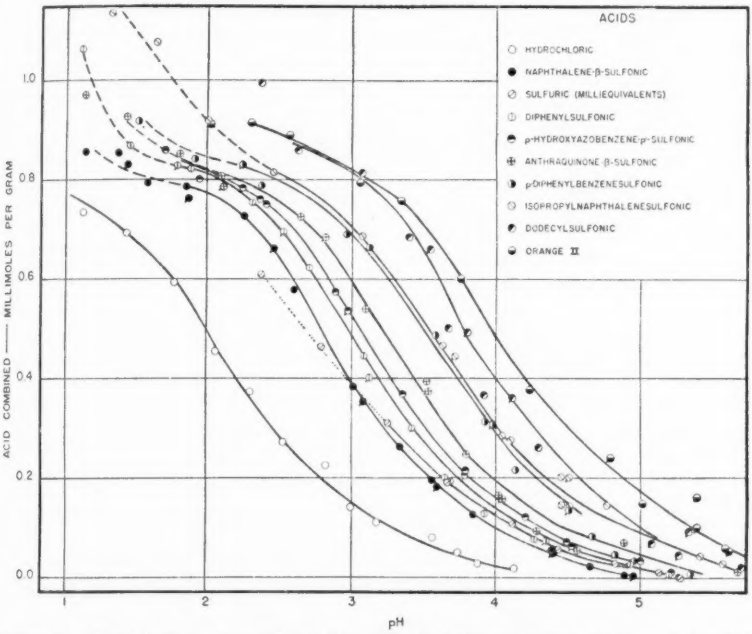

FIGURE 2.—*Combination of wool protein with 10 different strong acids as a function of* pH *at 50° C.*

The significance of the tagged circles is described in the text.

consistent with one another. This agreement constitutes proof that the anion-wool associations measured are fully reversible, and that the wool in combining with acid suffers no permanent alteration until amounts which approach 0.8 millimole per gram are combined.[3] In addition, such agreement eliminates the possibility that the results obtained are affected by the presence of acid impurities which differ appreciably in affinity from the substance under investigation. Other indications of the reversibility of the combination with acid have already been cited. Taken as a whole, they fully justify a theoretical treatment based on equilibrium considerations [12, 16].

[3] Data obtained with β-naphthoquinone-4-sulfonic acid did not fulfill this criterion of reversibility except for small amounts combined, and are therefore omitted from this paper. This exceptional behavior is consistent with the known reactivity of quinones with proteins. It is noteworthy that this dye changed color on combining with the fibers, and gave a curve of combination having an appreciably lower degree of dependence on pH than did all the other acids.

TABLE 1.—*Combination of wool protein with various strong acids, in the absence of added salt*

[Only new measurements, obtained with a single batch of wool, are included here. Italicized entries represent equilibria approached from the side of greater amounts combined]

A. RESULTS OBTAINED AT 0° C

Hydrochloric acid		[a] Phosphoric acid		Sulfamic acid		[b] Metaphosphoric acid		Isoamylsulfonic acid		[c] Sulfuric acid		[c] Pyrophosphoric acid		o-Phenolsulfonic acid	
pH	*Millimoles/g*	pH	*Millimoles/g*	pH	*Millimoles/g*	pH	*Millimoles/g*	pH	*Millimoles/g*	pH	*M-eq/g*	pH	*M-eq/g*	pH	*Millimoles/g*
0.830	0.871	1.584	0.745	1.253	0.773	1.449	0.783	1.592	0.776	0.97	1.045	1.126	1.006	0.708	0.893
1.051	.814	1.745	.616	1.402	.751	2.639	.433	1.848	.730	1.26	0.944	1.318	0.907	*1.075*	*.860*
1.315	.782	1.870	.562	1.598	.660	3.178	.259	*1.872*	*.690*	*1.53*	*.860*	1.525	.870	1.106	.809
1.546	.740	2.053	.484	1.818	.579	3.976	.097	2.173	.612	1.56	.857	1.711	.809	*1.589*	.887
1.788	.643	2.232	.382	2.077	.472	5.85	−.005	*2.388*	*.540*	1.81	.804	1.924	.795	1.445	.830
2.061	.528	2.400	.311	2.305	.385			2.427	.490	2.044	.770	*1.961*	*.722*	*1.716*	.768
2.308	.430	2.712	.207	2.493	.310			2.713	.350	*2.066*	*.742*	2.135	.705	1.812	.736
2.716	.267	2.980	.140	2.690	.244			*2.850*	*.310*	2.281	.683	*2.169*	*.698*	*2.068*	.666
3.040	.174	3.210	.098	2.905	.181			3.030	.247	*2.492*	*.624*	*2.359*	*.611*	2.134	.637
3.294	.114	3.510	.060	3.169	.129			3.295	.166	2.645	.573	*2.570*	*.561*	*2.341*	.562
3.636	.071	3.869	.034	3.395	.089			*3.566*	*.149*	2.901	.445	2.708	.505	2.418	.530
4.060	.043	4.349	.012	3.629	.061			3.498	.124	*3.056*	*.415*	*2.827*	*.460*	*2.665*	.490
4.465	.020			4.07	.034			3.800	.077	3.303	.336	2.950	.424	2.714	.403
5.010	.003			4.32	.018			*3.864*	*.071*	3.585	.231	*3.020*	*.379*	*2.832*	.383
5.22	−.007							4.066	.044	*3.655*	*.219*	3.170	.325	3.027	.285
								4.361	*.028*	3.884	.153	3.450	.269	*3.111*	.228
								4.367	.031	4.180	.105			3.302	.213
								4.507	.014	*4.235*	*.102*			*3.358*	.196
										4.513	.063			3.521	.139
										4.734	.035			*3.552*	.128
										4.791	*.034*			3.806	.100
										4.95	.022			*3.821*	.087
														4.030	.074
														4.055	.068
														4.256	.051
														4.584	.027

B. RESULTS OBTAINED AT 25° C

Octylsulfuric acid				Sulfosalicylic acid				Dodecylsulfuric acid				Dodecylsulfonic acid			
pH	Acid neutralized	Ammonia produced	Acid combined	pH	Acid neutralized	Ammonia produced	Acid combined	pH	Acid neutralized	Ammonia produced	Acid combined	pH	Acid neutralized	Ammonia produced	Acid combined
	Millimoles/g	*Millimoles/g*	*Millimoles/g*		*M-eq/g*	*Millimoles/g*	*M-eq/g*		*Millimoles/g*	*Millimoles/g*	*Millimoles/g*		*Millimoles/g*	*Millimoles/g*	*Millimoles/g*
1.735	0.875	0.020	0.855	1.082	1.620	0.026	1.594	1.727	1.193	0.177	1.016	2.129	1.055	0.121	0.934
2.007	.840	.011	.829	1.388	1.407	.020	1.387	*2.020*			*0.980*	*2.452*			.878
2.019			*.821*	1.696	1.169	.018	1.151	2.078	1.147	.152	.995	2.459	0.881	.047	.834
2.397			.784	1.952	0.986	.010	0.976	2.451	0.995	.128	.867	*2.778*			.805
2.595			*.757*	2.188			.850	*2.675*			.777	3.338	.698	.016	.682
2.858			.681	2.470			.719	3.044	.800	.058	.742	*3.459*			.668
3.180			.525	2.850			.584	3.743	.560	.034	.526	*3.760*			.500
3.199			*.499*	3.175			.460	3.85			*.478*	*4.03*			.375
3.477			.412	3.504			.364	*4.19*			*.358*	*4.60*			.273
3.412			*.396*	3.89			.246	*4.87*			*.254*	*4.88*			.157
3.84			.281	4.19			.177	*4.78*			*.181*	5.08			.104
3.77			.272	4.71			.117					*5.52*			.052
4.35			.167	5.06			.081					*5.67*			.025

[a] These measurements fall in the range of pH in which phosphoric acid is monobasic.
[b] Salt was present in these experiments, as explained in the text.
[c] Calculations have been made on the basis of 2 equivalents per mole.

TABLE 1.—*Combination of wool protein with various strong acids, in the absence of added salt*—Continued

C. RESULTS OBTAINED AT 50° C

Hydrochloric acid				β-Naphthalenesulfonic acid				•Sulfuric acid				Diphenylsulfonic acid			
pH	Acid neutralized	Ammonia produced	Acid combined	pH	Acid neutralized	Ammonia produced	Acid combined	pH	Acid neutralized	Ammonia produced	Acid combined	pH	Acid neutralized	Ammonia produced	Acid combined
	Millimoles/g	*Millimoles/g*	*Millimoles/g*		*Millimoles/g*	*Millimoles/g*	*Millimoles/g*		*M-eq/g*	*Millimoles/g*	*M-eq/g*		*Millimoles/g*	*Millimoles/g*	*Millimoles/g*
1.124	0.800	0.064	0.736	1.147	1.032	0.175	0.857	2.370	0.620	0.010	0.610	1.11	1.398	0.334	1.064
1.435	.730	.036	.694	1.380	.956	.081	.855	2.788			.466	1.46	1.015	.146	0.869
1.770	.609	.016	.593	*1.447*	.833	.039	*.852*	3.244			.313	*1.79*	0.875	.042	*.829*
2.055	.471	.014	.457	1.584	.805	.016	.794	3.661			.193	1.88	.772	.018	.833
2.295	.384	.010	.374	1.864			.787	4.107			.110	2.31	.630	.007	.754
2.525			.274	*1.873*			*.761*	4.428			.059	*2.52*			*.696*
2.816			.227	2.254			.727	4.823			.030	2.70			.623
2.990			.143	*2.458*			*.662*	5.130			.010	3.08			.437
3.169			.113	2.597			.579	5.28			.000	*3.12*			*.403*
3.553			.082	3.007			.384					3.41			.301
3.729			.053	*3.078*			*.354*					3.64			.203
3.870			.031	3.330			.265					*3.68*			*.195*
4.127			.021	3.554			.197					3.91			.130
				3.587			*.184*					4.25			.078
				3.842			.129					*4.34*			*.076*
				4.379			.056					*4.93*			*.029*
				4.396			*.051*					*5.20*			*.008*
				4.649			.025								
				4.890			.007								
				4.952			*.007*								

p-Hydroxyazobenzene-*p'*-sulfonic acid				Anthraquinone-β-sulfonic acid				Isopropylnaphthalene-sulfonic acid			
pH	Acid neutralized	Ammonia produced	Acid combined	pH	Acid neutralized	Ammonia produced	Acid combined	pH	Acid neutralized	Ammonia produced	Acid combined
	Millimoles/g	*Millimoles/g*	*Millimoles/g*		*Millimoles/g*	*Millimoles/g*	*Millimoles/g*		*Millimoles/g*	*Millimoles/g*	*Millimoles/g*
1.54	1.005	0.089	0.916	1.138	1.313	0.342	0.971	1.307	1.525	0.390	1.135
1.71	0.924	.065	.859	1.434	1.142	.215	.927	1.625	1.357	.282	1.075
1.83			*.905*	1.807	0.946	.095	.851	1.994	1.026	.106	.920
1.94	.849	.048	.801	2.092	.855	.048	.807	2.448	0.852	.036	.816
2.24	.785	.025	*.785*	*2.106*			*.785*	3.065	.701	.014	.687
2.36			.760	2.644	.742	.016	.726	3.627	.477	.009	.468
2.88			.573	*2.811*			*.684*	*3.710*			*.447*
2.97			*.537*	3.093	.551	.010	.541	4.039	.295	.009	.286
3.35			.369	3.512			.397	*4.096*			*.277*
3.78			.207	*3.526*			*.376*	4.447	.216	.011	.205
3.78			.217	3.792			.250	4.447			.146
4.20			.124	4.013			.167	*4.502*			*.204*
4.49			.070	*4.035*			*.160*	*4.502*			*.144*
4.53			*.065*	4.279			.095	4.768			.101
5.22			*.013*	4.557			.056	5.42			.045
5.27			.003					5.58			.029

TABLE 1.—*Combination of wool protein with various strong acids, in the absence of added salt*—Continued

p-Diphenylbenzenesulfonic acid				Dodecylsulfonic acid				Orange II			
pH	Acid neutralized	Ammonia produced	Acid combined	pH	Acid neutralized	Ammonia produced	Acid combined	pH	Acid neutralized	Ammonia produced	Acid combined
	Millimoles/g	*Millimoles/g*	*Millimoles/g*		*Millimoles/g*	*Millimoles/g*	*Millimoles/g*		*Millimoles/g*	*Millimoles/g*	*Millimoles/g*
1.525	1.083	0.165	0.918	2.370	1.224	0.228	0.996	2.020	1.125	0.212	0.913
1.915	0.914	.072	.842	2.629	0.943	.083	.861	2.300	1.072	.144	.928
2.239			*.820*	*3.068*			*.815*	2.568	0.972	.080	.892
2.366	.816	.027	.789	3.397	.701	.015	.686	3.053	.846	.050	.796
2.956	.700	.010	.690	*3.559*			*.662*	3.339	.783	.024	.759
3.119			*.665*	3.666			.503	3.749	.611	.010	.601
3.577			.489	*3.780*			*.495*	4.230			.379
3.920			.315	3.916			.368	*4.790*			*.244*
3.972			*.310*	*4.110*			*.362*	5.015			.151
4.132			.219	*4.290*			*.263*	*5.395*			*.163*
4.499			*.157*	*5.34*			.095	*5.395*			*.102*
4.663			.084	*5.08*			.070	5.595			.061
4.821			*.048*	*5.27*			.047	*5.625*			*.055*
4.965			.031	*5.72*			*.022*	*5.835*			*.029*
5.02			.016					5.90			.007
5.35			.009					*6.16*			*.006*

As in the results described earlier [16], considerable amounts in excess of 0.8 millimole appear to be bound when the most concentrated solutions of some of the acids are employed. Possible causes of this excess take-up of acid have been discussed in section II–4 and elsewhere [16]. The discussion of the affinity to wool of each of the anions dealt with in this paper is based entirely on the position with respect to the pH coordinate of the main S-shaped portion of the titration curve. In order to fix the position of this principal portion of each set of data, an effort has been made to draw continuous curves which represent the measurements fairly rather than to draw curves deliberately congruent with one another.

The curves which lie more than one to one and one-half pH units above the curve for hydrochloric acid must be considered as somewhat less accurately fixed by the experiments on three counts: (1) The pH values measured are those of very poorly buffered solutions; (2) the attainment of equilibrium is difficult, although the equilibrium curve can usually be fixed within narrow limits by comparing the measurements with the results of reversal experiments; (3) the relatively long periods at high temperatures required for attainment of equilibrium with acids of high affinity result in appreciable decomposition of the wool. This effect is intensified by the fact that decomposition is brought about more rapidly by acids of high affinity (table 1). Thus the choice of temperature at which each acid was investigated was governed in part by the desire to minimize as much as possible the aggregate effect of all of these factors as well as by the desire to obtain data at more than one temperature for a few acids of representatively different affinities. Acids having affinities equal to or greater than that of naphthalene-β-sulfonic acid were measured at either 25° or 50° C rather than at 0° C.

The bearing of the results on the general question of the factors influencing affinity is considered in section IV of this paper, but matters of special interest concerning a few of the substances worked with are discussed individually below.

Hydrochloric acid no longer occupies an extreme position at the low-affinity end of the diagram (fig. 1) as it did in the earlier paper. Two other acids give curves which indicate that their anions have affinities for wool lower than the affinity of chloride. Thus, titration curves of proteins, obtained with hydrochloric acid, are also clearly affected by the specific affinity of the chloride ion for the protein, and must not be regarded as representing a limiting case governed by the hydrogen-ion dissociation equilibrium of the carboxyl groups alone.

The lowest affinity is shown by phosphoric acid, and refers to the dihydrogen phosphate ion. The data for phosphoric acid are congruent with the other curves only for amounts combined of less than about 0.45 millimole per gram. This limitation is brought about by the fact that the first step in the dissociation of phosphoric acid is not complete in the range of pH below 2. The presence of appreciable amounts of un-ionized acid results in the combination of additional amounts of acid in the undissociated form, as is found with weak acids generally [13].

The data at 0° C include measurements with two acids, sulfuric and pyrophosphoric, which are dibasic in the pH ranges of their respective curves. The amounts combined are therefore plotted as milliequivalents per gram instead of millimoles per gram. The curves for both indicate that their doubly charged anions have relatively high affinities, considering their molecular weights. A part, at least, of their high affinity may be due to the double charge, but this cannot constitute a full explanation. Thus, pyrophosphate has a lower affinity than sulfate although its molecular weight is considerably higher.

The curve obtained with metaphosphoric acid is not strictly comparable with those obtained with the other acids because of the presence of chloride, divalent monohydrogen trimetaphosphate, and trivalent metaphosphate ions. Its position is probably determined predominantly by the affinity of the divalent ion (or its dimer), since the concentration of this acid ion increases almost proportionally to the increase in hydrogen ion, as is the case when curves are obtained with strong acids in the absence of salt. The higher affinity of the basic trimetaphosphate ion is probably indicated by the titration curves obtained by Briggs for the soluble protein, serum albumen [2]. Because the titration curves for soluble proteins fall in a region of higher pH values [12], in these experiments the metaphosphate is nearly all in the fully ionized form. Thus the difference between the curves obtained by Briggs with hydrochloric acid and with hydrochloric acid plus metaphosphate is much larger than the difference found here with wool.

Among the data given for 25° C are measurements made with a third divalent anion, sulfosalicylate, commonly used as a protein precipitant. The affinity, as would be expected, is high but not so high as that of two other protein precipitants of higher molecular weight, picric and flavianic acids [16]. As in the case of flavianic acid, amounts far in excess of 0.8 *milliequivalent* per g are bound at low pH values. The anion present in this region of pH is the monovalent ion, and a

plateau near 0.8 *millimole* rather than at 0.8 milliequivalent would presumably be found.

The results shown for octylsulfuric, dodecylsulfonic, and dodecylsulfuric acids are the first given for strong aliphatic acids of high molecular weight. The first of these has a molecular weight slightly above that of naphthalenesulfonic acid; its affinity for wool is obviously higher. The affinities of the two larger molecules are among the highest so far measured.[4] These results tend to contradict a suggestion made earlier [16], namely, that flat aromatic ions had higher affinities than linear ions, and are therefore discussed further elsewhere.

Among the data obtained at 50° C (fig. 2), the new measurements made with Orange II supersede those published earlier, since they have been corrected for the effect of the ash content of the fibers, and for the relatively rapid decomposition of the wool that occurs in the more concentrated solutions of this dye. The results therefore differ slightly from those published earlier.

With sulfuric acid the data at 50° C are much like those obtained at 0° C when the amounts combined are less than 0.3 milliequivalent per gram; beyond this point the increase in the amounts combined as the pH decreases is smaller than at the lower temperature. This anomaly may be attributed to the formation in the more acid solutions of the low-affinity *bisulfate* ion, a process which is enhanced by high temperature (the second dissociation constant of sulfuric acid decreases as the temperature is raised [4]). Thus at pH values below 3 there is considerably more bisulfate ion at 50° C than at 25° C. This effect of high temperatures in effectually diminishing the affinity of sulfuric acid is of importance in dyeing, where not only high temperature but the presence of sulfate in addition to sulfuric acid favors the formation of bisulfate ion.

2. THE SCALE OF ANION AFFINITIES

In order to compare the results obtained with different acids on other than an empirical basis, it is necessary to reduce the positions of the curves to corresponding values of K_A', the anion dissociation constant, defined in previous papers [12, 16]. The resulting series of constants, calculated from the pH values at which half the maximum amounts are combined, not only furnishes an affinity scale to which a quantitative significance can be attached, but also makes possible the calculation of the effects of other environmental factors, such as the presence of salts, in terms of a mass-action effect, or of the effect of temperature, in terms of heats of dissociation. A slight modification [11] in the original method of calculation has recently been introduced in order to extend the range of usefulness of the previously formulated equations. With this modification, the equations describe the relevant parts of the curves in full detail, and not merely the positions of the midpoints of the curves.

Using the new equations, values of K_A' for all the acids so far investigated have been calculated by employing the appropriate values of K_H' for each temperature [16]. The results of the calcula-

[4] The high affinity of dodecylsulfate is of special interest in view of its recent use as a protein denaturant [1]. As Smith [8] has shown, the effect of this substance, unlike that of other protein denaturants, is to disrupt at least one protein into fragments. The hydrolytic effect of dodecylsulfuric acid on wool protein shown in table 1, and further described elsewhere [17], is the greatest of any acid so far investigated. Since, in general, the hydrolytic effect increases with the affinity, the drastic effects of dodecylsulfate on soluble proteins may be shared in greater or lesser degree by other compounds of high molecular weight.

tion are assembled in table 2. The newly calculated values of $-\log K_A'$ for acids measured previously are compared in the table with the values given earlier. The revised values are not far different from those given by the old equations, especially in the range of lower affinities. The larger differences are found with the anions of highest affinity, since there is a slightly smaller degree of dependence of K_A' on the pH of half-maximum combination in the new equations.

TABLE 2.—*Calculation of anion affinity constants* $(1/K_A')$ *at three different temperatures*

	Molecular weight	pH of half-maximum combination	$-\log K_A'$	$-\log K_A'$ previously given
0° C				
Phosphoric	98.0	2.155	0.115	
Sulfamic	97.1	2.22	.20	
Hydrochloric	36.5	2.32	.43	0.45
Ethylsulfuric	126.1	2.33	.44	.45
Hydrobromic	80.9	2.47	.69	.74
Nitric	63.0	2.58	.89	.96
Isoamylsulfonic	152.2	2.58	.89	
Benzenesulfonic	158.2	2.63	1.00	1.05
p-Toluenesulfonic	172.2	2.66	1.035	1.10
o-Phenolsulfonic	174.2	2.66	1.035	
o-Xylene-*p*-sulfonic	186.2	2.71	1.12	1.21
Metaphosphoric [a]	$(80.0)_{3n}$	2.72	[a](1.14)	
Trichloroacetic	163.4	2.73	1.16	1.25
o-Nitrobenzenesulfonic	203.2	2.86	1.39	1.50
Pyrophosphoric [b]	178.0	2.94	1.53	
4-Nitrochlorobenzene-2-sulfonic	237.6	3.07	1.76	1.93
Sulfuric [b]	98.1	3.08	1.78	
2,5-Dichlorobenzenesulfonic	227.1	3.13	1.87	1.95
2,4-Dinitrobenzenesulfonic	248.2	3.17	1.94	2.09
Naphthalene-β-sulfonic	208.2	3.24	2.06	2.23
2,4,6-Trinitroresorcinol	245.1	3.64	2.73	3.02
Picric	229.1	3.86	3.08	3.34
Flavianic [b] [e]	314.2	4.24	3.67	3.94
25° C				
Hydrochloric	36.5	2.16	0.265	0.31
Naphthalene-β-sulfonic	208.2	3.03	1.82	1.97
Octylsulfuric	210.3	3.47	2.56	
Sulfosalicylic	218.1	3.34	2.34	
Picric	229.1	3.52	2.64	2.89
Dodecylsulfuric	266.4	4.02	3.42	
Flavianic [b]	314.2	4.07	3.495	3.77
Dodecylsulfonic [e]	250.4	4.08	3.51	
Orange II [e]	328.3	[e]4.63	[e]4.28	[e]4.53
50° C				
Hydrochloric	36.5	2.17	0.28	0.38
Naphthalene-β-sulfonic	208.2	2.95	1.68	
Sulfuric [b]	98.1	[d]2.97	1.71	
Diphenylsulfonic	234.3	3.16	2.04	
p-Hydroxyazobenzene-*p'*-sulfonic	278.3	3.24	2.18	
Anthraquinone-β-sulfonic	288.3	3.40	2.44	
p-Diphenylbenzenesulfonic	310.4	3.70	2.93	
iso-Propylnaphthalenesulfonic	250.3	3.74	2.99	
Dodecylsulfonic	250.4	3.96	3.33	
Orange II	328.3	4.17	[f]3.64	3.94

[a] The affinity indicated is minimal, for reasons explained in the text.
[b] The data given refer to combination with the divalent anion, but K_A' is expressed, for purposes of comparison, as if the anion were monovalent.
[e] The affinity given is minimal because equilibrium may not have been attained
[d] Extrapolated from the lower (normal) portion of the titration curve. The actual midpoint pH was 2.92.
[e] The midpoint pH of the curve obtained with Orange II at 25° C has been reevaluated by applying a correction for ash to these data. Both values of $-\log K_A$ are based on the reevaluated midpoint.
[f] This value is based on the revised midpoint pH given in the present paper.

3. EFFECT OF TEMPERATURE ON AFFINITY

The revised values of K_A' in table 2 entail a slight revision of the values previously given for ΔH, the heat of dissociation of the anions from the anion-wool complex.

The assumptions which enter into calculations, from titration data at two temperatures, of ΔH for the dissociation of a hydrogen ion from the protein have been discussed elsewhere [15, especially p. 535 and footnote 11]. The same assumptions are now applied to the calculation of the heat of dissociation of anions as well.

The new values are indicated in table 3; it will be seen that they are not greatly altered from those given previously. With one exception, they extend and confirm the regularity described earlier, namely, a pronounced tendency for the average heat of dissociation in a given temperature interval to increase as the affinity increases. The relatively small value for sulfate ion, which constitutes the exception noted, must be accepted with reservations on two counts: first, the affinity constants from which it has been calculated have only formal significance since they apply strictly to monovalent anions only. In addition, the value given for ΔH for this acid, unlike all others in the table, is an average value over the wide temperature interval 0° to 50° C. A comparison with the results obtained with hydrochloric acid suggests that the heat of dissociation of sulfate from the sulfate-wool complex may be approximately twice as great in the 0° to 25° C interval as the average value given in the table for the wider range.

TABLE 3.—*Calculation of heats of dissociation of anion-wool combinations*

Anion	Temperature interval	Ratio of dissociation constants	ΔH (average heat of dissociation)
	°C		*Calories*
Chloride	0 to 25	1.481	2,550
	25 to 50	0.975	−194
Sulfate	0 to 50	1.163	532
Naphthalene-β-sulfonate	0 to 25	1.755	3,640
	25 to 50	1.338	2,220
Picrate	0 to 25	2.75	6,550
Dodecylsulfonate	25 to 50	1.51	3,180
Orange II	25 to 50	>4.36	>11,300

IV. RELATION OF CHEMICAL STRUCTURE TO AFFINITY

The data collected in table 2 reveal a pronounced tendency for the affinity of anions for wool to rise with their molecular weights. Thus, the question of the existence of any additional factors modifying this tendency may best be examined by comparing the affinities of different substances or classes of substances on the basis of their sizes or molecular weights rather than by comparing the affinities themselves. Such a comparison is facilitated by figure 3, in which quantities proportional to the free energy of binding of the anions ($-\log K_A'$) of a large proportion of all the acids studied have been plotted against their respective molecular weights. Among the acids investigated, only the strong monobasic organic acids are represented in order to bring out simple relationships more clearly. To include as wide a range of molecular weights and of affinities as possible, data for two temperatures, 0° and 50° C, have been combined; a division between

the data at the two temperatures has been effected arbitrarily, with only slight overlapping, at log K'_A approximately equal to -2. Naturally it cannot be expected that there will be any continuity between the data obtained at the two different temperatures, but their combination serves to point a trend, and the data for each temperature may be compared among themselves.

The simple relations shown indicate an absence of any large specific effects of different substituents on the affinity within the two groups of acids represented. Thus, to point to only a few examples, *o*-phenolsulfonic and *p*-toluenesulfonic acids have nearly equal molecular weights and show practically identical affinities, although the properties of the OH and CH_3 groups (such as polarity, polarizability, and resonance energy) differ markedly. Likewise the differences in the

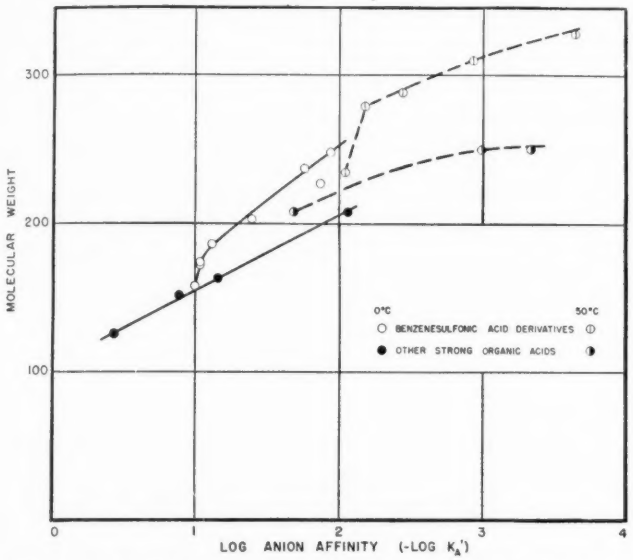

FIGURE 3.—*Molecular weights and values of log affinity for strong monobasic organic acids.*

Data for two temperatures, 0° and 50° C, are represented.

positions on the diagram of xylene-, nitrobenzene-, nitrochlorobenzene-, and dinitrobenzene-sulfonic acids are consistent with their relative molecular weights, despite similar large differences in the properties of their respective substituents. Such regularities in the relation between affinity and molecular weight as are shown in figure 3 imply that the effects of temperature on anion affinity are also fairly regular. This has already been indicated by the data presented in the preceding section.

However, the fact that the points in the diagram fall roughly into two groups is an indication that there are limits to the range of chemical structure within which marked specific effects fail to appear. Thus, among the strong organic acids, those which are benzenoid in character have lower affinities for wool than those which fall in other categories (aliphatic, naphthenoid, etc.). Since the simplest member of the benzenoid series, benzenesulfonic acid, falls on both curves, it

cannot be maintained that the benzene ring itself has a particularly low ratio of affinity to mass. Rather, it appears that the mass added by a substituent to the benzene ring is relatively less effective in increasing the affinity to wool than is the same mass added to aliphatic or conjugated ring compounds. This reduced effectiveness appears even when the substituent added is another benzene ring, as is shown in the strictly homologous series benzenesulfonic, diphenylsulfonic, diphenylbenzenesulfonic acids. It does not appear, or appears less strongly, when the rings are conjugated, as in naphthalenesulfonic acid. The existence of similar effects is suggested by the scantier data obtained at 25° C, which are not represented in the figure. The reason for these differences remains obscure.

If the affinities of other types of acids were included in figure 3, the existence of marked specific differences in affinity would be well shown. Thus points for the two strong phenolic acids, picric acid and trinitroresorcinol, would fall well below the curve for the benzenesulfonic acid derivatives; that is, these phenolic acids have relatively high ratios of affinity to mass, when compared with other benzenoid compounds. As would be expected, doubly charged anions, such as flavianate and sulfosalicylate, also have higher ratios of affinity to mass. The greatest specific differences appear among the inorganic acids, the points for which, if included in the figure, would scatter widely in its lower left-hand corner. Although all their affinities fall in the lower part of the range covered, all but sulfamic and the two phosphoric acids have relatively higher ratios of affinity to mass than do any of the organic acids. The common acids—hydrochloric, nitric, and sulfuric—are outstanding in this respect.

V. REFERENCES

[1] M. L. Anson, J. Gen. Physiol. **23,** 239 (1939).
[2] D. R. Briggs, J. Biol. Chem. **134,** 261 (1940).
[3] R. K. Cannan, Cold Spring Harbor Symposia Quant. Biol. **6,** 1 (1939).
[4] W. J. Hamer, J. Am. Chem. Soc. **54,** 860 (1934).
[5] R. S. Hisar, Kimiya Ann. **3,** 20 (1938).
[6] C. R. Noller and J. J. Gordon, J. Am. Chem. Soc. **55,** 1090 (1933).
[7] E. P. Partridge, V. Hicks, and G. W. Smith, J. Am. Chem. Soc. **63,** 454 (1941).
[8] E. Smith, J. Gen. Physiol. **24,** 583 (1941); **24,** 753 (1941).
[9] A. Sookne, C. H. Fugitt, and J. Steinhardt, J. Research NBS **25,** 61 (1940) RP1314; Textile Research **10,** 380 (1940); Am. Dyestuff Reptr. **29,** 1333 (1940).
[10] J. M. Sprague and T. B. Johnson, J. Am. Chem. Soc. **59,** 1837 (1937).
[11] J. Steinhardt, J. Research NBS **28,** 191 (1942) RP1452.
[12] J. Steinhardt and M. Harris. J. Research NBS **24,** 335 (1940) RP1286; Textile Research **10,** 181 (1940); Am. Dyestuff Reptr. **29,** 103 (1940).
[13] J. Steinhardt and M. Harris, Proc. Am. Soc. Biological Chemists XXXIV, J. Biol. Chem. **134,** xcvii (1940).
[14] J. Steinhardt and M. Harris, Proc. Am. Soc. Biological Chemists XXXV, J. Biol. Chem. **140,** cxxiv (1941). A more complete account is in preparation.
[15] J. Steinhardt, C. H. Fugitt, and M. Harris, J. Research NBS **25,** 519 (1940) RP1343; Textile Research **11,** 72 (1940); Am. Dyestuff Reptr. **29,** 607 (1940).
[16] J. Steinhardt, C. H. Fugitt and M. Harris, J. Research NBS **26,** 293 (1941) RP1377; Textile Research **11,** 259–284 (1941); Am. Dyestuff Reptr. **30,** 223 (1941).
[17] J. Steinhardt, J. Biol. Chem. **141,** 995 (1941).
[18] P. van Rysselberghe, J. Phys. Chem. **43,** 1049 (1939).

WASHINGTON, November 7, 1941.

U. S. DEPARTMENT OF COMMERCE NATIONAL BUREAU OF STANDARDS

RESEARCH PAPER RP1454

Part of Journal of Research of the National Bureau of Standards, Volume 28, February 1942

INTERCOMPARISON OF PLATINUM RESISTANCE THERMOMETERS BETWEEN −190° AND 445° C

By Harold J. Hoge and Ferdinand G. Brickwedde

ABSTRACT

Eight platinum resistance thermometers satisfying the requirements of the International Temperature Scale were calibrated on the International scale and intercompared from −190° to 445° C. The δ's of the Callendar-Van Dusen equations for seven of these thermometers ranged from 1.49375 to 1.49862. The δ for the eighth thermometer, *E*, was 1.51155. After minimizing the effects of relative calibration errors, the maximum difference between the readings of the group of seven thermometers was 7 millidegrees between −190° and 0° C and 1.3 millidegrees between 0° and 100° C. Maximum differences from the mean were 4.0 and 0.8 millidegree, respectively. For thermometer *E*, deviations from the mean of the other seven were 15 millidegrees at −110° C and 3 millidegrees at +50° C. Tables of differences between readings of platinum resistance thermometers arising from assumed calibration errors at the fixed points were calculated and are included.

CONTENTS

		Page
I.	Introduction	217
II.	Apparatus and procedure	219
III.	Adjustment of the data	221
IV.	Discussion of results	228
V.	Comparison with previous work	232
VI.	Conclusions	233
VII.	Appendix. Calibration errors	234
VIII.	References	240

I. INTRODUCTION

The International Temperature Scale below 660° C is defined in terms of a few fixed points and by interpolation formulas for strain-free, high-purity platinum resistance thermometers [1].[1] The platinum resistance thermometer was chosen as the basic instrument because of its precision, convenience, and reproducibility. The scale was made to agree, as closely as was possible at the time of its adoption, with the thermodynamic scale by selection of the fixed points and the temperatures assigned to them and by selection of the interpolation instrument and formulas. Exact agreement of the two scales, though desirable, is not necessary, provided the International scale is accurately reproducible, because then the relation between the two scales can be determined at any time within the limits of reproducibility.

[1] Figures in brackets indicate the literature references at the end of this paper.

The reproducibility of a temperature scale depends upon the agreement of the values obtained when different thermometers are used to measure the same temperature. If groups of thermometers are used, and if the mean reading of one group is compared with those of other groups, greater reproducibility is to be expected than when individual thermometers are compared. There are a number of factors that may influence the reading of a thermometer. Besides those factors associated with the calibrating and measuring apparatus and technique, there are others associated with the intrinsic properties of the thermometers themselves. The intrinsic differences in thermometers that result from variations in materials, construction, or annealing are limited by specifications for the thermometers.

The accumulated experience with resistance thermometers indicates that the reproducibility attainable in repeated measurements with an individual instrument is very satisfactory. A considerable amount of evidence in the literature indicates that the differences between various thermometers, while small, are consistent enough to show that they are real. The information on this point in the range below 0° C is somewhat scanty, consisting of that obtained in comparisons of resistance thermometers with gas thermometers [2, 3]. There is little direct evidence concerning the differences which may exist between groups of thermometers.

Direct evidence concerning the reproducibility of the International scale can be obtained by a systematic intercomparison of a group of thermometers used to maintain the scale. If such a comparison should show satisfactory agreement among all the thermometers, nothing more definite concerning reproducibility would be established than the probability that other similar thermometers would also show satisfactory agreement. If the agreement should not be as good as desired, it would indicate that a stricter definition of the scale might be advantageous, and the data obtained might or might not indicate in what respects the definition could be advantageously revised.

Eight thermometers, each satisfying the present requirements for the International Temperature Scale, were used for the intercomparisons reported here. The thermometers were made in three institutions, using wire from at least three manufacturers. All the thermometers were of the same type, consisting of a coiled helix supported on a mica frame. Obviously, any conclusions concerning reproducibility will be more limited than those which might have been drawn if thermometers of other types had been included. However, if the thermometers were really strain-free, as is indicated by their constancy of calibration after exposure to temperatures from 445° to −190° C, it is not to be expected that the behavior of other strain-free thermometers would differ appreciably from these, even though the manner of supporting the wire were different. Moreover, the thermometers used included not only a number which might be considered typical but also some selected from the available group so as to include the widest range of characteristics consistent with the requirements of the International Temperature Scale adopted in 1927.

The treatment of the data differs in one important respect from that followed in most of the previous work in resistance thermometry at this Bureau. It was found that the constancy of the thermometers and the accuracy of the resistance measurements were such that the resistance of each thermometer could be considered as depending

only on its temperature, at least over the limited period (less than 1 year) during which the calibrations and intercomparisons were made. With this procedure, the resistance at 0° C, R_0, for example, was treated as a constant rather than as a quantity subject to small variations from time to time. If the measurements had extended over a longer period of time or had been made in the summer months, when the humidity is likely to be high, this procedure might not have been possible, but in the present instance it appears to be justified by the results obtained. With this method, a further refinement in handling the data was possible. Making use of the intercomparisons at or near the calibration points, the calibration data were adjusted so as to bring the thermometers into as good agreement as possible at the calibration points. Using these adjusted calibration data for calculating temperatures at intermediate points, the differences found between the various thermometers would be those inherent in the instruments themselves, and would be almost independent of calibration errors.

II. APPARATUS AND PROCEDURE

The experimental work consisted of two parts: (a) The calibration of each individual thermometer on the International Temperature Scale, and (b) the intercomparison of the calibrated thermometers. Part (a) was carried out in the prescribed manner [1]. Part (b) was carried out in two different comparators, one covering the range from the sulfur point down to room temperature, and the other covering the range below 100° C. In the region of overlap, data were taken with both comparators, which served as a check on their satisfactory operation.

The high-temperature comparator consisted of a vertical furnace containing an aluminum block with wells in which the thermometers were placed. Outside this block were alternate layers of insulating material and aluminum, to promote temperature uniformity in the block. Above the comparison block and separated from it was a guard block through which the thermometers passed, so that their total depth of immersion was considerably greater than the minimum specified by the International Temperature Scale for sulfur-point calibrations. The furnace was controlled to better than 1° C by an automatic regulator, the precise regulation of the block being accomplished manually by means of an auxiliary heater on the comparison block. The guard block also carried a heater, by means of which its temperature was maintained approximately equal to that of the comparison block.

The low-temperature comparator, in which the larger part of the measurements were made, was designed for enclosure in a Dewar flask. It consisted of a copper comparison block with wells in which the thermometers were placed, surrounded by a heavy copper thermal shield. The block carried one heater and the shield two, by means of which their temperatures could be held constant through manual regulation of the heating currents. The block and shield were supported by a copper-nickel tube, which passed upward axially through the source of refrigeration. The latter was a deep container for liquid air or liquid hydrogen, located in the upper part of the Dewar flask, several inches above the comparison block. Oxygen or hydrogen gas

could be admitted to the axial copper-nickel tube. This gas condensed in the part of the tube surrounded by the refrigerant, ran down the tube, and evaporated in contact with the thermal shield of the block. By varying the pressure of the gas, the rate of removal of heat from the block could be controlled.

The resistance thermometers were of the same type as those used previously [4], each consisting of a coiled helix supported on a mica frame. Each thermometer was sealed into a helium-filled cylindrical platinum case (5 by 50 mm) by a soft-glass seal, through which the leads passed. In the low-temperature comparator the space between the platinum cases and the thermometer wells was filled with low-melting solder. For high-temperature work and for all calibrations at fixed points, these platinum-encased thermometers were placed at the bottom of long glass protecting tubes (1 by 60 cm). These tubes contained several mica baffles or plugs of glass wool to reduce convection in the section above the thermometer and were filled with helium. Constants of the resistance thermometers are given in tables 1 and 2.

In taking readings, the same general procedure was followed with both comparators. At a given temperature, approximate values of the resistances of all the thermometers were obtained while time was being allowed for the disappearance of temperature gradients and the reaching of a satisfactorily steady state. Thermometer P, which had been chosen as the primary thermometer, was then read alternately with the others until each of these had been read twice. The thermometer current was in all cases 1 milliampere. When the rate of drift was negligible, every third reading was made on the "primary" thermometer; otherwise every second reading was on the primary, including of course the first and last readings in either case. When the primary-thermometer readings before and after were not identical, a linear change of resistance with time was assumed in computing simultaneous resistances of a given thermometer and the primary. The rate of drift was kept as near zero as possible and seldom exceeded 2 millidegrees between successive readings of the primary thermometer. In the case of thermometers F and G, which had been previously calibrated, no measurements were made above 100° C. With the other thermometers, the high-temperature calibrations and intercomparisons were in general made first, so that any changes caused by the high temperatures would not affect the accuracy of the low-temperature work.

The four leads to each resistance thermometer enter the platinum case through a glass seal. Above 300° C this glass became slightly conducting, as evidenced by a slight initial kick of the galvanometer, followed by a drift back toward a position of equilibrium. A separate investigation of this effect showed that by taking proper precautions the error introduced by it could be made negligible.[2]

[2] These precautions are based on the rapid reduction in conductance that results from the polarization of the glass during the first few minutes after the electromotive force is applied. A preliminary report of the investigation was given at a meeting of the American Physical Society [5] and a more complete report is being prepared for publication.

III. ADJUSTMENT OF THE DATA

The original data obtained when the various resistance thermometers were calibrated at the sulfur, steam, ice, and oxygen points are given in table 1. The values in italics were obtained by averaging the original determinations. The constants α, δ, and β were computed from the italicized values in the ordinary way, each thermometer being entirely independent of the rest. Using these calibration constants, the simultaneous resistance values obtained by intercomparison were converted to simultaneous temperature indications. Representing the temperature indication of the ith thermometer by t_i and that of the particular thermometer chosen as the primary thermometer by t_P, the differences, $t_i - t_P$, were computed. The results of this reduction are shown in figure 1. To avoid confusion, the experimental points were omitted in preparing this figure for publication. However, the disposition of points relative to the curves which represent them is the same for both figure 1 and figure 2, and may be consulted in the latter figure, where each curve is plotted on separate axes.

It is apparent from figure 1 that, with this method of computation, the results obtained with thermometers F and G at $-110°$ C differed by about 10 millidegrees from the mean of the others, and that thermometer E differed by somewhat more in the opposite direction. Since the curves do not go through zero at the calibration points, it is apparent that the comparison data near these points are in some cases not in good agreement with the calibration data. The notable discrepancies are those for thermometers F and G at the ice and oxygen points, F at the steam point, and P (base line) at the sulfur point. The question is immediately raised as to how the curves would be altered if the effects of these discrepancies, which arise from the relative calibration errors of the thermometers, could be eliminated. The constants in table 1 were obtained by the independent calibration of each thermometer at the four fixed points, while as a result of the intercomparisons any one of the thermometers could be used to calibrate all the rest. Under these conditions the calibration constants given in table 1 may be improved upon by combining all the available data by the method of least squares. Thus through the medium of the intercomparisons, each individual calibration datum has a share in determining the constants of all the thermometers in the group.

The method of adjusting the calibration data will be explained briefly. We represent the reading of the ith thermometer, when the constants of table 1 are used, by t_i. This quantity has the dimensions of temperature, but because of the possibility of calibration errors it is not to be confused with the true temperature. We take the steam-point adjustment as an example, and represent by $(t_i)_{100}$ the reading of the ith thermometer when the true temperature is exactly 100° C. Then the original steam-point calibration of each thermometer yields an equation of the form

$$(t_i)_{100} = 100.$$

There is no inconsistency in the eight equations of this type and no improvement in the calibrations can be made without additional data.

TABLE 1.—*Calibration data for the eight thermometers intercompared*

[Original data are in ordinary type and averages in italics. Values of α, δ, and β were computed from the italicized data in the ordinary way, each thermometer being entirely independent of the rest.]

Thermometer	R_0		R_{100}		R_S		R_{S2}		α	δ	β
A	Nov. 2, 1940	23.24346	Oct. 24, 1940	32.32875	Oct. 23, 1940	61.55375	Nov. 7, 1940	5.74009			
	Nov. 4, 1940	46	Oct. 31, 1940	51	Oct. 29, 1940	228	ditto	23			
	Nov. 8, 1940	46	Nov. 4, 1940	65	Oct. 30, 1940	335	Nov. 8, 1940	46			
Average		*23.24346*		*32.32864*		*61.55313*		*5.74026*	0.003908704	1.49651	0.11183
B	Nov. 2, 1940	28.66101	Oct. 24, 1940	39.90011	Oct. 23, 1940	76.05181	Nov. 7, 1940	7.00648			
	Nov. 4, 1940	01	Nov. 1, 1940	11	Oct. 29, 1940	018	ditto	25			
	Nov. 8, 1940	01	Nov. 4, 1940	31	Oct. 30, 1940	176	Nov. 8, 1940	45			
	Jan. 8, 1941	10									
Average		*28.66103*		*39.90018*		*76.05125*		*7.00639*	0.003921405	1.49776	0.11232
C	Nov. 2, 1940	27.49012	Oct. 24, 1940	38.24775	Oct. 23, 1940	72.84892	Nov. 7, 1940	6.76148			
	Nov. 4, 1940	17	Nov. 1, 1940	802	Oct. 29, 1940	796	ditto	34			
	Nov. 8, 1940	12	Nov. 4, 1940	772	Oct. 31, 1940	818	Nov. 8, 1940	81			
	Jan. 8, 1941	21									
Average		*27.49016*		*38.24783*		*72.84835*		*6.76154*	0.003913280	1.49888	0.11287
D	Nov. 2, 1940	25.75597	Oct. 24, 1940	35.86399	Oct. 23, 1940	68.38110	Nov. 7, 1940	6.28402			
	Nov. 4, 1940	97	Nov. 1, 1940	425	Oct. 29, 1940	07	ditto	51			
	Nov. 8, 1940	99	Nov. 4, 1940	409	Oct. 30, 1940	43	Nov. 8, 1940	69			
	Dec. 27, 1940	98									
Average		*25.75598*		*35.86411*		*68.38120*		*6.28441*	0.003924576	1.49518	0.11086
E	Nov. 2, 1940	22.63930	Oct. 24, 1940	31.49937	Oct. 18, 1940	59.97864	Nov. 7, 1940	5.54790			
	Nov. 4, 1940	30	Oct. 31, 1940	03	Oct. 29, 1940	762	ditto	801			
	Nov. 8, 1940	30	Nov. 4, 1940	08	Oct. 30, 1940	814	Nov. 8, 1940	821			
	Dec. 27, 1940	31									
Average		*22.63930*		*31.49916*		*59.97815*		*5.54804*	0.003913487	1.51178	0.12170
F	Jan. 19, 1935	27.54605	Jan. 10, 1935	38.33267	Jan. 9, 1935	73.03269	May 21, 1935	6.77095			
	May 17, 1935	587	Jan. 18, 1935	262	Jan. 17, 1935	19	ditto	121			
			Mar. 26, 1935	301			May 22, 1935	112			
			Mar. 27, 1935	260			ditto	227			
Average		*27.54596*		*38.33278*		*73.03244*		*6.77159*	0.003915914	1.49547	0.10849
G	Jan. 19, 1935	27.52759	Jan. 10, 1935	38.30709	Jan. 9, 1935	72.98538	May 21, 1935	6.76998			
	May 17, 1935	46	Jan. 18, 1935	54	Jan. 17, 1935	19	ditto	656			
			Mar. 26, 1935	27			May 22, 1935	621			

G	Jan. 19, 1935	27.52759	Jan. 10, 1935	38.30709	Jan. 9, 1935	72.98538	May 21, 1935	6.76698			
	May 17, 1935	46	Jan. 18, 1935	54	Jan. 17, 1935	19	do	656			
			Mar. 26, 1935	27			May 22, 1935	621			
			Mar. 27, 1935	12			do	767			
Average		*27.52752*		*38.30726*		*72.98528*		*6.76686*	0.003915987	1.49493	0.10844
P	Nov. 2, 1940	28.91754	Oct. 24, 1940	40.25732	Oct. 23, 1940	76.73164	Nov. 7, 1940	7.07050			
	Nov. 4, 1940	54	Nov. 1, 1940	20	Oct. 29, 1940	042	do	6977			
	Nov. 8, 1940	61	Nov. 4, 1940	26	Oct. 30, 1940	158	Nov. 8, 1940	6975			
	Dec. 27, 1940	66									
	Jan. 8, 1941	67									
Average		*28.91760*		*40.25726*		*76.73121*		*7.07001*	0.003921370	1.49798	0.11189

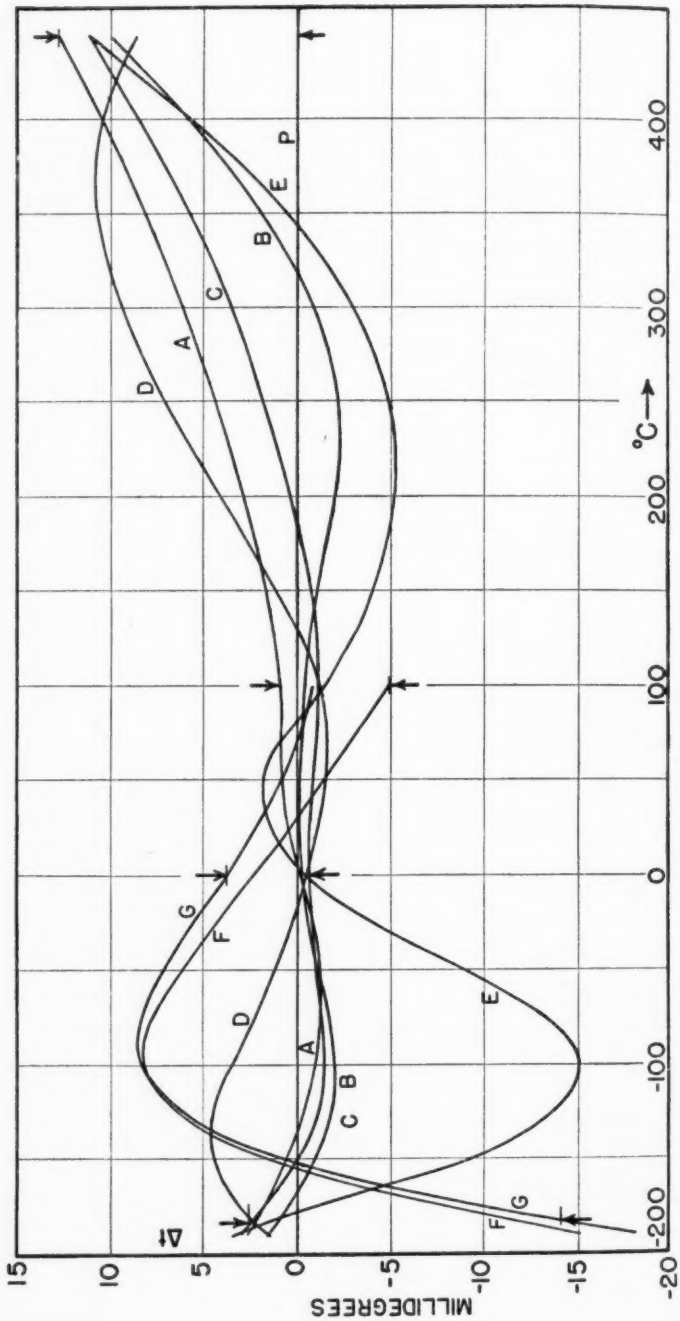

FIGURE 1.—*Deviations, $t_i - t_P$, of the readings of other thermometers from the reading of the primary thermometer.*

Temperatures computed with the unadjusted calibration constants.

We have additional data, however, in the difference curves of figure 1. By reading off the ordinates of the various curves at 100° C, we obtain seven equations of the form

$$(t_i - t_P)_{100} = a_i,$$

where a_i is the value read from the curve. The 15 equations contain 8 unknowns, and the least-squares solution yields the most probable value of the reading of each thermometer when the true temperature (as determined by the entire group) is exactly 100° C. For thermometer D, for example, it was found that $(t_D)_{100} = 99.9997$. Its calibration constants were therefore adjusted, so that in the neighborhood of the steam point the reading of the thermometer would be 0.0003 higher than before. Similar adjustments for all the thermometers were made at all the fixed points except where data were not available (F and G at the sulfur point). The adjusted calibration data are given in table 2. The adjusted value of α may of course be obtained immediately from the value of R_{100}/R_0.

TABLE 2.—*Adjusted calibration data*

[The figures in this table were obtained by utilizing both the data of table 1 and the results of the intercomparisons]

Thermometer	R_0	R_{100}/R_0	R_S/R_0	R_{O_2}/R_0	δ	β
A	23.24347	1.390875	2.648203	0.246967	1.49663	0.11160
B	28.66103	2140	53475	4454	1.49767	1240
C	27.49014	1326	49986	5965	1.49862	1297
D	25.75597	2457	54969	4001	1.49505	1087
E	22.63929	1346	49295	5063	1.51155	2183
F	27.54626	1560	51265	5760	1.49375	1080
G	27.52797	1576	51314	5749	1.49405	1042
P	28.91764	2138	53415	4480	1.49853	1183

The calibration data for thermometers F and G at the steam, ice, and oxygen points were given zero weight, so that in effect this adjustment was equivalent to recalibrating F and G at these points in terms of the calibration data for the other six thermometers. The reasons for considering the calibrations of these thermometers less accurate than the rest are given in section IV of this paper.

The original constants in table 1 had now served their purpose and were not further used. The intercomparison data were next recomputed with the adjusted constants and the differences, $t_i - t_P$, again found and plotted. The results are given in figure 2.

If the elimination of the effect of calibration errors had been the only purpose to be served by the adjustment of the data, the desired result could have been achieved by simpler methods—for example, by merely disregarding the original calibration data on all thermometers but one. However, this method of adjustment was used primarily to secure the most reliable calibration of each individual instrument for use as a thermometer, and this adjustment automatically eliminated the differences at the fixed points that are of concern in the present work.

The magnitude of the adjustments at the various calibration points is shown in table 3. In the neighborhood of each calibration point, temperatures computed with the unadjusted constants are greater

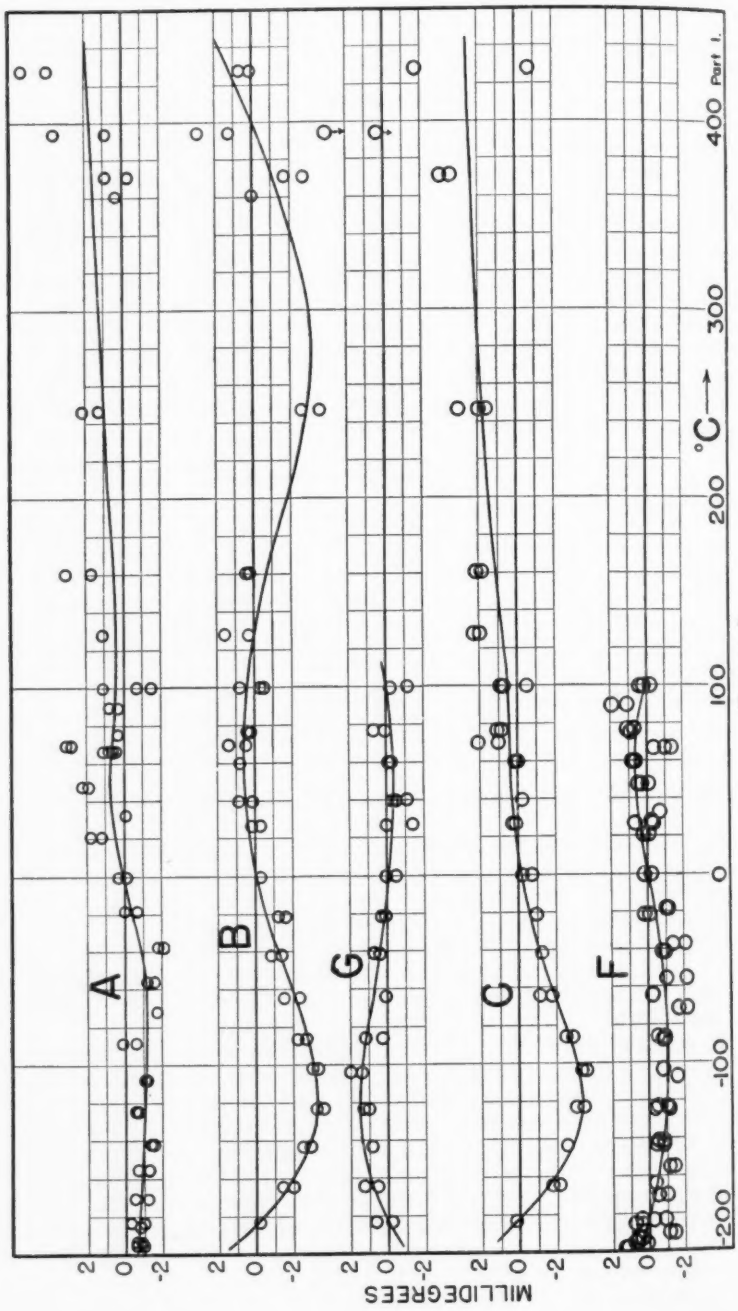

FIGURE 2.
(See also part 2, below.)

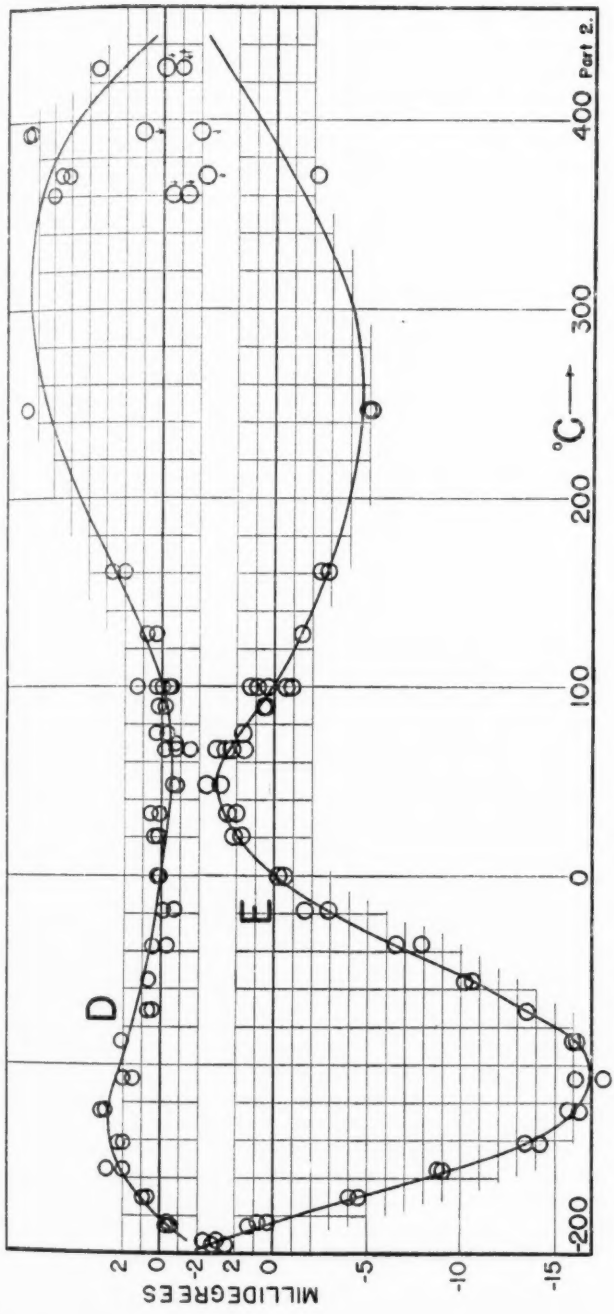

FIGURE 2 (Continued).—*Deviations,* $t_t - t_P$, *of the readings of other thermometers from the readings of the primary thermometer.*

Temperatures computed with the adjusted calibration constants.

435456—42——7

than those computed with the adjusted constants by the amounts given in table 3. It is apparent from table 3 that the adjustments have greatly reduced the larger discrepancies at the fixed points mentioned in an earlier paragraph. Comparison of figures 1 and 2 shows that for the six thermometers, *A*, *B*, *C*, *D*, *E*, and *P*, the new calibration data differ only slightly from the old, and that the differences between the indications of the thermometers at temperatures other than those of the calibration points have not been decreased appreciably. On the other hand, the agreement of thermometers *F* and *G* with the others has been very greatly improved, both at the calibration points and at intermediate points.

TABLE 3.—*Magnitude of the adjustments*

[This table gives the amounts, in millidegrees, by which temperatures computed with the unadjusted constants are greater than those computed with the adjusted constants]

Thermometer	t(unadjusted) $-t$(adjusted) at—			
	−182.97° C	0° C	100° C	444.60° C
A	1.1	0.1	1.3	3.7
B	−0.7	.0	−0.1	0.8
C	.6	−.2	−.8	1.5
D	.6	−.1	−.3	1.1
E	.1	−.1	−.8	0.4
F	−13.6	2.7	−4.2	.0
G	−15.8	4.1	0.0	.0
P	−1.8	0.3	.8	−7.1

There may still be a question as to whether the small remaining relative calibration errors represented by the differences at the calibration points in figure 2 could appreciably affect the differences between these points. A mathematical treatment of the problem of calibration errors is given in the Appendix, where a general expression for the effect of any combination of calibration errors is derived. In addition, four special cases are treated in which respectively only the ice point, steam point, sulfur point, or oxygen point is assumed to be in error. The curves for these four cases, showing the relative error as a function of temperature, were included in a paper by Mueller [6]. As shown in table 5, page 238, the effect at −110° C of an error made in the sulfur-point calibration is 8.0 percent of the magnitude of the original error. Hence a relative change in the δ of a thermometer corresponding to a change of 4 millidegrees at the sulfur point would change the difference $(t_i - t_P)$ for that thermometer at −110° C by +0.3 millidegree. It is therefore concluded that the differences in the readings of the various thermometers shown by figure 2 are chiefly due to intrinsic differences in the thermometers themselves. In the case of the two thermometers not intercompared above 100° C (*E* and *G*), there is no independent evidence concerning the existence of calibration errors at the sulfur point. For these, we can only estimate the probable relative error at 444.60° C and consider the curves at −110° C to be uncertain by 8.0 percent of this amount.

IV. DISCUSSION OF RESULTS

It is apparent from figure 2 that thermometer *E* differs greatly from the other seven thermometers, and that conclusions as to the reproducibility of the International Temperature Scale, especially

below 0° C, by means of a single thermometer will depend largely on whether or not this thermometer is included. Examination of the data shows that thermometer E has a fairly high fundamental coefficient, α, but that the value of δ is unusually large, especially for such a value of α. It has been pointed out [6] that the limitation on R_s/R_0 as given in the International Temperature Scale does not constitute an effective limitation on δ, and that this might well be replaced by the requirement that $(R_s-R_0)/(R_{100}-R_0)$ shall be between 4.216 and 4.218. Since the temperature assigned to the sulfur point is 444.60° C, this corresponds to limiting δ to the range 1.4882 to 1.5012. Such a requirement would definitely exclude thermometer E. While the existence of such a thermometer and the fact that it complies with the present requirements of the International Temperature Scale cannot be disregarded, it appears legitimate to state the conclusions that would result if thermometer E were excluded from the group, as well as those resulting if it is retained.

If thermometer E is included, it appears that two thermometers meeting the requirements of the International Temperature Scale may differ by about 20 millidegrees near −110° C, whereas if E is excluded, the maximum difference below 0° C falls to about 7 millidegrees, and the difference between the indication of any one thermometer and the mean of the group is not more than about 4 millidegrees.

The results show that if a reproducibility considerably better than 10 millidegrees is required, it is necessary to exclude thermometers like E. This could be done very simply by setting limits such as those mentioned above for the value of δ. From the nature of the case, it is not possible to prove that such a restriction would also be sufficient.

The comparison of the thermometers, after minimizing relative calibration errors (fig. 2), reveals differences in the temperature scales arising from inherent differences of the thermometers. Comparison of the curves of thermometers F and G in figures 1 and 2 shows that relative calibration errors can be of greater importance than the inherent differences of the thermometers. These thermometers were calibrated 5 years earlier than the other six thermometers of the group investigated, and by a different person using a different Mueller bridge. Also, the apparatus used in making the earlier oxygen-point calibrations was not of the same type as that now in use [7]. It was to be expected that the relative calibration errors of these thermometers, on the one hand, and the other six thermometers of the group, on the other, would be larger than the relative calibration errors of the members of the group of six thermometers. We do not believe that the observed differences are due to changes in the thermometers, but attribute them to the factors above mentioned. It is thought, however, that the differences are too large to be typical of calibrations made at different times and with different equipment.

It is instructive to consider the differences that may arise from assumed calibration errors. As reasonable limits for calibration errors at the ice and steam points, we may assume 1 and 3 millidegrees, respectively. Table 5, page 238, shows that the differences between the scales arising from these assumed errors are 5.4 millidegrees at −110° C and 1.2 millidegrees at +50° if the errors are of opposite sign, and 1.6 millidegrees at −110° C and 2.1 millidegrees at +50°

if they are of the same sign. These do not include the smaller differences that arise from calibration errors at the oxygen and sulfur points. The figures indicate that with present technique and apparatus relative calibration errors may give rise to differences in scales nearly as large as those arising from inherent differences in the seven thermometers investigated, whose δ's lie between 1.4936 and 1.4986. Differences of 0.01° at −110° and a few thousandths at +50° may be expected occasionally from not unreasonably large calibration errors.

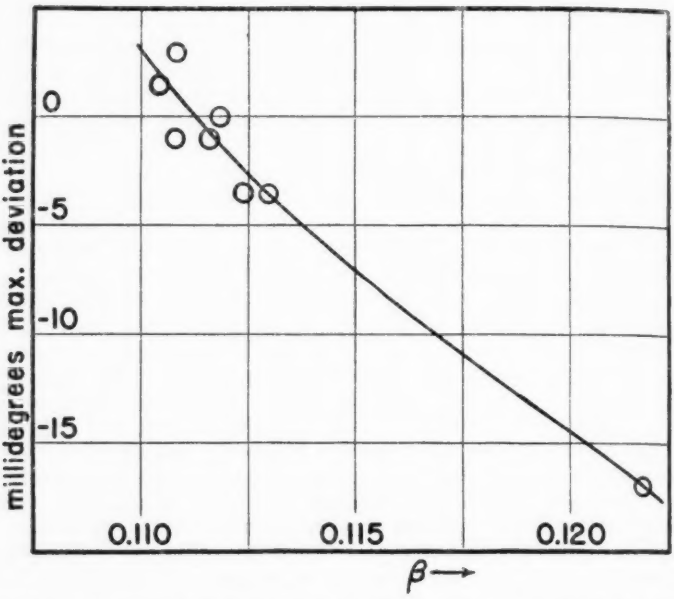

FIGURE 3.—*Maximum deviation* (t_i—t_P) *between* —182.97° *and* 0° C, *versus the calibration constant,* β.

Each resistance thermometer gives one experimental point.

The use of the same bridge for the calibration of a thermometer and for temperature measurements is recommended for obtaining the best reproducibility of a temperature scale. However, the use of the same bridge is not always feasible. In this connection, it should be realized that resistance coils of bridges and potentiometers are subject to seasonal as well as secular changes, and should be calibrated as frequently as is necessary to obtain the desired accuracy of resistance measurement.

The maximum values of t_i—t_P were read from the curves in figure 2 and recorded in table 4. To exhibit any relationships that might be present in the data, figures 3 and 4 were prepared. In figure 3 the values in the second column of table 4 are plotted against the values of β. Even without the point representing thermometer E there is some indication of a relationship, but the differences involved are small.

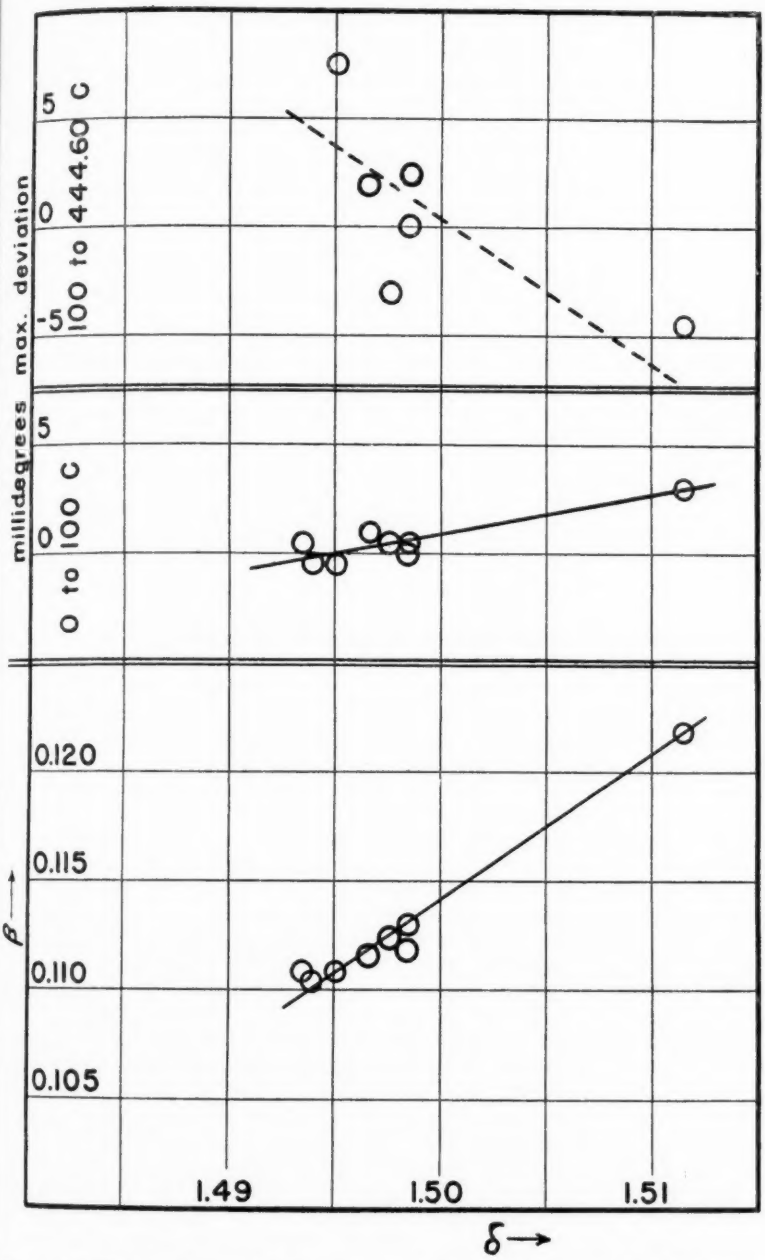

FIGURE 4.—*Top, maximum deviation* ($t_i - t_P$) *between 100° and 444.60° C; middle, maximum deviation,* $t_i - t_P$, *between 0° and 100° C; bottom, calibration constant,* β.

The abscissa for the three curves is the calibration constant, δ.

TABLE 4.—*Maximum deviation in millidegrees of the reading of a given thermometer from the reading of the primary thermometer*

Values were read from the curves in figure 2.

Thermometer	Maximum deviation between—		
	−182.97° and 0° C	0° and 100° C	100° and 444.60° C
A	−1.0	1.0	2.0
B	−3.5	0.5	−3.0
C	−3.5	.5	2.5
D	3.0	−0.5	7.5
E	−17.0	3.0	−4.5
F	−1.0	.5	
G	1.5	−0.5	
P	0.0	0.0	0.0

In figure 4, three quantities are plotted as functions of δ: (1) the maximum deviation between 0° and 100° C, (2) the maximum deviation between 100° and 444.60° C, and (3) β. Values of the maximum deviations are taken from table 4. Omitting the points representing thermometer *E*, the first two show very little correlation. A relation between β and δ is indicated, but again it is doubtful whether the relation is definite enough to serve as a basis for specifications.

V. COMPARISON WITH PREVIOUS WORK

Heuse and Otto [2] compared two platinum resistance thermometers with each other and with a gas thermometer between −130° and 0° C. They also report a few isolated measurements on two other thermometers. Keesom and Dammers [3] compared five thermometers with a gas thermometer between −153° and 0° C and made a few comparisons of four of these thermometers with each other. From these data the differences in reading of various resistance thermometers were obtained and plotted. Keesom and Dammers report their direct observations of the quantity $t_{A\alpha}-t_{Int.}$ (gas thermometer reading minus resistance-thermometer reading) and also give a table of smoothed values of the same quantity. It was found preferable to obtain the difference in reading of various resistance thermometers from the original data rather than from the smoothed values, as the difference curves obtained from the original data are more regular in shape. Over the range covered by the data, the points from both papers appeared to lie on curves similar to those in our figure 1.

With the exception of one thermometer (Leiden No. 69), differences between pairs of Leiden [3] thermometers and between a pair of PTR [2] thermometers satisfying the specifications of the International Temperature Scale were of the order of a few millidegrees from 0° to −190° C and did not exceed 7 millidegrees. Leiden thermometer 69 differed from four other Leiden thermometers by about 0.03° at −140° C. Its constants (α=0.0039074, δ=1.495, β=0.111) do not characterize this thermometer as abnormal. Since the intercomparisons were not continued down to the oxygen point, there is the possibility that if they had been continued, an appreciable difference at this point might have been found.

Confirmation for the relation between β and the maximum deviation found for the eight thermometers of the present investigation was looked for in the results of the comparisons made by Keesom and Dammers and by Heuse and Otto. Although there was some confirmation, there were almost as many exceptions as agreements. How many of the exceptions it would be possible to attribute to calibration errors, it is difficult to say.

Blaisdell and Kaye [8] determined the temperature of the mercury boiling point (356.57° C.) with 12 platinum resistance thermometers, with δ ranging from 1.492 to 1.496. The temperatures obtained had a spread of 10.7 millidegrees, the thermometers with the highest δ's, in general yielding the lowest temperatures. They state, however, that not all of the variation in reading can be attributed to differences in δ. This dependence of the thermometer reading on δ above 0° is consistent with the dependence on β at low temperatures found in the present work and indicates that thermometers with large values of δ give values that are too low between −182.97° and 0° C, too high between 0° and 100°, too low again between 100° and 444.60°, and presumably too high between 444.60° and 660°.

In addition to the above-mentioned papers, there are others which give some relevant information, often limited to a single fixed point whose value has been determined with more than one thermometer. A number of these were investigated by plotting for each set of observations deviations from the mean temperature indication against deviations from the mean δ or β, a process which takes full advantage of the internal consistency of the data. The scattering of these data was in general so great that they could not be said to confirm or disprove the results in the present work. This may mean, as Blaisdell and Kaye have already pointed out for the dependence of the mercury boiling temperature on δ, that the relation between thermometer readings and δ or β depends upon the kinds of impurities in the platinum wire and the construction of the thermometer.

VI. CONCLUSIONS

1. After minimizing relative calibration errors, differences between the temperatures determined with seven of the eight platinum resistance thermometers investigated, having δ's ranging from 1.49375 to 1.49862, were of the order of a few thousandths of a degree between 0° and −190° C. and were in no case greater than 7 millidegrees. Maximum differences from the mean of the group were not over 4 millidegrees. The eighth thermometer, E, though it satisfied the requirements of the International Temperature Scale, had an unusually large δ (for its α) and deviated 15 millidegrees at −110° C. from the mean of the other seven thermometers. These results indicate that the reproducibility of the International Temperature Scale below 0° C. can be considerably improved by setting limits to the admissible values of δ, which is equivalent to setting limits on $(R_s-R_0)/(R_{100}-R_0)$.

2. Between 0° and 100° C. deviations from the mean were less than 1 millidegree except for thermometer E, which, at 50° C. deviated by about 3 millidegrees from the mean of the other seven.

3. It might be said that for the seven normal thermometers of the group investigated, differences between the scales of thermometers arising from errors in calibrations carefully made are a little smaller

than the differences between the scales attributable to inherent differences in thermometers themselves. Not unreasonably large calibration errors, however, may lead to differences between the scales of these thermometers that are larger than differences arising from inherent differences in the thermometers.

4. In general, it does not seem that the agreement between thermometers can be substantially improved by setting limits for β as well as δ. Such limits might be useful in excluding unusually large calibration errors or thermometers having unusual characteristics not found in those used in this intercomparison.

5. Since there are good reasons for excluding thermometer *E*, there is only one thermometer, Leiden 69, which differs by more than 0.01° from others with which it was compared. On the whole, it seems a reasonable expectation that very few thermometers, if carefully calibrated according to the International Temperature Scale, will differ from each other by more than 0.01° C below 0° C.

The authors are pleased to acknowledge the valuable assistance received from E. F. Mueller in the preparation of this paper.

VII. APPENDIX. CALIBRATION ERRORS

Temperatures on the International Temperature Scale are computed from the Callender-Van Dusen equation, which may be written in either of the forms:

$$R/R_0 = 1 + At + Bt^2 + C(t-100)t^3 \tag{1}$$

or

$$t = \frac{1}{\alpha}\left(\frac{R}{R_0}-1\right) + \delta\left(\frac{t}{100}-1\right)\frac{t}{100} + \beta\left(\frac{t}{100}-1\right)\left(\frac{t}{100}\right)^3 \tag{2}$$

the terms containing C and β being retained only below the ice point. Although the discussion which follows is based on the latter form, the final results apply equally well to both, since they are mathematically equivalent.[3]

If we write eq 2 in the form

$$\phi = 0 = t - \frac{1}{\alpha}\left(\frac{R}{R_0}-1\right) - \delta\left(\frac{t}{100}-1\right)\frac{t}{100} - \beta\left(\frac{t}{100}-1\right)\left(\frac{t}{100}\right)^3 \tag{3}$$

and compute $\Delta\phi$ by partial differentiation, we obtain, since $\Delta\phi = 0$, a relation which may be used to compute the error Δt resulting from the errors $\Delta\alpha$, ΔR, ΔR_0, $\Delta\delta$, and $\Delta\beta$. The usefulness of this expression is strictly limited, however, by the fact that the errors involved are not all independent errors of observation.[4]

The directly observed and independent quantities from which the calibration constants are computed are R_0, R_{100}, R_S, and R_{O_2}, and an error equation containing these quantities rather than α, δ, and β is required. The subscripts 0, 100, S, and O_2 refer to values at exactly 0°, 100°, 444.60°, and −182.97° C, respectively. In the discussion which follows, it will be assumed, as may be done without loss of generality, that the temperature is always known exactly and that only meas-

[3] It is easily shown that the constants of the two equations are related as follows:

$$A = \alpha(1+10^{-2}\delta) \qquad \alpha = A + 100B$$

$$B = -10^{-4}\alpha\delta \qquad \delta = -\frac{10^4 B}{A+100B} = -\frac{10^4 B}{\alpha}$$

$$C = -10^{-8}\alpha\beta \qquad \beta = -\frac{10^8 C}{A+100B} = -\frac{10^8 C}{\alpha}$$

[4] Beattie, Benedict, Blaisdell, and Kaminsky (reference [9] p. 358–360, [10] p. 373–374, and [11] p. 385) have published tables of values of the errors in temperature caused by errors in α, δ, etc. Because they do not take into account the relationship between the various calibration constants, these tables are inapplicable to the types of error which are most likely to occur in practice. For example, suppose that the sulfur-point resistance is correctly determined but is used with an incorrect α to obtain δ. Then δ will be in error by an amount just sufficient to compensate at 444.60° C for the error in α, so that in the neighborhood of the sulfur point the total calibration error will be zero.

ured resistance is subject to error. It is convenient to make the replacement of α, δ, and β in two steps, introducing first the "platinum temperature" defined by

$$p \equiv \frac{1}{\alpha}\left(\frac{R}{R_0}-1\right) \tag{4}$$

and finally expressing all platinum temperatures in terms of resistances. Substituting eq. 4 in eq. 3,

$$\phi = 0 = t - p - \delta(\tau-1)\tau - \beta(\tau-1)\tau^3, \tag{5}$$

where, for convenience, $t/100 \equiv \tau$ has been written.

The conditions by which δ and β are determined are $\phi_S = 0$ and $\phi_{O_2} = 0$, or

$$0 = t_S - p_S - \delta(\tau_S - 1)\tau_S$$
$$0 = t_{O_2} - p_{O_2} - \delta(\tau_{O_2} - 1)\tau_{O_2} - \beta(\tau_{O_2} - 1)\tau_{O_2}^3.$$

Eliminating δ and β between these equations and eq 5, ϕ may be put in the symmetrical form

$$\phi = 0 = t - p - (t_S - p_S)\frac{(\tau-1)\tau}{(\tau_S-1)\tau_S}\left(1-\frac{\tau^2}{\tau_{O_2}^2}\right) - (t_{O_2}-p_{O_2})\frac{(\tau-1)\tau^3}{(\tau_{O_2}-1)\tau_{O_2}^3}. \tag{6}$$

In terms of these variables, we have, since $\Delta\phi = 0$,

$$\frac{\partial\phi}{\partial t}\Delta t + \frac{\partial\phi}{\partial p}\Delta p + \frac{\partial\phi}{\partial p_S}\Delta p_S + \frac{\partial\phi}{\partial p_{O_2}}\Delta p_{O_2} = 0,$$

or

$$\frac{\partial\phi}{\partial t}\Delta t = \Delta p - \frac{(\tau-1)\tau}{(\tau_S-1)\tau_S}\left(1-\frac{\tau^2}{\tau_{O_2}^2}\right)\Delta p_S - \frac{(\tau-1)\tau^3}{(\tau_{O_2}-1)\tau_{O_2}^3}\Delta p_{O_2}. \tag{7}$$

In eq 4 we replace $1/\alpha$ by its value in terms of resistances, obtaining

$$p \equiv \frac{100R_0}{R_{100}-R_0}\,\frac{R-R_0}{R_0}$$

$$\equiv 100\frac{R-R_0}{R_{100}-R_0}$$

In terms of resistance intervals, writing $R - R_0 \equiv I$ and $R_{100} - R_0 \equiv F$ (the fundamental interval)

$$p = 100\frac{I}{F}$$

whence

$$\Delta p = 100\frac{\Delta I}{F} - p\frac{\Delta F}{F}.$$

Substituting into eq 7, we obtain

$$\frac{\partial\phi}{\partial t}\Delta t = 100\frac{\Delta I}{F} - p\frac{\Delta F}{F}$$

$$-\left(100\frac{\Delta I_S}{F} - p_S\frac{\Delta F}{F}\right)\frac{(\tau-1)\tau}{(\tau_S-1)\tau_S}\left(1-\frac{\tau^2}{\tau_{O_2}^2}\right)\cdot$$

$$-\left(100\frac{\Delta I_{O_2}}{F} - p_{O_2}\frac{\Delta F}{F}\right)\frac{(\tau-1)\tau^3}{(\tau_{O_2}-1)\tau_{O_2}^3}\cdot$$

The terms in p, p_S, and p_{O_2} may be replaced by similar terms in t, utilizing the symmetrical equation, 6, giving

$$\frac{\partial\phi}{\partial t}\Delta t = 100\frac{\Delta I}{F} - t\frac{\Delta F}{F} - \left(100\frac{\Delta I_S}{F} - t_S\frac{\Delta F}{F}\right)\frac{(\tau-1)\tau}{(\tau_S-1)\tau_S}\left(1-\frac{\tau^2}{\tau_{O_2}^2}\right) - \left(100\frac{\Delta I_{O_2}}{F} - t_{O_2}\frac{\Delta F}{F}\right)\frac{(\tau-1)\tau^2}{(\tau_{O_2}-1)\tau_{O_2}^2}. \quad (8)$$

The partial derivative, $\partial\phi/\partial t$, has a simple physical significance. Written in full to show what variables are held constant, it is

$$\left(\frac{\partial\phi}{\partial t}\right)_{p,\, p_S,\, p_{O_2}}.$$

If we solve eq 6 for p and consider p as a function of t, p_S, and p_{O_2}, and calculate $\partial p/\partial t$, we find that

$$\left(\frac{\partial\phi}{\partial t}\right)_{p,\, p_S,\, p_{O_2}} = \left(\frac{\partial p}{\partial t}\right)_{p_S,\, p_{O_2}}.$$

It is also easily shown, by using eq. 5 and 6, that

$$\left(\frac{\partial p}{\partial t}\right)_{p_S,\, p_{O_2}} = \left(\frac{\partial p}{\partial t}\right)_{\delta,\beta}$$

which is simply the rate of change of platinum temperature with ordinary temperature. Substituting this, eq 8 becomes

$$\left(\frac{\partial p}{\partial t}\right)_{\delta,\beta}\Delta t = \frac{100}{F}\left[\Delta I - \tau\Delta F - (\Delta I_S - \tau_S\Delta F)\frac{(\tau-1)\tau}{(\tau_S-1)\tau_S}\left(1-\frac{\tau^2}{\tau_{O_2}^2}\right) - (\Delta I_{O_2} - \tau_{O_2}\Delta F)\frac{(\tau-1)\tau^2}{(\tau_{O_2}-1)\tau_{O_2}^2}\right]. \quad (9)$$

This is the general expression and may be used to compute the total effect of any combination of errors that is likely to occur. It should not be forgotten that *all terms originating from the oxygen-point calibration are to be dropped above 0° C.* Some care is required in assigning values to the various errors, particularly when R_0, R_{100}, R_S, R_{O_2}, and R have been measured at widely different times or with different equipment.

The types of error to be expected under various experimental conditions have been discussed fully by Mueller [6] and will not be treated here.

In many cases it is reasonable to assume that the same pair of values should be used for R_{100} and R_0 wherever they occur in eq 9. Making this assumption, it is of interest to treat five special cases of error, in which, respectively, only one of the five resistances, R_0, R_{100}, R_S, R_{O_2}, and R, is incorrectly determined.

Case 1.—$\Delta R_0 \neq 0$, no other errors

In this case, eq 9 reduces to

$$\Delta t\frac{\partial p}{\partial t} = \frac{100\Delta R_0}{F}(\tau-1)\left[1-\frac{\tau}{\tau_S}\left(1-\frac{\tau^2}{\tau_{O_2}^2}\right)-\frac{\tau^3}{\tau_O^3}\right]. \quad (10)$$

This equation is relatively simple in form because both sides are in terms of platinum temperature, in which the Callendar-Van Dusen equation is explicit. The error ΔR_0 is equivalent to an error $100\Delta R_0/F$ in platinum temperature at the

ice point. The function of τ on the right gives the relative importance of the error at any temperature. As would be expected, it vanishes at all calibration points except the ice point, at which it has the value -1. The negative sign signifies that if in calibration the value assigned to R_0 is too high, subsequent measurements of temperature near the ice point will yield values which are too low.

Because different thermometers have different values of R_0, values of ΔR_0 may not be directly comparable. Hence it is more convenient to estimate the calibration error in terms of temperature. To permit this, eq 10 may be evaluated for $\tau=0$, giving

$$\Delta t_0\left(\frac{\partial p}{\partial t}\right)_0=\frac{100\Delta R_0}{F}(-1),$$

where Δt_0 is simply the error at the ice point resulting from the calibration error ΔR_0. Dividing eq 10 by this, we obtain

$$\frac{\Delta t}{\Delta t_0}=\frac{\left(\frac{\partial p}{\partial t}\right)_0}{\left(\frac{\partial p}{\partial t}\right)}(1-\tau)\left[1-\frac{\tau}{\tau_S}\left(1-\frac{\tau^2}{\tau_{O_2}^2}\right)-\frac{\tau^3}{\tau_{O_2}^3}\right], \tag{11a}$$

which, above the ice point becomes

$$\frac{\Delta t}{\Delta t_0}=\frac{\left(\frac{\partial p}{\partial t}\right)_0}{\left(\frac{\partial p}{\partial t}\right)}(1-\tau)\left(1-\frac{\tau}{\tau_S}\right). \tag{11b}$$

The quantities $(\partial p/\partial t)_0$ and $\partial p/\partial t$ contain the constants δ and β. Assuming δ and β to be 1.495 and 0.111, respectively, values of eq 11 were computed at 10-degree intervals. The values are given in column 2 of table 5.

Case 2.—$\Delta R_{100}\neq 0$, no other errors.

In this case, eq 9 reduces to

$$\Delta t\frac{\partial p}{\partial t}=\frac{100\Delta R_{100}}{F}\tau\left[-1+\frac{\tau-1}{\tau_S-1}\left(1-\frac{\tau^2}{\tau_{O_2}^2}\right)+\frac{(\tau-1)\tau^2}{(\tau_{O_2}-1)\tau_{O_2}^2}\right]. \tag{12}$$

Most of the discussion of case 1 is applicable. Following the procedure of that section, we obtain

$$\frac{\Delta t}{\Delta t_{100}}=\frac{\left(\frac{\partial p}{\partial t}\right)_{100}}{\frac{\partial p}{\partial t}}\tau\left[1-\frac{\tau-1}{\tau_S-1}\left(1-\frac{\tau^2}{\tau_{O_2}^2}\right)-\frac{(\tau-1)\tau^2}{(\tau_{O_2}-1)\tau_{O_2}^2}\right], \tag{13a}$$

which above the ice point becomes

$$\frac{\Delta t}{\Delta t_{100}}=\frac{\left(\frac{\partial p}{\partial t}\right)_{100}}{\frac{\partial p}{\partial t}}\tau\,\frac{\tau_S-\tau}{\tau_S-1}. \tag{13b}$$

Function 13 has the value 1 at 100° C and vanishes at all other calibration points. Values computed at 10-degree intervals are given in table 5.

Case 3.—$\Delta R_S\neq 0$, no other errors.

In this case, we obtain

$$\frac{\Delta t}{\Delta t_S}=\frac{\left(\frac{\partial p}{\partial t}\right)_S}{\frac{\partial p}{\partial t}}\frac{(\tau-1)\tau}{(\tau_S-1)\tau_S}\left(1-\frac{\tau^2}{\tau_{O_2}^2}\right) \tag{14a}$$

below the ice point, and above the ice point

$$\frac{\Delta t}{\Delta t_S}=\frac{\left(\frac{\partial p}{\partial t}\right)_S}{\frac{\partial p}{\partial t}}\frac{(\tau-1)\tau}{(\tau_S-1)\tau_S} \tag{14b}$$

This function has the value 1 at 444.60° C, and vanishes at all other calibration points. Values computed at 10-degree intervals are given in table 5.

Case 4.—$\triangle R_{O_2}\neq 0$, no other errors.

With this type of error we have below the ice point

$$\frac{\Delta t}{\Delta t_{O_2}}=\frac{\left(\frac{\partial p}{\partial t}\right)_{O_2}}{\frac{\partial p}{\partial t}}\frac{(\tau-1)\tau^3}{(\tau_{O_2}-1)\tau_{O_2}^3}. \tag{15}$$

This function has the value 1 at − 182.97° C, vanishes at 0° C, and is of course not to be used at higher temperatures. Values computed at 10-degree intervals are given in table 5.

Case 5.—$\triangle R\neq 0$, no other errors.

In this case,

$$\Delta t=\frac{1}{\frac{\partial p}{\partial t}}\frac{100\Delta R}{F}. \tag{16}$$

This is included for completeness. The error is not connected with the calibration but with the subsequent use of the thermometer.

TABLE 5.—*Numerical values of functions 11, 13, 14, and 15*

For use in finding the errors at temperature t when the errors Δt_0, Δt_{100}, Δt_S, and Δt_{O_2} resulting from calibration are known]

t	$\Delta t/\Delta t_0$	$\Delta t/\Delta t_{100}$	$\Delta t/\Delta t_S$	$\Delta t/\Delta t_{O_2}$
°C				
−200	−1.067	0.765	−0.060	1.365
−190	−.405	.287	−.022	1.141
−182.97	*0*	*0*	*0*	*1*
−180	.157	−.110	.008	.944
−170	.625	−.433	.033	.773
−160	1.008	−.687	.052	.625
−150	1.312	−.879	.065	.498
−140	1.546	−1.016	.075	.391
−130	1.716	−1.102	.080	.302
−120	1.831	−1.144	.081	.228
−110	1.896	−1.148	.080	.169
−100	1.918	−1.119	.077	.121
−90	1.904	−1.062	.071	.084
−80	1.860	−.983	.064	.056
−70	1.791	−.885	.056	.036
−60	1.703	−.773	.048	.021

TABLE 5.—*Numerical values of functions 11, 13, 14, and 15*—Continued

t	$\Delta t/\Delta t_0$	$\Delta t/\Delta t_{100}$	$\Delta t/\Delta t_S$	$\Delta t/\Delta t_{O_2}$
°C				
−50	1.600	−.651	.039	.012
−40	1.487	−.523	.030	.006
−30	1.367	−.391	.021	.002
−20	1.244	−.258	.013	.001
−10	1.121	−.127	.006	.000
0	*1*	*0*	*0*	*0*
10	.882	.123	−.005	
20	.769	.240	−.009	
30	.659	.353	−.012	
40	.552	.461	−.014	
50	.450	.564	−.014	
60	.352	.662	−.014	
70	.258	.755	−.012	
80	.168	.841	−.009	
90	.082	.923	−.005	
100	*0*	*1*	*0*	
110	−.078	1.071	.006	
120	−.151	1.137	.014	
130	−.221	1.198	.023	
140	−.286	1.252	.033	
150	−.347	1.302	.044	
160	−.403	1.346	.057	
170	−.455	1.384	.071	
180	−.503	1.416	.086	
190	−.546	1.443	.103	
200	−.585	1.464	.120	
210	−.619	1.479	.140	
220	−.648	1.488	.160	
230	−.673	1.491	.182	
240	−.693	1.488	.205	
250	−.709	1.479	.230	
260	−.720	1.464	.256	
270	−.725	1.442	.283	
280	−.726	1.415	.312	
290	−.722	1.381	.342	
300	−.714	1.340	.373	
310	−.700	1.293	.406	
320	−.681	1.240	.441	
330	−.657	1.180	.477	
340	−.628	1.113	.514	
350	−.593	1.040	.553	
360	−.554	.960	.594	
370	−.508	.872	.636	
380	−.458	.778	.680	
390	−.402	.678	.725	
400	−.341	.570	.772	
410	−.274	.454	.820	
420	−.202	.332	.870	
430	−.124	.202	.922	
440	−.040	.065	.975	
444.60	*0*	*0*	*1*	
450	.049	−.079	1.030	
460	.144	−.231	1.086	
470	.245	−.390	1.145	
480	.352	−.557	1.205	
490	.465	−.732	1.267	
500	.585	−.915	1.330	
510	.710	−1.105	1.396	
520	.841	−1.304	1.463	
530	.979	−1.510	1.532	
540	1.123	−1.725	1.602	
550	1.273	−1.948	1.675	
575	1.677	−2.542	1.865	
600	2.123	−3.190	2.067	
625	2.611	−3.892	2.281	
650	3.143	−4.650	2.508	
660	3.368	−4.970	2.602	

VIII. REFERENCES

[1] George K. Burgess, *The International Temperature Scale*, BS J. Research 1, 635 (1928) RP22.

[2] W. Heuse and J. Otto, *The agreement of the legal and the thermodynamic emperature scales below 0° C*, Ann. Physik **14,** 181 (1932).

[3] W. H. Keesom and B. G. Dammers, *Comparison of some platinum thermometers with the helium thermometer between 0° and −183° C.* Physica 2, 1080 (1935) (Leiden Commun. 239e).

[4] Harold J. Hoge and Ferdinand G. Brickwedde, *Establishment of a temperature scale for the calibration of thermometers between 14° and 83° K.* J. Research NBS **22,** 351 (1939) RP1188.

[5] Harold J. Hoge, *Electrical conduction in the glass insulation of resistance thermometers* [abstract], Phys. Rev. **59,** 921 (1941).

[6] E. F. Mueller, *Precision resistance thermometry*, Temperature—Its Measurement and Control in Science and Industry, p. 162 (Reinhold Publishing Corporation, New York, N. Y., 1941).

[7] Russell B. Scott, *Calibration of thermocouples at low temperatures*, J. Research NBS **25,** 459 (1940) RP1339.

[8] B. Edwin Blaisdell and Joseph Kaye, *The location of the normal sulfur and mercury boiling points on the thermodynamic temperature scale*, Temperature—Its Measurement and Control in Science and Industry, p. 127 (Reinhold Publishing Corporation, New York, N. Y., 1941).

[9] James A. Beattie, Manson Benedict, and B. Edwin Blaisdell, *The reproducibility of the sulfur point. The effect of pressure on the sulfur point*, Proc. Am. Acad. Arts Sci. **71,** 327 (1937).

[10] James A. Beattie and B. Edwin Blaisdell, *The reproducibility of the steam point. The effect of pressure on the steam point*, Proc. Am. Acad. Arts Sci. **71,** 361 (1937).

[11] James A. Beattie, B. Edwin Blaisdell, and Joseph Kaminsky, *The reproducibility of the mercury boiling point. The effect of pressure on the mercury boiling point*, Proc. Am. Acad. Arts Sci. **71,** 375 (1937).

WASHINGTON, October 10, 1941.